



上海交通大学
SHANGHAI JIAO TONG UNIVERSITY



INPAC
INSTITUTE OF NUCLEAR AND PARTICLE PHYSICS



中能重离子碰撞与核物质对称能

陈列文

(上海交通大学 物理与天文学院/粒子与核物理研究所)

lwchen@sjtu.edu.cn

“原子核结构与中高能重离子碰撞交叉学科理论讲习班”，
湖州师范学院，湖州，浙江，2021年7月21日



- ① 重离子碰撞与极端条件下的核物理简介
 - ② 中能重离子碰撞微观输运理论模型
 - ③ 中能重离子碰撞与核物质对称能
 - ④ 对称能研究进展
 - ⑤ 展望
-



一、重离子碰撞与极端条件下的核物理简介

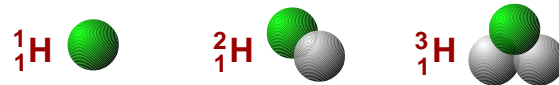
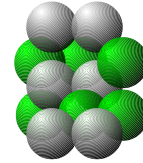
- 核反应的基本概念
 - 重离子碰撞的特点
 - 极端条件下的核物理
-



原子核的组成

- 原子核由**质子**和**中子**组成
- 核素: 给定中子数和质子数的原子核
- 元素: 给定质子数的原子核
- 同位素: 相同质子数但不同中子数的原子核
- **重离子**: 质量数大于4的离子, 亦即比 α 粒子 (${}^4\text{He}$) 重的离子

Mass number — 12 ${}^{12}\text{C}$
Charge number — 6 ${}^6\text{C}$

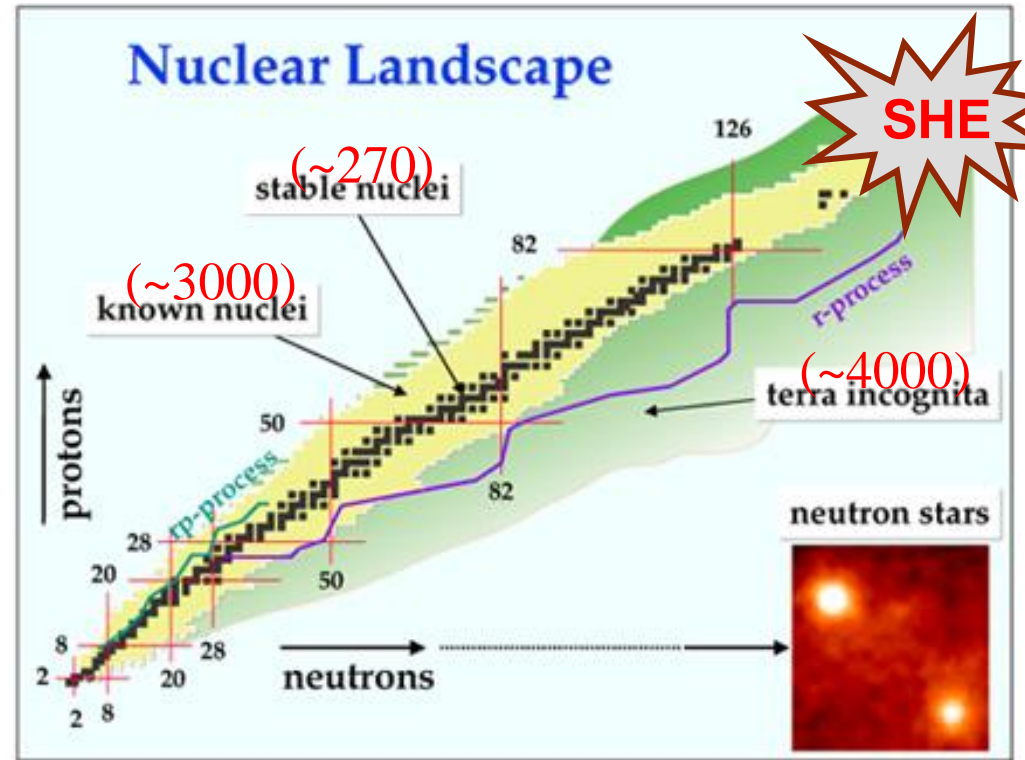


- **同位旋**: 就核力的性质而言, 质子与中子之间没有明显区别, 因此把质子和中子看成同一种粒子(统称为核子)的两种不同状态, 类比自旋的概念引入抽象的同位旋(**isospin**)空间, 质子和中子是同位旋 I 相同, 同位旋第3分量 I_3 不同的两种状态, 由此可确定它们的同位旋 $I = 1 / 2$, 质子的 $I_3 = 1 / 2$, 中子的 $I_3 = -1 / 2$, 它们组成同位旋二重态 ... (**海森堡, 1932年**)。在强相互作用, 同位旋是一个好量子数。



核素示意图

- 已知118种元素
- 只有不到300个稳定核(对此我们有一定认识)
- 对大部份不稳定核有所知,但知之不多
- 对其余几千个远离稳定区的核则一无所知
- 这些核素为人们提供了丰富的重离子源





什么是核反应？

- 两个原子核互相碰撞，或者在外场（如：库仑场）作用下，原子核内部发生变化，称为核反应。在强激光作用下发生的核反应叫“激光核反应”。关键是相对运动原子核，能够达到核力程范围，使核子之间发生作用！
- 由重离子诱发的反应称为重离子反应，又称重离子碰撞 (Heavy Ion Collisions – HIC's)
- 低能核反应通常表示为(2 → 2反应过程)



a: Projectile; A: Target; b: Exited partilce (lighter); B: Residue nucleus

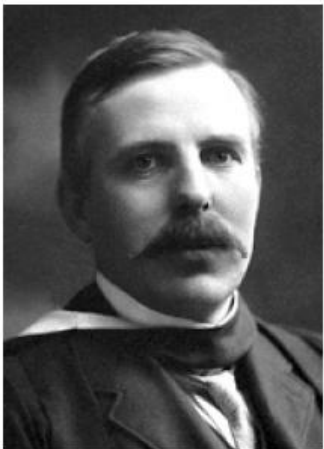


早期的核反应

- 卢瑟福模型：1911年，基于 α 粒子 (^4He) 轰击原子实验 (卢瑟福散射，卢瑟福“影子”，开创了通过散射来研究物质结构的先河)
- 质子的发现 (卢瑟福，1919年)：人类第一次实现人工核反应，人工“点金术”



The projectile α is from ${}^{212}\text{Po}$ decay (7.68 MeV).



Ernest Rutherford



The Nobel Prize in **Chemistry** 1908

"for his investigations into the disintegration of the elements, and the chemistry of radioactive substances"



早期的核反应

- 第一个在加速器上进行的核反应：



The projectile p was accelerated to 0.5 MeV and α has kinetic energy of 8.9 MeV. Release Energy!

- 第一个产生放射性核素的反应



- 导致发现中子的核反应 (J. Chadwick, NP in Physics 1935)



James Chadwick



Walther Bothe



The Nobel Prize in Physics 1954

Max Born, Walther Bothe

The Nobel Prize in Physics 1954 was divided equally between Max Born "for his fundamental research in quantum mechanics, especially for his statistical interpretation of the wavefunction" and Walther Bothe "for the coincidence method and his discoveries made therewith".



核反应的分类

- According to exited particles
 - Nuclear Scattering: $A(a,a)A$, $A(a,a')A^*$
 - Nuclear Conversion: $A(a,b)B$, $a \neq b$
- According to Incident Energy
 - $E_{in} < \text{几十 MeV/u}$: Low energy reactions
 - $\text{几十 MeV/u} < E_{in} < \text{几个 GeV/u}$: **Intermediate energy reactions**
 - $\text{几个 GeV/u} < E_{in} < \text{几十 GeV/u}$: High energy reactions
 - $E_{in} > \text{几十 GeV/u}$: Ultra-relativistic energy reactions
- According to Reaction Mechanism
 - Direct Reactions
 - Compound Reactions
 - Coulomb Excitation
 - Deep Inelastic Collisions (DIC's)
 - Fission
 - Fusion
- According to nucleus type
 - Light nucleus reaction
 - Heavy-ion reactions/Collisions (HIC's)



一、重离子碰撞与极端条件下的核物理简介

- 核反应的基本概念
 - 重离子碰撞的特点
 - 极端条件下的核物理
-



重离子反应研究的历史

- ④ 20世纪50、60年代，随着加速器技术的发展，人们能够加速 ^{12}C 、 ^{14}N 、 ^{16}O 等轻的重离子，能量很低，束流强度很弱
- ④ 1969年，预言了超重元素，推动了重离子物理的发展，引发了建造重离子加速器、合成超重核和挖掘滴线核素的热潮
- ④ 1972年在LBL实验室加速了GeV/u的重离子，为研究热的、高压缩的核物质提供了可能性，扩展了关于核的远离平衡的核状态方程
- ④ 1973年发现重离子深部非弹性碰撞(强阻尼碰撞) 机制
- ④ 80年代开始，相继建成了一些中能(10 MeV/u~1GeV/u) 重离子加速器，如HIRFL-CSR、GSI、GANIL、MSU 和RIKEN 等，可用来研究中能重离子碰撞，开创了核物理的新领域
- ④ 90年代开始极端相对论重离子碰撞实验，研究从强子相(Hadronic)到夸克-胶子等离子体相QGP (Quark-Gluon Plasma) 的相变，以及在地球上实现一个研究早期宇宙的实验室(SPS/RHIC/LHC)
- ④ 放射性核束引起的重离子反应(核存在的极限)
- ④ 超重元素合成



- ① 重离子反应具有以下特点：
 - ✓ 库仑作用强：原子核低激发态(库仑激发)
 - ✓ 形成高激发复合核：热核，高温高密核物质
 - ✓ 高角动量复合核：原子核的高自旋态
 - ✓ 重离子波长短：低能散射可用半经典模型
 - ✓ 入射粒子种类多：放射性核素的产生大大增加了入射重离子的数目



重离子反应的特点

粒子在不同动能E时的德布罗意波长

λ (fm)	γ	e	π	p	α	^{16}O	^{40}Ar	^{208}Pb
E (MeV)								
1	197	140	12	4.57	2.30	1.14	0.72	0.32
10	19.7	18.7	3.7	1.4	0.72	0.36	0.23	0.10
100	1.97	2.0	1.0	0.45	0.23	0.11	0.07	0.03
1000	0.20	0.2	0.17	0.12	0.07	0.04	0.02	0.01



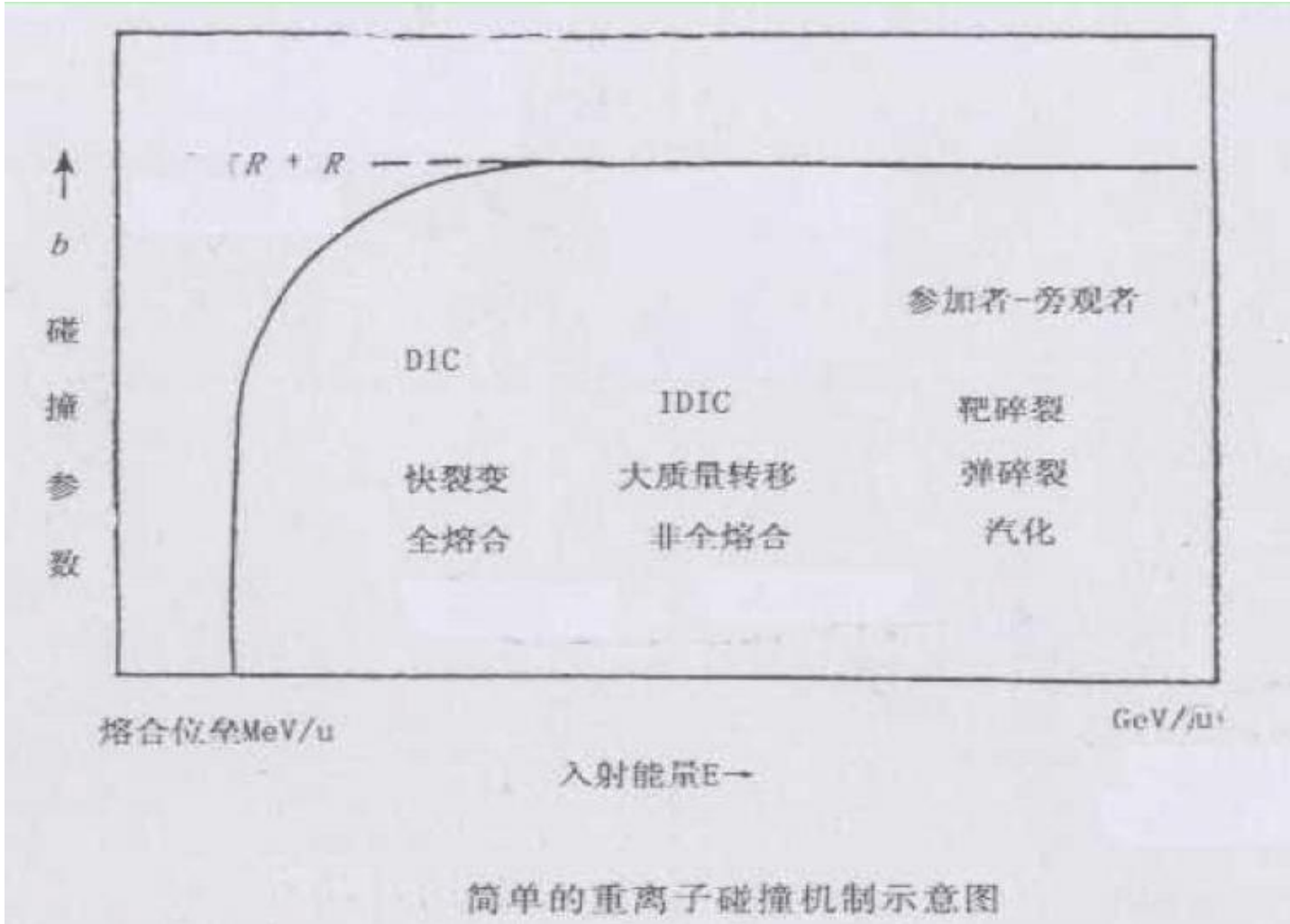
重离子碰撞能区：

- ✓ **低能区：** 库仑位垒 ~ 10 MeV/u (库仑位垒 ~ 6 MeV/u. 核子集体自由度主导)
- ✓ **中能区：** 10 MeV/u ~ 1 GeV/u (核子自由度主导，并高度激发)
- ✓ **高能区：** 1 GeV/u \sim 几十 GeV/u (介子自由度和奇异性自由度开始大量出现)
- ✓ **极端相对论能区：** 几十 GeV/u 以上 (强子自由度开始向夸克-胶子自由度过渡)



重离子反应的特点

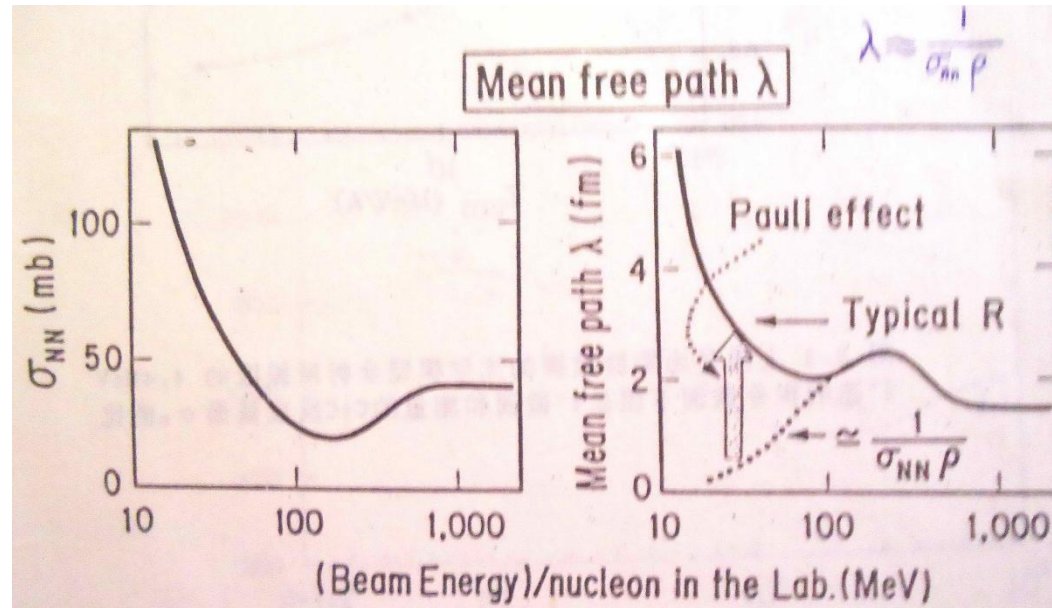
重离子反应机制与碰撞能量和碰撞参数的关系





中能重离子反应的特点

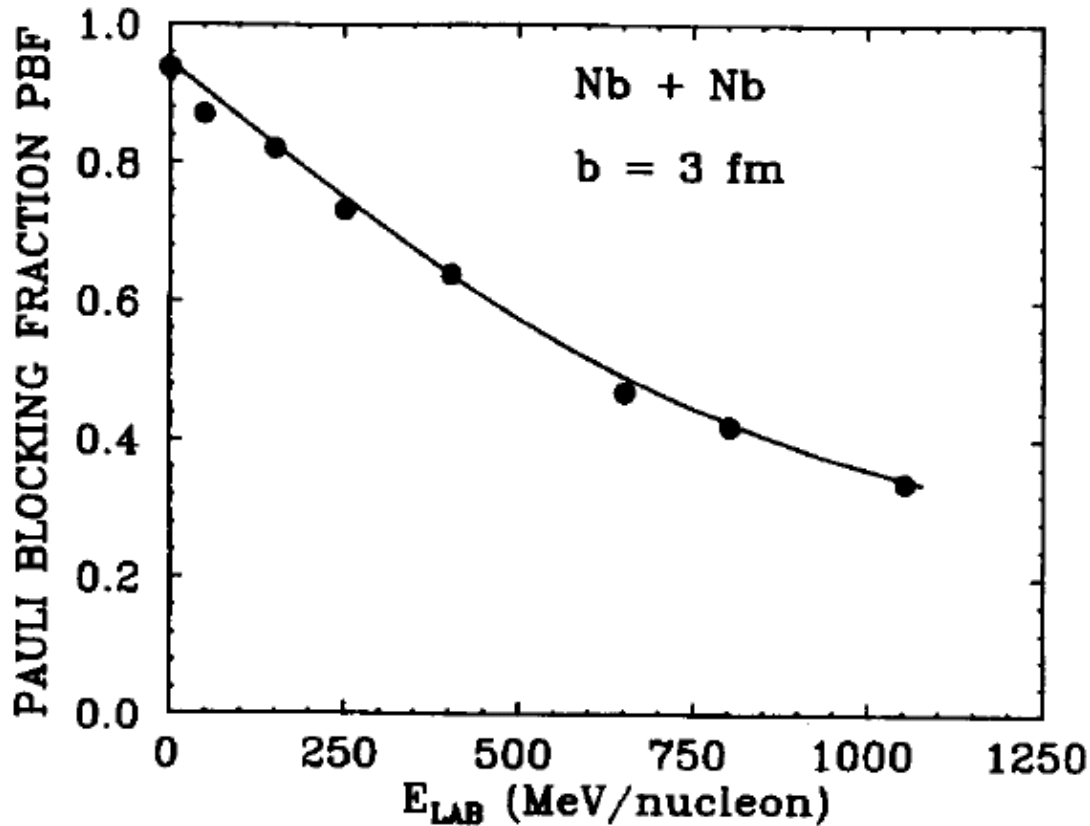
- 低能区：核子的平均自由程 $>$ 原子核的尺度 \rightarrow 平均场起主导作用
- 高能区：核子的平均自由程 $<$ 原子核的尺度 \rightarrow 核子-核子碰撞起主导作用
- 中能区：核子的平均自由程 \sim 原子核的尺度 \rightarrow 平均场、核子-核子碰撞以及Pauli阻塞效应都起作用，称为中能重离子碰撞的三要素



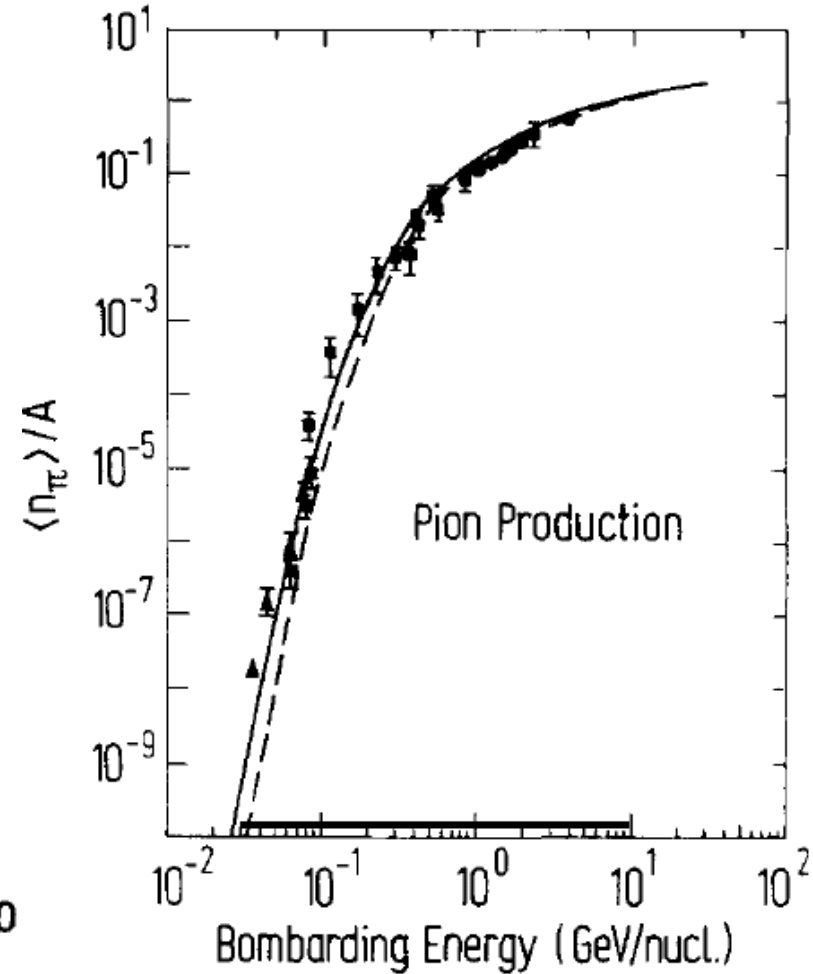


中能重离子反应的特点

Stock/Greiner, Phys. Rep. 137 (1986)277



Fraction of Pauli-blocked collisions in the VUU theory versus energy for the Nb + Nb system at $b = 3$ fm



Pion multiplicities per nucleon versus bombarding energy



重离子加速器

中能重离子加速器

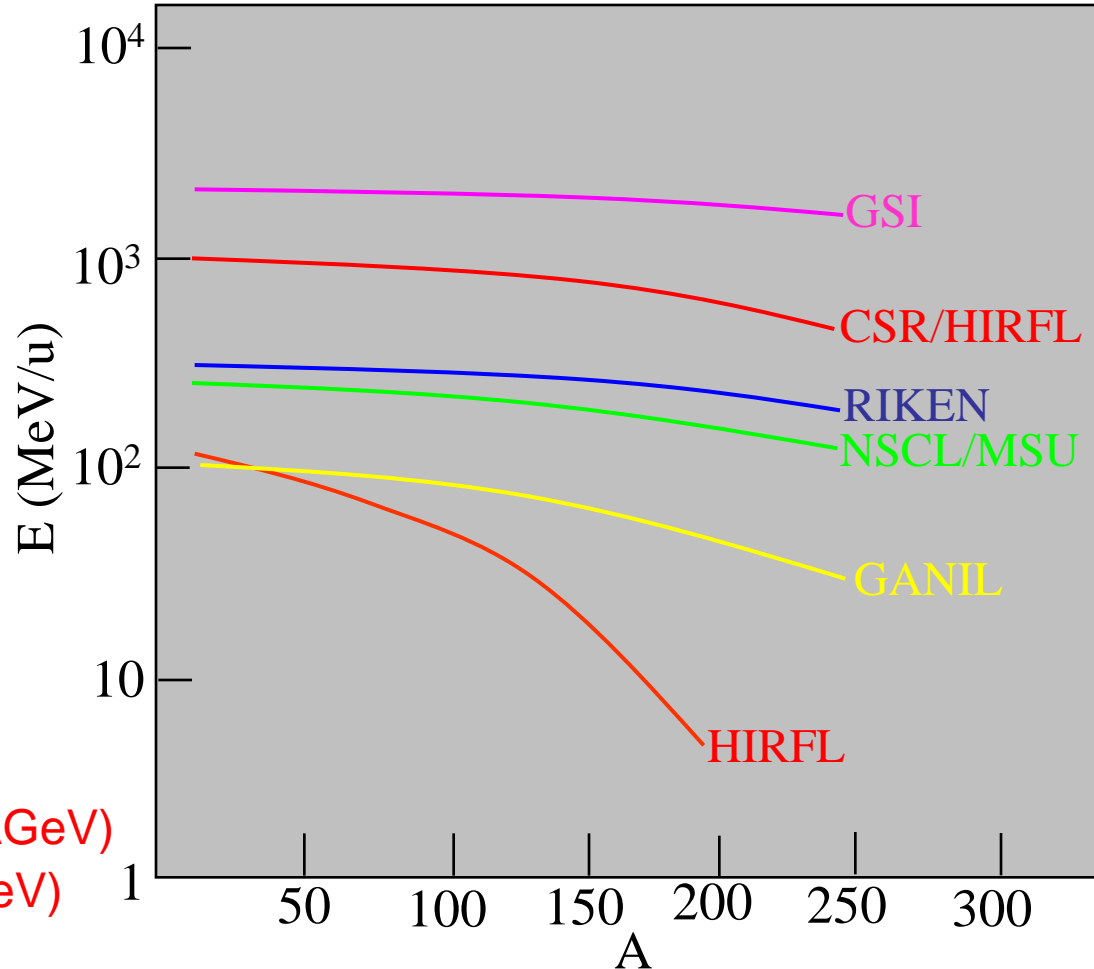
- ④ HIRFL, CSR/HIRFL (中国,兰州)
- ④ GANIL (France)
- ④ GSI (Germany)
- ④ NSCL/MSU (FRIB)
- ④ RIKEN (Japan)

- ④ Dubna, LBL, ORNL, TAMU,
- ④ INFN, KVI,...

高能重离子加速器

- ④ Bavalac / LBL (1 GeV/u)
- ④ SIS / GSI (1 GeV/u)
- ④ AGS / BNL (10 GeV/u)
- ④ SPS / CERN (100 GeV/u)
- ④ RHIC / BNL (质心能量: 200 AGeV)
- ④ LHC / BNL (质心能量: 5.5 ATeV)

中能重离子加速器

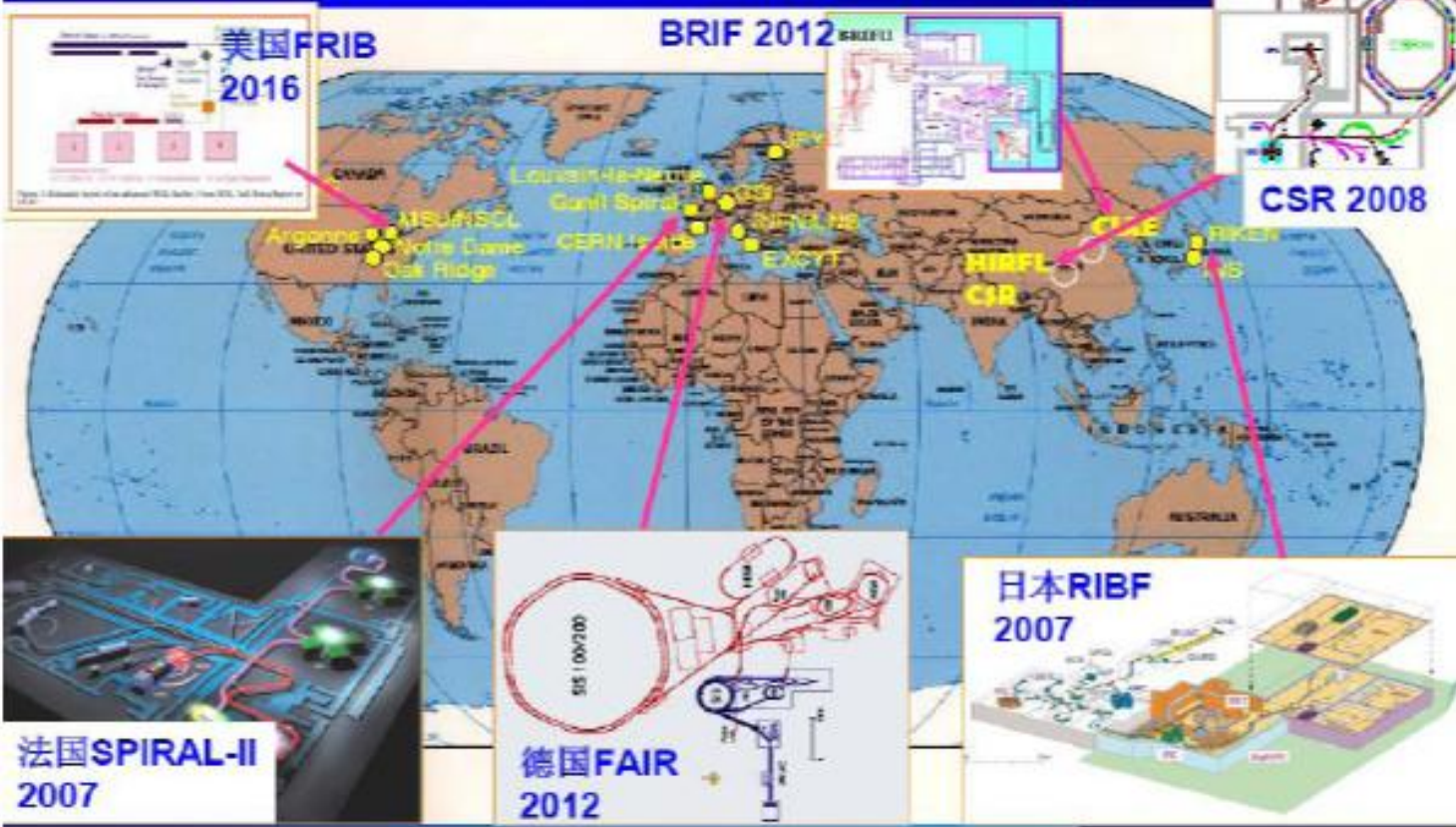




放射性核束装置

Radioactive beam facilities are being built around the world

正在发展的放射性核束大科学装置



HIAF:
(2018-2025)
U:0.8-17 AGeV

HIAF-U:
(2027-2032)
U:3-7 AGeV

BISOL

Providing new opportunities for both nuclear physics and astrophysics

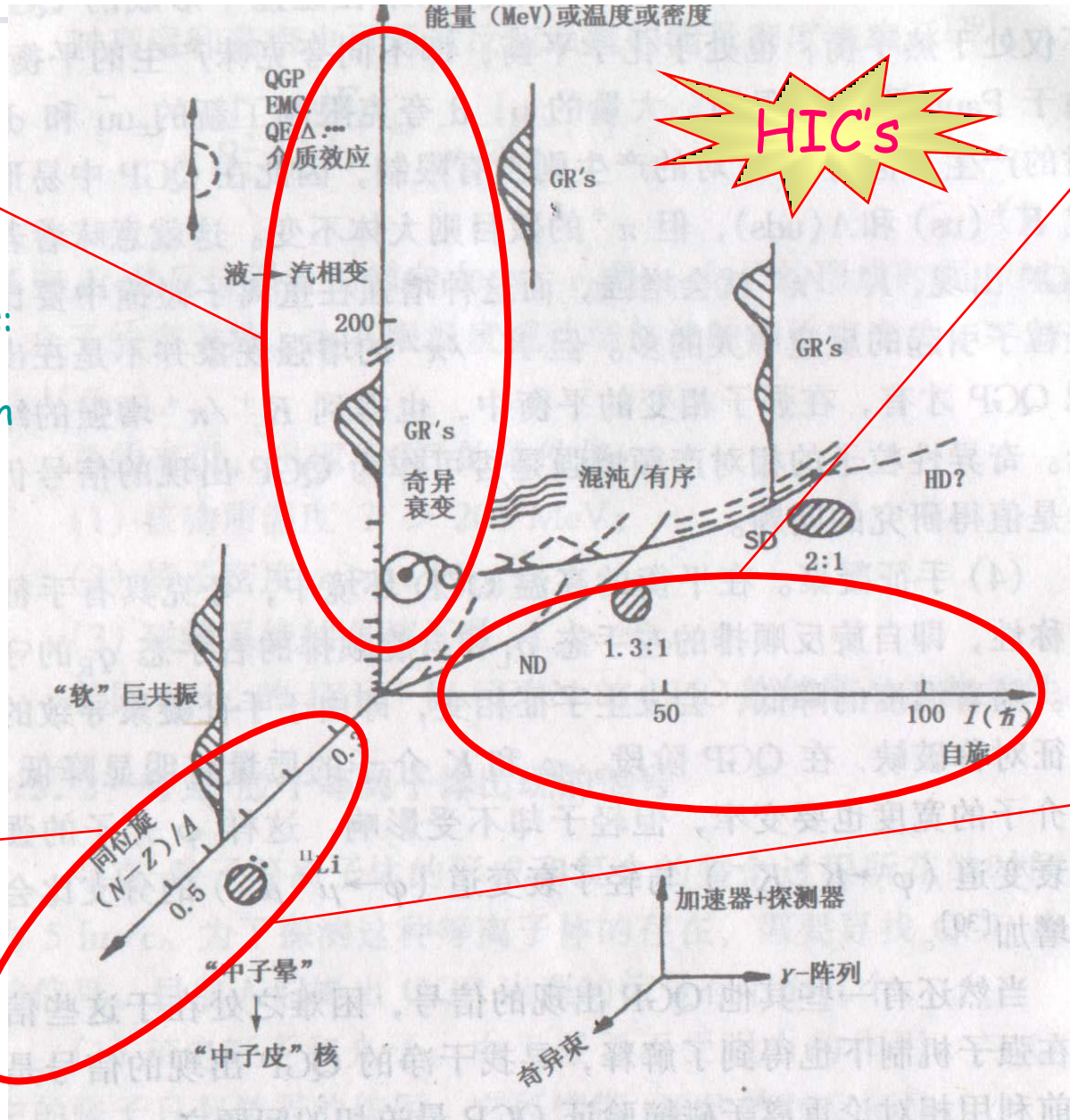


一、重离子碰撞与极端条件下的核物理简介

- 核反应的基本概念
 - 重离子碰撞的特点
 - 极端条件下的核物理
-



极端条件下的核物理



Energy,
Temperature,
Density
(高温高密):
Phase Transitions:
Liquid-Gas;
Chiral Restoration
QGP-Hadrons
.....

Spin(自旋):
High Spin
State and,
SD (Super-
Deformed),
HD (Hyper-
Deformed)
.....

Isospin:
(同位旋)
Nuclei far
from Beta-
Stability Line
.....

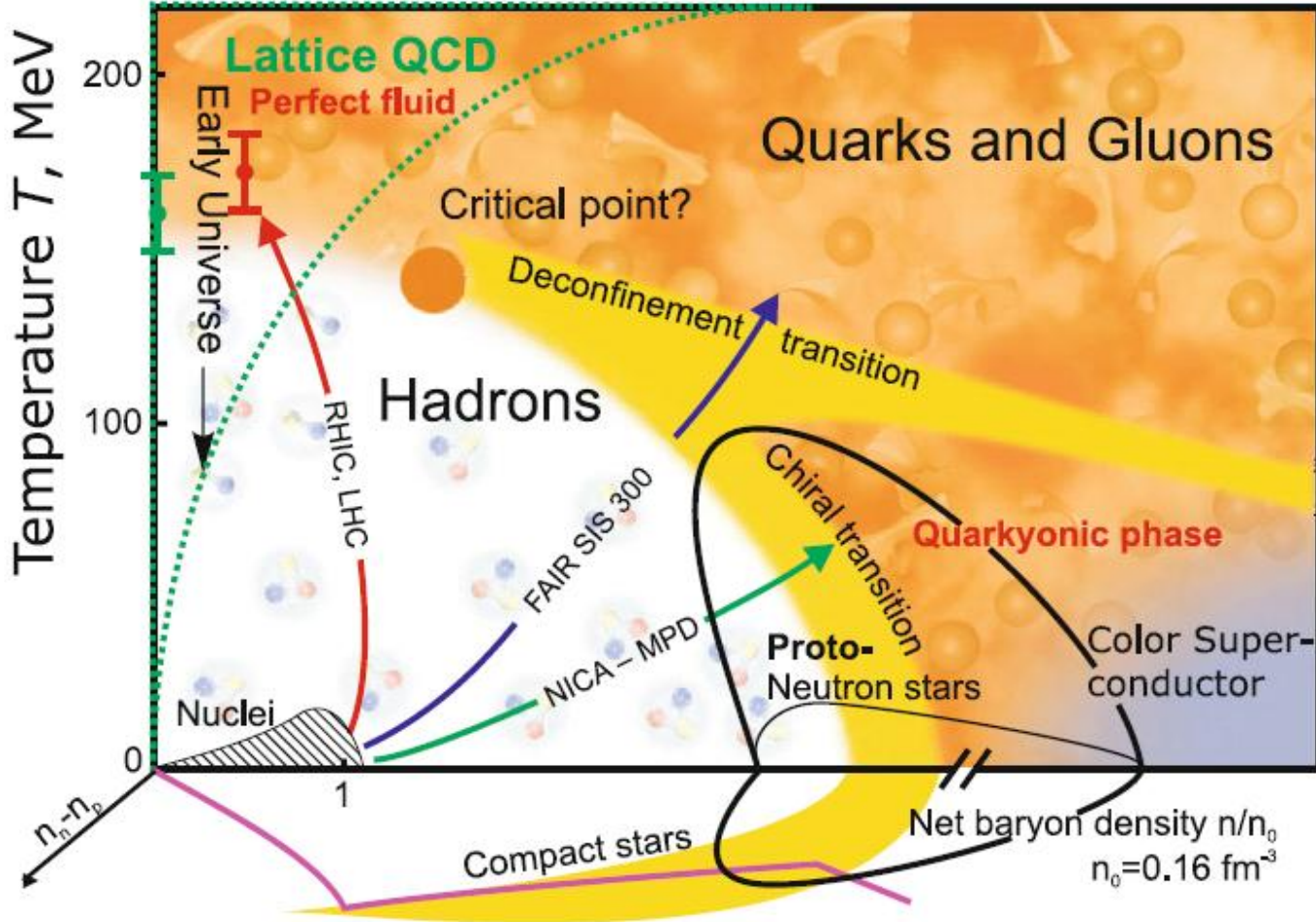
A and Z
(超重元素):
SHE
(Super-Heavy
Elements)
.....



强相互作用物质相图

QCD Phase Diagram in 3D: density, temperature, and isospin

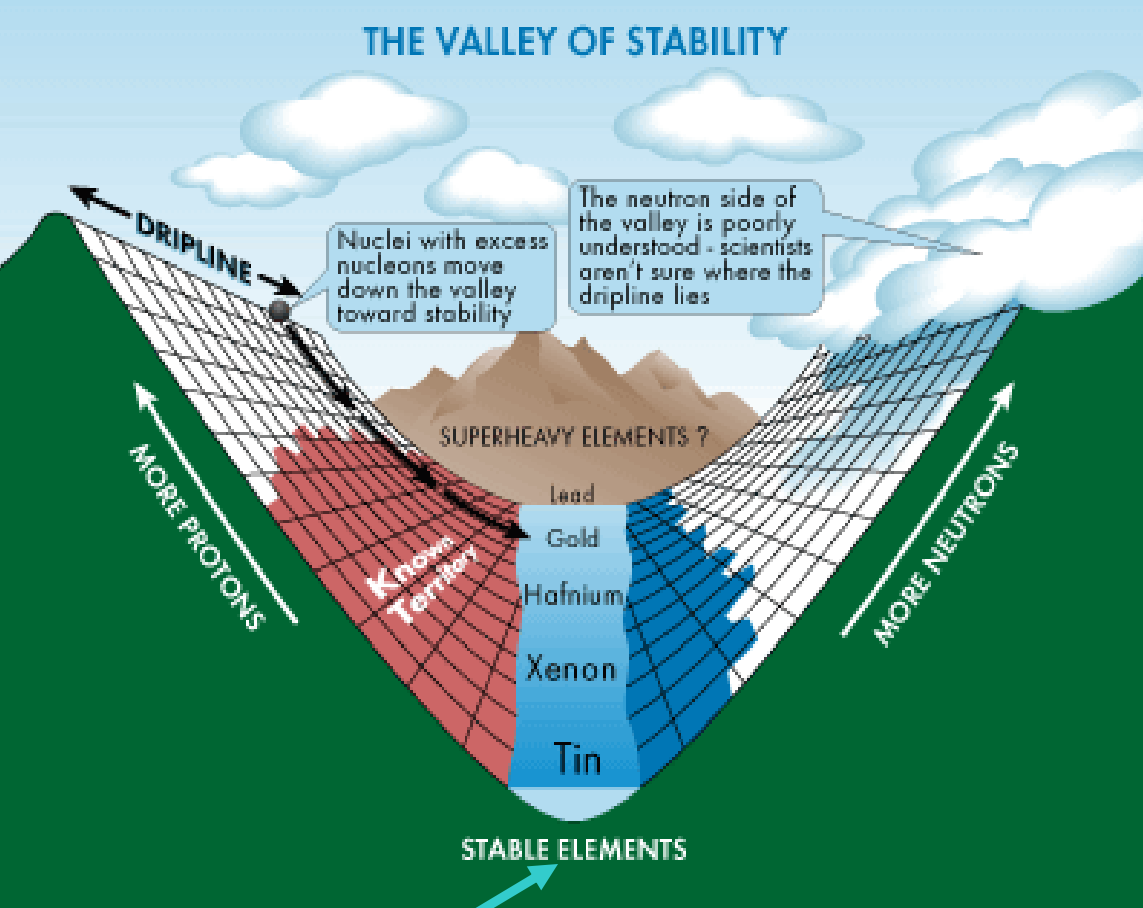
V.E. Fortov, *Extreme States of Matter – on Earth and in the Cosmos*, Springer-Verlag Berlin Heidelberg 2011



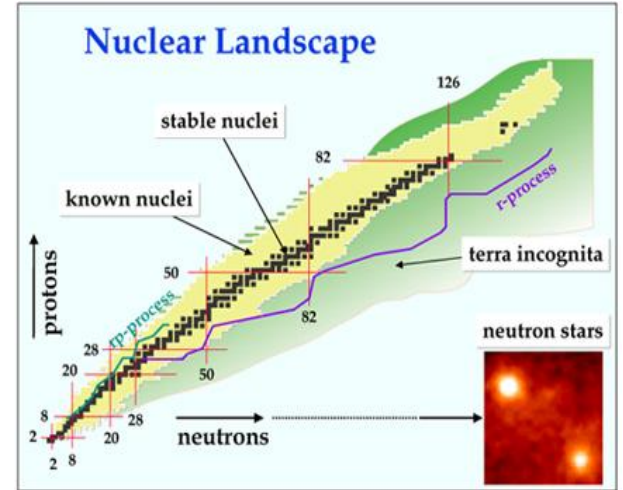


极端同位旋核物理

THE VALLEY OF STABILITY



Very small isospin asymmetry



Studied extensively

$$E(\rho_n, \rho_p)$$

Symmetric matter
 $\rho_n = \rho_p$

density

$$\rho = \rho_n + \rho_p$$

???

A new dimension

Isospin asymmetry $\delta = (\rho_n - \rho_p) / \rho$



超重核的合成

<http://www.webelements.com/>

Periodic Table

Og-118: PRC 74, 044602 (2006)

Ts -117: PRL 104, 142502 (2010)

1 H																	2 He
3 Li	4 Be											5 B	6 C	7 N	8 O	9 F	10 Ne
11 Na	12 Mg											13 Al	14 Si	15 P	16 S	17 Cl	18 Ar
19 K	20 Ca	21 Sc	22 Ti	23 V	24 Cr	25 Mn	26 Fe	27 Co	28 Ni	29 Cu	30 Zn	31 Ga	32 Ge	33 As	34 Se	35 Br	36 Kr
37 Rb	38 Sr	39 Y	40 Zr	41 Nb	42 Mo	43 Tc	44 Ru	45 Rh	46 Pd	47 Ag	48 Cd	49 In	50 Sn	51 Sb	52 Te	53 I	54 Xe
55 Cs	56 Ba	57 La	72 Hf	73 Ta	74 W	75 Re	76 Os	77 Ir	78 Pt	79 Au	80 Hg	81 Tl	82 Pb	83 Bi	84 Po	85 At	86 Rn
87 Fr	88 Ra	89 Ac	104 Rf	105 Db	106 Sg	107 Bh	108 Hs	109 Mt	110 Uun	111 Ds	112 Rg	113 Cn	114 Nh	115 Mc	116 Lv	117 Ts	118 Og

58 Ce	59 Pr	60 Nd	61 Pm	62 Sm	63 Eu	64 Gd	65 Tb	66 Dy	67 Ho	68 Er	69 Tm	70 Yb	71 Lu
90 Th	91 Pa	92 U	93 Np	94 Pu	95 Am	96 Cm	97 Bk	98 Cf	99 Es	100 Fm	101 Md	102 No	103 Lr

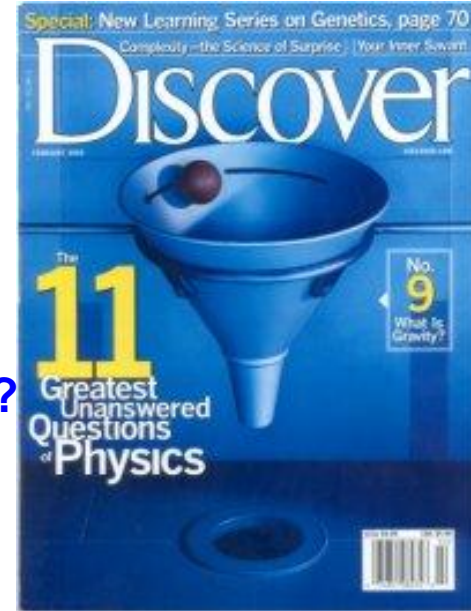
原子序数	英文名称	中文名称	符号
113	nihonium	鉈	Nh
115	moscovium	镆	Mc
117	tennessine	砷	Ts
118	oganesson	气	Og

新造字“砷 (tián)”和“气 (ào)”得到国家语言文字工作委员会同意，纳入国家规范用字。



本世纪11个最重要的物理问题 (美国《发现》2002)

1. What is dark matter
2. What is dark energy
3. How were the heavy elements from iron to uranium made?
从铁到铀等重元素是如何形成的? -高同位旋、高密度
4. Do neutrinos have mass?
5. Where do ultrahigh-energy particles come from?
6. Is a new theory of light and matter needed to explain what happens at very high energies and temperatures?
7. Are there new states of matter at ultrahigh temperatures and densities?
极端高温、高密条件下会出现新物态吗? -高温、高密度
8. Are protons unstable?
9. What is gravity?
10. Are there extra dimensions?
11. How did the universe begin?





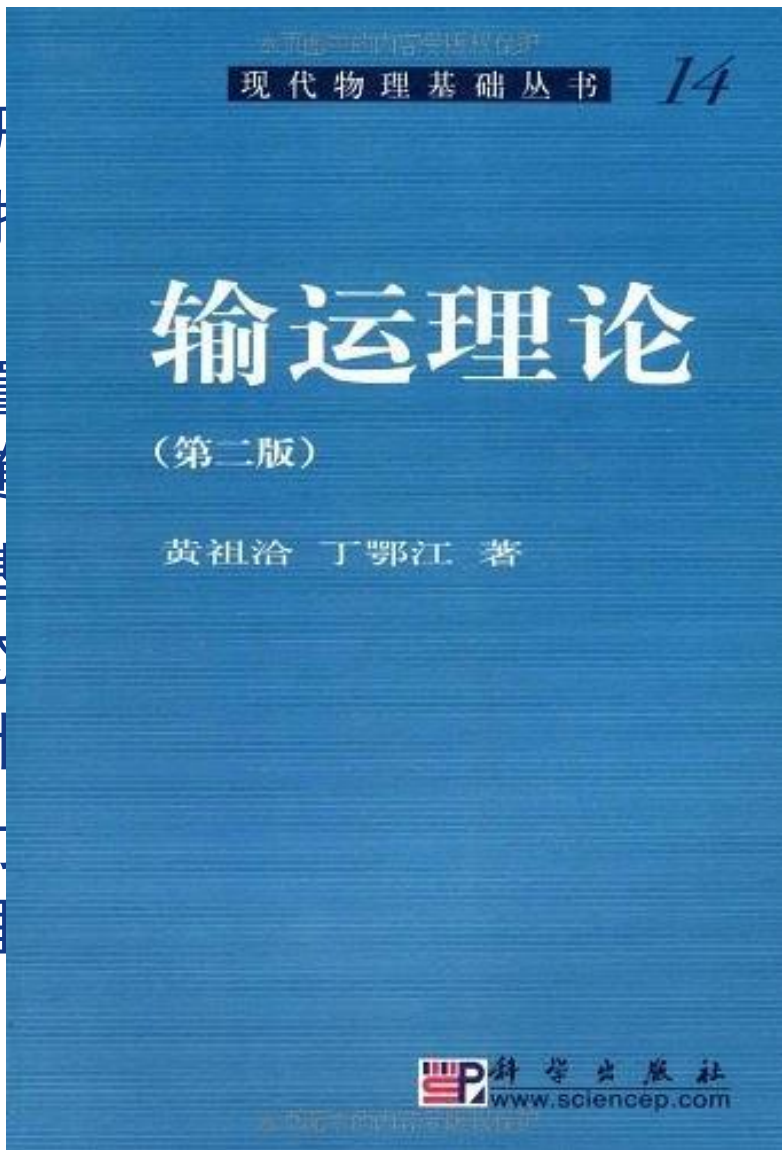
二、中能重离子碰撞微观输运理论模型

- 输运理论的基本概念
- 中能重离子碰撞输运模型
- BUU和QMD的数值实现



什么是输运理论？

- ① 输运理论是研
量粒子(或可
市中的居民,
于各粒子位置
有关物理量随
- ② 输运理论的基
态和非平衡态
非平衡态统计
- ③ 平衡态统计力
统计力学的理



运过程是当大
道中的车辆、城
质中运动时，由
而引起的各种

内容包括平衡
究的问题属于

，而非平衡态



什么是输运理论？

非平衡态统计力学研究方法

- 运动论方法，又称动理论(kinetics)：是从微观动力学出发，通过单粒子分布函数来讨论系统的宏观性质的理论。单粒子分布函数所满足的方程称为运动论方程，又称输运方程。于是输运理论是运动论的一部分，而运动论是非平衡态统计力学的一种重要研究方法。
- 线性响应理论方法：R. Kubo, *Lectures in Theoretical Physics (Boulder)* Vol. I(1958) p. 120; R. Zwanzig, *Ann. Rev. Phys. Chem.* 16(1965), 67.
- 闭合时间路径Green函数方法：Schwinger, Keldysh et al. See, e.g., K.C. Chou(周光召), Z.B. Su(苏肇冰), B.L. Hao(郝柏林), L. Yu(于渌), *Phys. Rep.* 118, 1-131 (1985))
- 耗散结构理论方法：Prigogine et al., 主要用于开放的非线性非平衡系统 (See, e.g., G. Nicolis and I. Prigogine, "*Self-organization in nonequilibrium systems*", Wiley, (1977).)



非平衡态统计力学三种不同层次的描述

- ① 微观层次的描述
- ② 运动论层次的描述
- ③ 流体动力学层次的描述

运动论层次的描述是通过单粒子分布函数来描述系统状态的一种方式。有比运动论更为详细的描述方式，即**微观层次**的描述。也有比运动论描述更为简化的方式，即**流体动力学层次**的描述。

在具体应用中选择哪一层次的描述，主要取决于所研究现象的类型。比如研究流动过程，流体动力学层次就足够了。研究粒子在某些介质中的迁移或散射，就要用到运动论层次的描述。研究激光与等离子体的散射等超短波长的高频行为时，就要用到微观层次的描述。



微观层次的描述

考虑由 N 个粒子所组成的系统。如果这是一个经典系统，那么原则上允许同时确定每个粒子的坐标和动量。所以，三维空间中的 N 粒子系统需要有 $6N$ 个变量来描述，其中 $3N$ 个变量 q_1, q_2, \dots, q_{3N} 描述每个粒子的坐标，另外 $3N$ 个变量 p_1, p_2, \dots, p_{3N} 描述每个粒子的动量。描述系统某一时刻状态的 $6N$ 个变量 $\{q_r, p_r\}$, ($r = 1, 2, \dots, 3N$)，可以看成某 $6N$ 维空间中某个点的坐标。我们称这个 $6N$ 维空间为**(系统的)相空间**，称这个点为系统的代表点，它代表了系统在该时刻的微观态。随着时间的推移，系



微观层次的描述

统的微观态发生变化,相应地在 $6N$ 维相空间中的代表点发生移动,形成一条轨迹. 我们用 Γ_N 表示相空间中的代表点:

$$\Gamma_N = \{q_r, p_r; r = 1, 2, \dots, 3N\};$$

假定系统的 Hamilton 量是

$$H = H(\Gamma_N).$$

那么,代表点的轨迹将由运动方程:

$$\begin{cases} \dot{p}_r = -\frac{\partial H}{\partial q_r}, \\ \dot{q}_r = \frac{\partial H}{\partial p_r}, \end{cases} \quad r = 1, 2, \dots, 3N. \quad (1.2.1)$$

来决定. 这里圆点表示对时间的微商.



微观层次的描述

统计力学所讨论的系统是由大量粒子组成的。我们事实上无法弄清一个代表点的轨迹。因此，J. W. Gibbs 提出了**系综**的概念。设想相空间中有一群代表点，它们代表着不同的微观态。引入**系综分布函数** $\rho = \rho(\Gamma_N, t)$ ，使得当代表点总数为 \mathcal{N} 时， $\mathcal{N}\rho(\Gamma_N, t)d\Gamma_N$ 表示 t 时刻在相空间 Γ_N 点附近体积元 $d\Gamma_N$ 中的代表点数。这里要求 \mathcal{N} 充分大，否则 ρ 就没有意义。此外， $d\Gamma_N$ 既要足够大以保证其中有相当数目的代表点，又要足够小以保证其中代表点的分布大致均匀。这样的体积元称为‘**物理上无穷小**’，而不是严格数学意义上的无穷小。由 $\rho(\Gamma_N, t)$ 的定义马上得出归一化条件：

$$\int d\Gamma_N \rho(\Gamma_N, t) = 1. \quad (1.2.2)$$



微观层次的描述

可以证明系综分布函数满足
$$\frac{\partial \rho}{\partial t} + \sum_{r=1}^{3N} \left(\frac{\partial \rho}{\partial q_r} \dot{q}_r + \frac{\partial \rho}{\partial p_r} \dot{p}_r \right) = 0. \quad (1.2.4)$$

这就是 **Liouville 方程**。利用(1.2.1)式及 **Poisson 括号**

$$\{H, \rho\} \equiv \sum_{r=1}^{3N} \left(\frac{\partial H}{\partial q_r} \frac{\partial \rho}{\partial p_r} - \frac{\partial H}{\partial p_r} \frac{\partial \rho}{\partial q_r} \right),$$

可以把(1.2.4)式改写成

$$\frac{\partial \rho}{\partial t} = \{H, \rho\}. \quad (1.2.5)$$

注意到 $\rho = \rho(\Gamma_N, t)$ ，可以看出(1.2.4)式左边就是跟随代表点运动时所观察到的 ρ 的变化率。将这个变化率记为 $D\rho/Dt$ ，于是 Liouville 方程也可以写成

$$\frac{D\rho}{Dt} = 0. \quad (1.2.6)$$

该方程说明，跟随代表点运动时所观察到的 ρ 是固定不变的。换句话说，如果考虑一个包含代表点并随之一起运动的小体积元，那么这小体积元的体积是不随时间变化的。这就是 Liouville 方程所表示的、相空间体积守恒的性质。



微观层次的描述

我们对一个**动力学变量**(以下简称**物理量**) A 的测量不是瞬时完成的。测量总要持续一段时间, 因此测量的结果实际上是时间平均值:

$$\langle A(t) \rangle_{\text{时间}} = \frac{1}{T} \int_{-\frac{T}{2}}^{\frac{T}{2}} dt' A(\Gamma_N(t+t')), \quad (1.2.11)$$

其中 T 是测量持续时间。系统的微观态变化是很快的, 例如气体中分子以很高的速度运动, 分子之间十分频繁地发生碰撞, 都使系统的微观态发生改变。但是, 系统的宏观态(例如气体的体积、局域温度、局域密度等等)明显变化所需要的时间却比微观态变化所需的时间长得多。(1.2.11)式中所取的时间间隔 T 在微观意义上很长, 而在宏观意义上却是极短暂的。只要 T 的大小属于这一范围, $\langle A(t) \rangle_{\text{时间}}$ 实际上就与 T 无关。如(1.2.11)式中取时间平均之后, 抹去了系统微观态剧烈变化所造成的物理量的快速涨落, 但仍保留了宏观态的较慢变化所对应的物理量随时间的演变。



Gibbs: 时间平均等于系综平均

微观层次的描述

然而, (1.2.11) 式并未真正解决如何计算物理量测量的结果这一问题, 因为我们无法计算代表点 Γ_N 的轨道. Gibbs 又假定: 一系统状态的时间平均 $\langle A(t) \rangle_{\text{时间}}$ 就等于系综平均 $\langle A(t) \rangle$:

$$\langle A(t) \rangle \equiv \int d\Gamma_N \rho(\Gamma_N, t) A(\Gamma_N) = \langle A(t) \rangle_{\text{时间}} \quad (1.2.12)$$

Gibbs 关于时间平均等于系综平均的假定并不是明显成立的, 因此, 这一假定引起了许多讨论. 本书不拟讨论这一假设成立的根据, 而是简单地承认这一假定. 这里只是指出, 对于平衡态, 物理量的测量值不再随时间改变, 因此 T 也可以任意长; 与此同时, ρ 也不随时间改变. 这时, (1.2.12) 式可以改写成

$$\int d\Gamma_N \rho(\Gamma_N) A(\Gamma_N) = \lim_{T \rightarrow \infty} \frac{1}{T} \int_0^T dt A(\Gamma_N(t)). \quad (1.2.15)$$

这个式子的右边是时间平均, 也就是物理量 A 的测量值; 左边是系综平均, 也就是按照先验等几率假设计算出的物理量 A 的平均值. 因此 (1.2.15) 式就是平衡态统计力学中的先验等几率假设. 由此可见, Gibbs 关于系综平均等于时间平均的假设是统计力学的基本假设. 全部统计力学, 不论所研究的是平衡态还是非平衡态, 都建立在这一假设的基础之上.

以上讨论的是经典系统, 对于量子力学系统, 可作相应推广



运动论层次的描述

在许多物理问题中，我们感兴趣的物理量 $A(\Gamma_N)$ 可能具有比较简单的形式。它可能只与单个粒子的广义坐标及动量有关，如

$$A(\Gamma_N) = A(\mathbf{q}_j, \mathbf{p}_j), \quad 1 \leq j \leq N \quad (1.3.1)$$

或

$$A(\Gamma_N) = \sum_{j=1}^N A(\mathbf{q}_j, \mathbf{p}_j). \quad (1.3.2)$$

例如由 N 个同样粒子所组成系统的总动能就是每个粒子的动能之和。对于这种较简单形式的物理量，求系综平均时，有可能简化手续。对于(1.3.1)式，有

$$\begin{aligned} \langle A(t) \rangle &= \int d\Gamma_N \rho(\Gamma_N, t) A(\mathbf{q}_j, \mathbf{p}_j) \\ &= \int d\mathbf{q}_j d\mathbf{p}_j \left[\int d\Gamma_{N-1} \rho(\Gamma_N, t) \right] A(\mathbf{q}_j, \mathbf{p}_j), \end{aligned}$$

这里

$$\int d\Gamma_{N-1} \cdots$$

表示对除第 j 个粒子以外的其他 $N-1$ 个粒子的广义坐标及动量积分。记

$$f(\mathbf{q}_j, \mathbf{p}_j, t) = \int d\Gamma_{N-1} \rho(\Gamma_N, t). \quad (1.3.3)$$



运动论层次的描述

若 $\rho(\Gamma_N, t)$ 对于 N 个粒子为对称(在我们所考虑的、由 N 个同样粒子组成系统的情形下, 这条件显然是成立的), 则(1.3.3)式中函数 f 的形式与 i 无关. 于是有

$$\langle A(t) \rangle = \int d\mathbf{q} d\mathbf{p} f(\mathbf{q}, \mathbf{p}, t) A(\mathbf{q}, \mathbf{p}). \quad (1.3.4)$$

我们省略了 $\mathbf{q}_i, \mathbf{p}_i$ 的下标 i , 因为 $\mathbf{q}_i, \mathbf{p}_i$ 都是积分变量. $f(\mathbf{q}, \mathbf{p}, t)$ 称为**单粒子分布函数**.

对于(1.3.2)式, 由于每个粒子在系统中的地位都是平等的, 故有

$$\begin{aligned} \langle A(t) \rangle &= \int d\Gamma_N \rho(\Gamma_N, t) \sum_i A(\mathbf{q}_i, \mathbf{p}_i) \\ &= N \int d\mathbf{q} d\mathbf{p} f(\mathbf{q}, \mathbf{p}, t) A(\mathbf{q}, \mathbf{p}). \end{aligned} \quad (1.3.5)$$

在这些情形下, 可以把系统相空间中的分布函数约化为单粒子分布函数来讨论系综平均. 用 \mathbf{q} 和 \mathbf{p} 的六个分量作独立变量所构成的空间称为**粒子相空间**.



运动论层次的描述

考虑粒子相空间的**密度算子**

$$\hat{n}(\mathbf{r}, \mathbf{p}, t) = \sum_{j=1}^N \delta(\mathbf{r} - \mathbf{q}_j(t)) \delta(\mathbf{p} - \mathbf{p}_j(t)), \quad (1.3.6)$$

这里 $\mathbf{q}_j(t)$ 与 $\mathbf{p}_j(t)$ 分别是 t 时刻第 j 个粒子的坐标和动量。粒子相空间密度算子的系综平均值就是粒子相空间的**密度分布函数**：

$$\begin{aligned} n(\mathbf{r}, \mathbf{p}, t) &\equiv \langle \hat{n}(\mathbf{r}, \mathbf{p}, t) \rangle \\ &= N \int d\mathbf{q}_j d\mathbf{p}_j \delta(\mathbf{r} - \mathbf{q}_j(t)) \delta(\mathbf{p} - \mathbf{p}_j(t)) f(\mathbf{q}_j, \mathbf{p}_j, t) \\ &= N f(\mathbf{r}, \mathbf{p}, t), \end{aligned} \quad (1.3.7)$$

其中用到(1.3.5)式。因此

$$f(\mathbf{r}, \mathbf{p}, t) = \frac{1}{N} n(\mathbf{r}, \mathbf{p}, t). \quad (1.3.8)$$

由 $n(\mathbf{r}, \mathbf{p}, t)$ 的定义可以知道, $n(\mathbf{r}, \mathbf{p}, t) d\mathbf{r} d\mathbf{p}$ 表示 t 时刻在 \mathbf{r} 附近 $d\mathbf{r}$ 中而动量在 \mathbf{p} 附近 $d\mathbf{p}$ 中的粒子数期望值, 因此 $f(\mathbf{r}, \mathbf{p},$



运动论层次的描述

$t)drdp$ 表示 t 时刻相应粒子出现的几率，由(1.2.2)式及(1.3.3)式知道， $f(\mathbf{r}, \mathbf{p}, t)$ 是归一化了的：

$$\int drdp f(\mathbf{r}, \mathbf{p}, t) = 1. \quad (1.3.9)$$

利用(1.3.8)及(1.3.9)式，立即得到

$$\int drdp n(\mathbf{r}, \mathbf{p}, t) = N. \quad (1.3.10)$$

有时，为方便起见，可用粒子速度 \mathbf{v} 代替动量 $\mathbf{p} = m\mathbf{v}$ 作自变量。这时应要求

$$f(\mathbf{r}, \mathbf{p}, t)d\mathbf{p} = f(\mathbf{r}, m\mathbf{v}, t)m d\mathbf{v} = \tilde{f}(\mathbf{r}, \mathbf{v}, t)d\mathbf{v},$$

其中 \tilde{f} 表示一个和 f 不同的函数。以下为了简单，去掉 \tilde{f} 上的 \sim 号。于是 $f(\mathbf{r}, \mathbf{p}, t)d\mathbf{p}$ 将直接改写为 $f(\mathbf{r}, \mathbf{v}, t)d\mathbf{v}$ 。将 $n(\mathbf{r}, \mathbf{p}, t)d\mathbf{p}$ 改写为 $n(\mathbf{r}, \mathbf{v}, t)d\mathbf{v}$ 时，也应如此理解。

$f(\mathbf{r}, \mathbf{v}, t)$ 或 $n(\mathbf{r}, \mathbf{v}, t)$ 所满足的方程称为 **输运方程或运动论方程**。为实现在运动论层次上的描述，一方面必须导出输运方程，另一方面还要说明输运方程适用的条件。



流体动力学层次的描述

微观层次的描述方式适合于讨论 $6N$ 维(系统)相空间中的分布函数 $\rho(\Gamma_N, t)$, 而运动论层次的描述方式适合于讨论 6 维(粒子)相空间中的分布函数 $f(\mathbf{r}, \mathbf{v}, t)$, 这种方式简单得多了. 但是, 在大多数情况下, 运动论层次的描述仍然是相当复杂的, 所以, 还可以考虑进一步简化描述方式. 当然, 随着描述方式的进一步简化, 信息的损失也增多了.

所谓流体动力学层次的描述, 实质上是只讨论单粒子分布函数 $f(\mathbf{r}, \mathbf{v}, t)$ 的前三次矩:

$$f_0(\mathbf{r}, t) = \int d\mathbf{v} f(\mathbf{r}, \mathbf{v}, t), \quad (1.4.1)$$

$$\mathbf{f}_1(\mathbf{r}, t) = \int d\mathbf{v} \mathbf{v} f(\mathbf{r}, \mathbf{v}, t), \quad (1.4.2)$$

$$f_2(\mathbf{r}, t) = \int d\mathbf{v} v^2 f(\mathbf{r}, \mathbf{v}, t). \quad (1.4.3)$$

它们分别称为单粒子分布函数的零次矩、一次矩和二次矩. 以下可见, 它们分别和流体的密度、速度和能量密度密切相关.



流体动力学层次的描述

考虑粒子数密度算子

$$\hat{N}(\mathbf{r}, t) = \sum_{j=1}^N \delta(\mathbf{r} - \mathbf{q}_j(t)). \quad (1.4.4)$$

它的系综平均值 $N(\mathbf{r}, t)$ 称为粒子数密度分布函数。由(1.3.5)式,将自变量 \mathbf{p} 换成 \mathbf{v} 后,求得

$$\begin{aligned} N(\mathbf{r}, t) &= \langle \hat{N}(\mathbf{r}, t) \rangle \\ &= N \int d\mathbf{q} d\mathbf{v} f(\mathbf{q}, \mathbf{v}, t) \delta(\mathbf{r} - \mathbf{q}(t)) \\ &= N \int d\mathbf{v} f(\mathbf{r}, \mathbf{v}, t) = \int d\mathbf{v} n(\mathbf{r}, \mathbf{v}, t), \end{aligned} \quad (1.4.4a)$$

最后一步利用了(1.3.8)式,和(1.4.1)式对比,得

$$N(\mathbf{r}, t) = N f_0(\mathbf{r}, t),$$

或

$$f_0(\mathbf{r}, t) = \frac{1}{N} N(\mathbf{r}, t). \quad (1.4.5)$$

由定义知, $N(\mathbf{r}, t)d\mathbf{r}$ 表示 t 时刻在 \mathbf{r} 附近 $d\mathbf{r}$ 中的粒子数期望值,因此 $f_0(\mathbf{r}, t)d\mathbf{r}$ 表示 t 时刻在 \mathbf{r} 附近 $d\mathbf{r}$ 中粒子出现的几率。这当然和 $f_0(\mathbf{r}, t)$ 的定义(1.4.1)式所表达的意义是一致的。



流体动力学层次的描述

流体中 t 时刻 \mathbf{r} 附近的**宏观流速** $\mathbf{c} = \mathbf{c}(\mathbf{r}, t)$ 等于该时该处的粒子平均速度:

$$\begin{aligned}\mathbf{c} = \mathbf{c}(\mathbf{r}, t) &= \frac{\int \mathbf{v} f(\mathbf{r}, \mathbf{v}, t) d\mathbf{v}}{\int f(\mathbf{r}, \mathbf{v}, t) d\mathbf{v}} \\ &= \frac{\mathbf{f}_1(\mathbf{r}, t)}{f_0(\mathbf{r}, t)}.\end{aligned}\quad (1.4.7)$$

而 t 时刻 \mathbf{r} 附近单位质量流体所具有的**内能**为

$$\begin{aligned}U = U(\mathbf{r}, t) &= \frac{\int d\mathbf{v} \frac{m}{2} (\mathbf{v} - \mathbf{c})^2 f(\mathbf{r}, \mathbf{v}, t)}{\int d\mathbf{v} m f(\mathbf{r}, \mathbf{v}, t)} \\ &= \frac{1}{2} [f_2(\mathbf{r}, t) - 2\mathbf{c} \cdot \mathbf{f}_1(\mathbf{r}, t) \\ &\quad + c^2 f_0(\mathbf{r}, t)] / f(\mathbf{r}, t).\end{aligned}\quad (1.4.8)$$

U 也称为**比内能**。(1.4.6)–(1.4.8)式将单粒子分布函数的前三次矩与流体力学中的基本物理量联系起来。

依描述对象的不同,前三次矩或流体力学量所满足的方程也有所不同。



二、中能重离子碰撞微观输运理论模型

- 输运理论的基本概念
- 中能重离子碰撞输运模型
- BUU和QMD的数值实现



中能重离子碰撞大概可以划分为以下四个阶段

- ① **初始阶段**：炮弹核被加速到一定的入射能量，靶核和炮弹核都处于基态，它们的性质是已知的。
- ② **压缩阶段**：靶核和炮弹核相互作用，在碰撞中心区域形成高温高密核物质，其密度可达到2-3倍 ρ_0 (ρ_0 为对称核物质饱和密度)。这一阶段核物质的性质显然是人们希望知道的。
- ③ **碰撞阶段**：被压缩的核物质向外扩展，核物质密度下降到低于 ρ_0 ，核物质中产生小质量的集团，可能发生液-气相变和多重碎裂(Multifragmentation)。这一阶段的性质也是人们感兴趣的。
- ④ **实验可观测阶段**：实验上可测量核子、核子集团以及其它强子的角分布、能谱等。



中能重离子碰撞微观运输理论模型的意义

问题：

人们感兴趣的压缩 / 膨胀阶段只是整个重离子碰撞过程中寿命很短的中间阶段(intermediate stage)，实验上无法直接观察和分析这些中间阶段核物质的性质。

微观运输理论的作用：

因此人们需要一种理论方法，即微观运输理论(transport theory)，用这种方法人们可以追踪重离子碰撞的动力学演化，从其初始阶段经过人们感兴趣的中间阶段，一直到最后的实验可观察阶段。这样人们可以从已知的初始条件及可观察和测量的末态性质推断出人们感兴趣的中间阶段核物质的性质，从而获得在广泛的密度和温度范围内核物质的状态方程。



中能重离子碰撞微观理论模型

- ① 重离子碰撞是一个非常复杂的过程。不同能区的重离子碰撞有各自不同的特点，寻找一个恰当和合理的描述重离子碰撞动力学演化的微观理论是重离子碰撞理论研究的重要课题
- ② 低能重离子碰撞：以通过单体耗散(one-body dissipation)由非平衡态向平衡态过渡为主要特点，平均场和泡利原理(Pauli blocking)在起主要的作用，由于泡利原理的限制，两体碰撞(two-body collision)基本上可忽略不计。时间相关的Hartree-Fock (TDHF)以及其半经典近似下的Vlasov方程是研究低能重离子碰撞的主要微观理论。有关的计算表明，对于许多实验可观察量，TDHF方程(量子)和Vlasov方程(半经典)给出基本一致的结果。



中能重离子碰撞微观理论模型

- ① **高能重离子碰撞**：由于相空间(phase space)的增大，Pauli阻塞效应明显减弱，两体碰撞起主导作用。平均场和Pauli原理可以被忽略。研究这一能区重离子碰撞动力学演化的主要理论方法有级联模型(cascade model)及核内级联模型(intranuclear cascade model)
- ② **中能区重离子碰撞**：兼有低能区和高能区特征的交叉区，是**平均场**，**Pauli阻塞效应**及**两体碰撞**多个因素交织作用的过程，因此也是研究核多体系统非平衡动力学行为的有效途径。由于中能重离子碰撞涉及平均场，泡利原理和两体碰撞，任何一个描述其动力学行为的微观理论必须同时包含这三方面的因素，从而导致中能重离子碰撞微观理论的复杂性。



中能重离子碰撞微观理论模型-BUU方程简介

- 对于中能重离子碰撞，一个自然的做法是将核子-核子相互作用分为平均场与残余相互作用两部分(TDHF方程中计入了平均场部分，残余相互作用导致核子间的关联，即两体碰撞)，从而得到推广的时间相关Hartree-Fock(ETDHF)方程。ETDHF方程同时包含了平均场，泡利阻塞效应及两体碰撞，但这一方程比较复杂(它是关于单粒子波函数的时间演化方程)，至今无法严格求解，必须利用相当多的近似，其中比较成功的是弛豫时间方法(relaxation time method)，即对ETDHF方程中的碰撞积分(Collision integral)作弛豫时间近似(类似于求解经典Boltzmann方程所作的弛豫时间近似)。
- 正如对TDHF方程作半经典近似可以得到Vlasov方程一样，对ETDHF方程通常也采用半经典近似,以期在数值计算方面得到一定的简化。其结果就是在中能重离子反应中用得非常广泛和成功的Boltzmann-Uehling-Uhlenbeck(BUU)方程，这一方程也被称为Vlasov-Uehling-Uhlenbeck(VUU)方程，Boltzmann-Nordheim方程以及Landau-Vlasov方程。



中能重离子碰撞微观理论模型-BUU方程简介

- BUU方程描述的是单体相空间分布函数的时间演化，它恰当地包含了中能重离子反应机制的三个要素：平均场、泡利原理和两体碰撞。
- 当平均场占优势时，BUU方程约化为Vlasov方程，即半经典近似下的TDHF方程，
- 当平均场和两体碰撞相竞争时，BUU方程是ETDHF方程的半经典形式。
- 如果仅考虑两体碰撞，BUU方程等价于级联模型。
- 自从十九世纪Boltzmann提出玻尔兹曼方程来研究非平衡态物理问题后，二十世纪二、三十年代，首先是Nordheim，然后是Uehling和Uhlenbech将Pauli不相容原理引入玻尔兹曼方程而得到BUU方程。多年来已有一些作者或从统计学基本原理，或从量子力学方程出发来推导BUU方程。一些流行的推导主要利用非平衡态Green函数技术或量子多体关联动力学方法。



中能重离子碰撞微观理论模型-BUU方程简介

- 在实际应用中人们并不直接求解BUU方程，而是将平均场部分和两体碰撞部分分开处理。实际求解的是与Vlasov方程等价的Hamilton运动方程，而两体碰撞则是在演化过程中人为加入的。
- 由于把核子看作点粒子，在用Skyrme力作为核子-核子相互作用时，Vlasov方程中用到的核子平均场出现非常大的涨落(fluctuation)。为了避免这一困难，人们在数值求解BUU方程(或Hamilton运动方程时)引入了试验粒子(test particle)的概念。通过引入试验粒子人们可以得到在坐标空间平缓变化的平均场，但同时核子间的关联被平均掉了。BUU方程只能用于描述单体可观察量而无法研究多体关联可观察量，特别是无法用于处理中能重离子反应过程中十分重要的集团形成(Cluster formation)及多重碎裂(multi-fragmentation)现象。因为这些现象实际上反映了低密度核系统中存在的强的核子关联及大的物理的平均场涨落(不同于由于点粒子所引入的非物理的平均场涨落)。



中能重离子碰撞微观理论模型-QMD模型简介

- 为了既能得到平缓变化的平均场又能描述象多重碎裂这样涉及多体关联的物理现象，人们提出了量子分子动力学(QMD)模型。如果忽略量子效应(泡利阻塞)，QMD方法退化为经典物理中常用的分子动力学方法(molecular dynamics)。QMD模型中核子不再被看作点粒子而被看作是坐标空间及动量空间具有有限宽度的高斯波包(Gaussian packet)。由于它不必引入试验粒子就能得到平缓变化的平均场，因而它包含了核子间的关联及平均场的物理涨落。QMD已被成功地用于描述多重碎裂现象。
- BUU和QMD**是目前主要的研究中能重离子碰撞的微观理论。平均场和两体碰撞反映了核子-核子相互作用的两个方面。平均场考虑的是核子-核子相互作用中的中程部分，两体碰撞即反映了核子-核子相互作用的短程排斥行为。这两个物理量(平均场及反映核子-核子碰撞的散射截面)决定了BUU和QMD的动力学行为。



BUU方程的推导

在非相对论极限下,核多体系统的动力学演化是由关于A-体密度矩阵 ρ_A 的 *Neumann* 方程所决定的:

$$i \frac{\partial \rho_A}{\partial t} = [H_A, \rho_A] \quad (2.1)$$

在只限于两体核子-核子相互作用 v_{ij} 的情况下, A体哈密顿量 H_A 可表示为:

$$H_A = \sum_{i=1}^A t(i) + \sum_{i<j} v_{ij} \quad (2.2)$$

其中 t_i 是第*i*个粒子的动能,引入*n*阶($n \leq A$)约化密度矩阵 ρ_n ,

$$\rho_n = 1/(A-n)! \text{Tr}_{(n+1, \dots, A)} \{ \rho_A \} \quad (2.3)$$

*Neumann*方程(2.1)式等价于一组关于 ρ_n 的耦合方程:

$$i \frac{\partial \rho_n}{\partial t} = \left[\sum_{i=1}^n t_i, \rho_n \right] + \left[\sum_{i=j}^{n-1} v_{ij}, \rho_n \right] + \text{Tr}_{(n+1)} \left[\sum_{i=1}^n v_{i, n+1}, \rho_{n+1} \right] \quad (2.4)$$



BUU方程的推导

特别地如果引入由下式定义的两体关联函数 $C_2(ij, i' j')$,

$$C_2(ij, i' j') = \rho_2(ij, i' j') - \rho_{20}(ij, i' j') \quad (2.5)$$

$$\begin{aligned} \rho_{20}(ij, i' j') &= \rho(ii')\rho(jj') - \rho(ij')\rho(ji') \\ &= \mathcal{A}_{ij} \rho(ii')\rho(jj') \end{aligned} \quad (2.6)$$

其中 \mathcal{A}_{ij} 是由置换算符 P_{ij} 定义的费米子反对称化算符:

$$\mathcal{A}_{ij} = 1 - P_{ij}$$

我们可以得到关于单体密度矩阵 $\rho(ii', t)$ 及两体关联函数 $C_2(ij, i' j', t)$ 的方程:

$$\begin{aligned} \dot{\rho}(ii', t) &= [t(i) + U(i)]\rho(ii', t) - \rho(ii', t)[t(i') + U(i')] \\ &+ \sum_{(j=j')}^{Tr} [v(ij)C_2(ij, i' j', t) - C_2(ij, i' j', t)v(i' j')] \end{aligned} \quad (2.7)$$



BUU方程的推导

$$\begin{aligned}
 i\dot{C}_2(ij, i' j', t) = & [t(i) + t(j) + U(i) + U(j) + Q_{ij}v(ij)]C_2(ij, i' j', t) \\
 & - C_2(ij, i' j', t)[t(i') + t(j') + U(i') + U(j') + v(i' j')Q_{i'j'}] \\
 & + [Q_{ij}v(ij)\rho_{20}(ij, i' j', t) - \rho_{20}(ij, i' j', t)v(i' j')Q_{i'j'}]
 \end{aligned}$$

时间相关的G矩阵理论 (2.8a)

$$\begin{aligned}
 & + \text{Tr}_{(l=l')} [v(il) \delta_{il} \delta_{i'l'} - v(i'l') \delta_{i'l'} \delta_{il}] \\
 & \cdot \rho(i'l', t) C_2(jl, j'l', t)
 \end{aligned}$$

$$\begin{aligned}
 & + \text{Tr}_{(l=l')} [v(jl) \delta_{jl} \delta_{j'l'} - v(j'l') \delta_{j'l'} \delta_{jl}] \\
 & \cdot \rho(jj', t) C_2(il, i'l', t)
 \end{aligned}$$

量子关联动力学 (2.8b)

$$\begin{aligned}
 & + \text{Tr}_{(l=l')} [v(il) + v(jl)] C_3(ijl, i' j' l', t) \\
 & - C_3(ijl, i' j' l', t) [v(i'l') + v(j'l')]
 \end{aligned}$$

三体关联 (2.8c)



BUU方程的推导

其中 $U(i, t)$ Q_{ij} 及 $C_s(ij|l, i' j' l')$ 分别为平均场, 泡利阻塞算符及三体关联函数。 $U(i)$ 和 Q_{ij} 的形式:

$$U(i) = \text{Tr}_{(l=l')} [v(i|l) \rho(l|l', t)] \quad (2.9)$$

$$Q_{ij} = 1 - \text{Tr}_{(l=l')} (P_{ij} + P_{ji}) \rho(l|l', t) \quad (2.10)$$

上述几式中的求迹号 $\text{Tr}_{(l=l')}$ 表明在 $l=l'$ 的情况下对自旋 $\sigma(l)$, 同位旋 $\tau(i)$ 的求和以及对坐标空间的积分。

下面我们将从时间相关 G 矩阵理论出发推导BUU方程。(2.8a)的形式解为:

$$C_2(t) = -\frac{i}{8\pi^2} \iiint d\omega d\omega' dt' \exp[-i(\omega - \omega')(t - t')] \hat{G}_{12}(\omega) [Q_{ij} \rho_{ij}(t') - \rho_{ij}(t') v Q^+] \hat{G}_{12}^+(\omega') \quad (2.11)$$

其中包括残余相互作用的传播子为:

$$\hat{G}_{12}(\omega) = \{\omega - [t(1) + t(2) + U(1) + U(2) + Q_{ij}] + i\epsilon\}^{-1} \quad (2.12)$$



BUU方程的推导

引入算符 Ω_{12} 使得:

$$\hat{G}_{12}(\omega) = \Omega_{12}(\omega) g_{12}(\omega) \quad (2.13)$$

其中平均场传播子为:

$$g_{12}(\omega) = \{\omega - [t(1) + t(2) + U(1) + U(2)] + i\epsilon\}^{-1} \quad (2.14)$$

由此(2.11)式可表示为:

$$\begin{aligned} C_2(t) = & -\frac{i}{8\pi^2} \int \int \int d\omega d\omega' dt' \exp[-i(\omega - \omega')(t - t')] \\ & \cdot \{ [\Omega_{12}(\omega) \rho_{20}(t') g_{12}^+(\omega') - \Omega_{12}(\omega) g_{11}(\omega) \rho_{20}(t') \Omega_{12}^+(\omega')] \\ & - [\rho_{20}(t') \hat{G}_{12}^+(\omega') - \hat{G}_{12}(\omega) \rho_{20}(t')] \} \end{aligned} \quad (2.15)$$

对 $\Omega(\omega)$ 和 $\Omega(\omega')$ 作近似, 完成对 $d\omega$ 的积分, 最后得到

$$\rho_2 = \Omega_{12} \rho_{20} \Omega_{12}^+$$

式:

$$v \rho_2 v^+ = G \rho_{20} G^+ \quad (2.16)$$



BUU方程的推导

(2.16)式将裸相互作用 v 相对于严格二体密度 ρ_2 的矩阵元同有效相互作用 G 相对于非微扰二体密度矩阵 ρ_{20} 的矩阵元相联系，有效相互作用 G 由下式给出，

$$G(E) = v + v g_{12} Q G(E) \quad \text{Bethe-Goldstone Eq.} \quad (2.17)$$

这是一个关于 G 矩阵的自洽迭代积分方程。

利用 G 矩阵的实部定义平均场，

$$[U_{\text{BHF}}, \rho] = \text{Tr}_{(1)} [R_e(G), \rho_{2q}] \quad (2.18)$$

把(2.7)式中涉及二体关联函数的其余部分归结为两体碰撞项，

$$I_2(t) = -i \text{Tr}_{(1)} [i G^+ Q E I_m(g_{12}) \rho_{20} - i \rho_{20} I_{mb}(g_{12}^+) G^+ Q G + G \rho_{20} G^+ Q^+ g_{12}^+ - g_{12} Q G \rho_{20} G^+] \quad (2.19)$$



BUU方程的推导

利用Wigner变换，并对单体相空间分布函数 $f(r, p, t)$ 作核物质近似，对平均场部分作半经典近似，最后得到BUU方程：

$$\begin{aligned}
 & \left(\frac{\partial}{\partial t} + \frac{p_1}{m} \frac{\partial}{\partial r_1} - \frac{\partial}{\partial r_1} U_{\text{BHF}}(r, t) \cdot \frac{\partial}{\partial p_1} \right) f(r_1, p_1, t) \\
 & = \left(-\frac{\partial f}{\partial t} \right)_{\text{Coll}} \\
 & = \frac{4}{(2\pi)^3} \int \int dp_2 dp_3 \int d\Omega |v_{12}| \frac{d\sigma}{d\Omega} (p_2 - p_4) \delta(p_1 + p_2 - p_3 - p_4) \\
 & \quad \times \{ f(r, p_3, t) f(r, p_4, t) [1 - f(r, p_1, t)] [1 - f(r, p_2, t)] \\
 & \quad - f(r, p_1, t) f(r, p_2, t) [1 - f(r, p_3, t)] [1 - f(r, p_4, t)] \}
 \end{aligned} \tag{2.20}$$



BUU方程的推导

其中 $|v_{12}|$ 是碰撞核子的相对速度。时间相关平均场 U_{BHF} 以及介质中核子-核子截面 $\frac{d\sigma}{d\Omega}$ 可由 G 矩阵得到:

$$U_{\text{BHF}}(r, t) = \int dr' R_e G_a(t-r') \rho(r', t) \quad (2.21)$$

$$\frac{d\sigma}{d\Omega} = \frac{m^2}{16\pi^2} G(\mathbf{q}) G_a^+(\mathbf{q}) \quad (2.22)$$

其中 $\rho(r, t)$ 是定域核子密度。 \mathbf{q} 表示核子-核子碰撞过程中的动量转移。(2.20) 式暂时忽略了平均场的动量相关。

若已知BUU方程中的平均场及核子-核子截面, 我们可以求解BUU方程得到相空间分布的时间演化。而平均场和核子-核子截面是由 G 矩阵给出的。所以得首先求解 *Bethe-Goldstone* 方程(2.17)式, 其中涉及裸核子-核子相互作用及系统的组态分布。因此(2.17)和(2.20)构成一个耦合的方程组, 涉及自洽求解的问题。在实际应用中或将 G 矩阵参数化, 或将平均场及核子-核子相互作用参数化, 以求简化数值计算。

QMD方程的“推导” J. Aichelin, Phys. Rep. 202, 233 (1991)

关于QMD的推导文献J. Aichelin, Phys. Rep.202, 233 (1991)有详细的讨论，其基本出发点同样是多体薛定谔方程，约化密度矩阵以及对BBGKY系列的截断，但一开始就引入相空间的概念，即对密度矩阵作富里叶变换得到所谓的Wigner密度(或称Wigner表示)。从而直接将多体薛定谔方程表示为类似于经典输运方程的形式，这里我们给出有关的主要公式。

在QMD中粒子波函数具有下列形式：

$$\phi_i(\mathbf{r}, t) = \frac{1}{(2\pi L)^{3/4}} \exp\left[-\frac{(\mathbf{r} - \mathbf{r}_i)^2}{4L}\right] \cdot \exp\left(\frac{i\mathbf{p}_i \cdot \mathbf{r}}{\hbar}\right) \quad (1)$$

式中 L 是固定的，它相关于相空间中的波包宽度，一般取为 1.08 fm^2 。 $\mathbf{r}_i(t)$ 和 $\mathbf{p}_i(t)$ 分别为坐标空间与动量空间的高斯分布波包中心。整个系统的 n 体波函数取为(1)式的直积，即

$$\Phi(\mathbf{r}, t) = \prod_i \phi_i(\mathbf{r}, \mathbf{r}_i, \mathbf{p}_i, t) \quad (2)$$

注意这里整个系统的 n 体波函数没有取成(1)式所构成的行列式，于是忽略了波函数的反对称化。 **AMD/FMD考虑了波函数的反对称化**



QMD方程的“推导”

相应的密度矩阵的Wigner表示是动量与坐标空间的高斯波包，

$$\begin{aligned} f(\mathbf{r}, \mathbf{p}, t) &= \frac{1}{(2\pi)^3} \int e^{-i\mathbf{p} \cdot \mathbf{r}_{12}} \psi_i \left(\mathbf{r} + \frac{\mathbf{r}_{12}}{2}, t \right) \psi_i^* \left(\mathbf{r} - \frac{\mathbf{r}_{12}}{2}, t \right) d\mathbf{r}_{12} \\ &= \frac{1}{\pi^3} e^{-\frac{(\mathbf{r} - \mathbf{r}_{i0}(t))^2}{2L} - \frac{(\mathbf{p} - \mathbf{p}_{i0}(t))^2}{2L}} \end{aligned} \quad (2.24)$$

QMD认为高斯波包中心 $\mathbf{r}_{i0}(t)$ 和 $\mathbf{p}_{i0}(t)$ 是随时间演化,而其宽度 \sqrt{L} 则是不随时间变化的。因此这不是严格的量子波包。

由(2.24)式可以得到坐标空间和动量空间的单体密度

$$\begin{aligned} \rho(\mathbf{r}, t) &= \int f(\mathbf{r}, \mathbf{p}, t) d\mathbf{p} = \sum_i \frac{1}{(2\pi L)^{3/2}} \exp\left[-\frac{(\mathbf{r} - \mathbf{r}_i)^2}{2L}\right] \\ g(\mathbf{p}, t) &= \int f(\mathbf{r}, \mathbf{p}, t) d\mathbf{r} = \sum_i \left(\frac{2L}{\pi\hbar^2}\right)^{3/2} \exp\left[-\frac{(\mathbf{p} - \mathbf{p}_i)^2 \cdot 2L}{\hbar^2}\right] \end{aligned}$$



QMD方程的“推导”

参数 $r_i(t)$ 和 $p_i(t)$ 的初始值由模型的初始化抽样所决定, 抽样结果要求给出弹核和靶核中的密度分布和动量分布以及弹核和靶核的一些基态性质。有了系统的波函数及初始条件, 我们就可以通过广义变分原理来决定多体系统的演化方程^[21]。Hamiltonian 量 H 可以表示为:

$$H = \sum_i T_i + \frac{1}{2} \sum_{j \neq i} V_{ij} \quad (3)$$

式中 T_i 和 V_{ij} 分别代表动能部分和势能部分。由广义变分原理可得到 $r_i(t)$ 和 $p_i(t)$ 的时间演化方程

$$\dot{r}_i = \frac{p_i}{m} + \nabla_{p_i} \sum_{j \neq i} \langle V_{ij} \rangle = \nabla_{p_i} \langle H \rangle \quad (4)$$

$$\dot{p}_i = - \nabla_{r_i} \sum_{j \neq i} \langle V_{ij} \rangle = - \nabla_{r_i} \langle H \rangle \quad (5)$$

QMD方程的“推导”

以上式子中 $\langle V_{ij} \rangle$ 为

$$\langle V_{ij} \rangle = \int d^3 r_1 d^3 r_2 \phi_1^* \phi_2^* V(\mathbf{r}_1, \mathbf{r}_2) \phi_1 \phi_2 \quad (6)$$

这样变分原理就将核反应系统的 n 体 Schrödinger 方程的时间演化约化成了 $6(A_P + A_T)$ 个参数的时间演化方程 (A_P, A_T 分别为弹、靶核子数)。(4)和(5)式可以进一步写成

$$\dot{\mathbf{r}}_i = \frac{\partial \langle H \rangle}{\partial \mathbf{p}_i} \quad (7)$$

$$\dot{\mathbf{p}}_i = -\frac{\partial \langle H \rangle}{\partial \mathbf{r}_i} \quad (8)$$

可见与经典的 Hamilton 正则方程有相同的形式,参数 $\mathbf{r}_i(t)$ 和 $\mathbf{p}_i(t)$ 分别代表粒子的坐标和动量。



QMD方程的“推导”

在包括两体和三体相互作用的情况下,粒子 i 贡献的 Hamiltonian 量为

$$H_i = T_i + \frac{1}{2} \sum_{j \neq i} U_{ij}^{(2)} + \frac{1}{3} \sum_{j \neq k \neq i} U_{ijk}^{(3)} \quad (13)$$

其中 T_i 为动能,即

$$T_i = \frac{p_i^2}{2m_i} \quad (14)$$

而 $U_{ij}^{(2)}$ 和 $U_{ijk}^{(3)}$ 分别为两体和三体势,可表示为

$$U_{ij}^{(2)} = \int f_i(\mathbf{r}, \mathbf{p}, t) V_{ij}^{(2)}(\mathbf{r}, \mathbf{r}', \mathbf{p}, \mathbf{p}') f_j(\mathbf{r}', \mathbf{p}', t) d\mathbf{r} d\mathbf{p} d\mathbf{r}' d\mathbf{p}' \quad (15)$$

$$U_{ijk}^{(3)} = \int f_i(\mathbf{r}, \mathbf{p}, t) f_j(\mathbf{r}', \mathbf{p}', t) f_k(\mathbf{r}'', \mathbf{p}'', t) V_{ijk}^{(3)}(\mathbf{r}, \mathbf{r}', \mathbf{r}'', \mathbf{p}, \mathbf{p}', \mathbf{p}'') d\mathbf{r} d\mathbf{p} d\mathbf{r}' d\mathbf{p}' d\mathbf{r}'' d\mathbf{p}'' \quad (16)$$



QMD方程的“推导”

在 IQMD 模型中,两体相互作用 $V_{ij}^{(2)}$ 包括局域部分 V_{ij}^{loc} (即零程的 Skyrme 相互作用)、Yukawa 部分 V_{ij}^{Yuk} 、对称能部分 V_{ij}^{sym} 、动量相关相互作用 V_{ij}^{MDI} 以及库仑相互作用 V_{ij}^{Coul} , 即,

$$V_{ij}^{(2)} = V_{ij}^{\text{loc}} + V_{ij}^{\text{Yuk}} + V_{ij}^{\text{sym}} + V_{ij}^{\text{MDI}} + V_{ij}^{\text{Coul}} \quad (17)$$

其中

$$V_{ij}^{\text{loc}} = t_1 \delta(\mathbf{r}_i - \mathbf{r}_j) \quad (18)$$

$$V_{ij}^{\text{Yuk}} = t_3 \frac{\exp(-\mu |\mathbf{r}_i - \mathbf{r}_j|)}{\mu |\mathbf{r}_i - \mathbf{r}_j|} \quad (19)$$

$$V_{ij}^{\text{sym}} = \frac{C}{2\rho_0} \tau_{z_i} \tau_{z_j} \delta(\mathbf{r}_i - \mathbf{r}_j) \quad (20)$$

$$V_{ij}^{\text{MDI}} = t_4 \ln^2 [t_5 (\mathbf{p}_i - \mathbf{p}_j)^2 + 1] \delta(\mathbf{r}_i - \mathbf{r}_j) \quad (21)$$

$$V_{ij}^{\text{Coul}} = \frac{Z_i Z_j e^2}{|\mathbf{r}_i - \mathbf{r}_j|} \quad (22)$$



QMD方程的“推导”

局域的三体相互作用为

$$V_{ijk}^{(3)} = t_2 \delta(\mathbf{r}_i - \mathbf{r}_j) \delta(\mathbf{r}_i - \mathbf{r}_k) \quad (23)$$

以上式子中, τ_z 为粒子同位旋自由度的第三分量, 对中子和质子分别等于 1 和 -1 。 Z_i 为粒子的电荷数。 C 为对称能强度系数, 取为 32 MeV。 t_1, t_2 为 Skyrme 势参数, 参数 t_3, t_4, t_5 及 μ 的取值分别为: $t_3 = -7$ MeV; $t_4 = 1.57$ MeV; $t_5 = 5.0 \times 10^{-4} (\text{MeV}/c)^{-2}$; $\mu = 0.8 \text{ fm}^{-1}$ 。相应地在 IQMD 模型中, 由(15)和(16)式, 系统的总的相互作用势可表示为

$$U^{\text{tot}} = U_{\text{loc}}^{(2)} + U_{\text{loc}}^{(3)} + U^{\text{Yuk}} + U^{\text{sym}} + U^{\text{MDI}} + U^{\text{Coul}} \quad (24)$$

其中 $U_{\text{loc}}^{(2)}, U_{\text{loc}}^{(3)}, U^{\text{Yuk}}, U^{\text{sym}}, U^{\text{MDI}}$ 和 U^{Coul} 分别表示局域的两体 Skyrme 势、局域的三体 Skyrme 势、Yukawa 势(表面势)、对称能项、动量相关势和库仑势, 其中



QMD方程的“推导”

$$U_{\text{loc}}^{(2)} = \sum_{j \neq i} t_1 \frac{1}{(4\pi L)^{3/2}} \exp\left[-\frac{(\mathbf{r}_i - \mathbf{r}_j)^2}{4L}\right] \quad (25)$$

$$U_{\text{loc}}^{(3)} = \sum_{j \neq k \neq i} \frac{t_2}{3^{3/2}(2\pi L)^3} \exp\left[-\frac{(\mathbf{r}_i - \mathbf{r}_j)^2 + (\mathbf{r}_i - \mathbf{r}_k)^2 + (\mathbf{r}_j - \mathbf{r}_k)^2}{6L}\right] \quad (26)$$

$$U^{\text{Yuk}} = \frac{t_3}{2} \sum_{j \neq i} \frac{1}{r_{ij}} \exp(L\mu^2) [\exp(-\mu r_{ij}) \text{erfc}(\sqrt{L}\mu - r_{ij}/\sqrt{4L}) - \exp(\mu r_{ij}) \text{erfc}(\sqrt{L}\mu + r_{ij}/\sqrt{4L})] \quad (27)$$

$$U^{\text{sym}} = \frac{C}{2\rho_0} \sum_{j \neq i} t_{z_i} t_{z_j} \frac{1}{(4\pi L)^{3/2}} \exp\left[-\frac{(\mathbf{r}_i - \mathbf{r}_j)^2}{4L}\right] \quad (28)$$

$$U^{\text{MDI}} = \delta \ln^2 \left[\epsilon \left(\frac{\rho}{\rho_0} \right)^{2/3} + 1 \right] \sum_{j \neq i} \frac{1}{(4\pi L)^{3/2}} \exp\left[-\frac{(\mathbf{r}_i - \mathbf{r}_j)^2}{4L}\right] / \rho_0 \quad (29)$$

$$U^{\text{Coul}} = \frac{e^2}{4} \sum_{j \neq i} \frac{(1 - t_{z_i})(1 - t_{z_j}) [1 - \text{erfc}(r_{ij}/\sqrt{4L})]}{r_{ij}} \quad (30)$$

QMD方程的“推导”

以上式子中，

$$r_{ij} = |\mathbf{r}_i - \mathbf{r}_j| \quad (31)$$

$erfc(x)$ 代表余误差函数。为了探索核物质的状态方程，可以引入相互作用密度

$$\rho_{\text{int}}^i(\mathbf{r}_i) = \frac{1}{(4\pi L)^{3/2}} \sum_{j \neq i} \exp\left[-\frac{(\mathbf{r}_i - \mathbf{r}_j)^2}{4L}\right] \quad (32)$$

这样，包括局域的两体、三体相互作用的势能部分可以化为^[15]

$$U = \alpha \left(\frac{\rho_{\text{int}}}{\rho_0}\right) + \beta \left(\frac{\rho_{\text{int}}}{\rho_0}\right)^\gamma \quad (33)$$

式中 ρ_0 为基态时的饱和密度。不同的势参数 α 、 β 和 γ 对应不同的核物质状态方程 (EOS)，最常用的有两组参数，即所谓的硬势(H)及软势(S)，分别对应硬的及软的 EOS，见表 1。以下将 ρ_{int} 记为 ρ 。

表 1 不考虑动量相关势时软势及硬势的势参数

$\alpha(\text{MeV})$	$\beta(\text{MeV})$	γ	K(MeV)	EOS
-124	70.5	2	380	H
-356	303	7/6	200	S



QMD方程的“推导”

这样总的相互作用势可以参数化为：

$$U^{\text{tot}} = \alpha \left(\frac{\rho}{\rho_0} \right) + \beta \left(\frac{\rho}{\rho_0} \right)^\gamma + U^{\text{Yuk}} + U^{\text{sym}} + U^{\text{MDI}} + U^{\text{Coul}} \quad (34)$$

式中 $\rho_0 = 0.16 \text{ fm}^{-3}$, 为基态时的饱和密度; ρ 、 ρ_n 和 ρ_p 分别是总的、中子的和质子的相互作用密度。

在数值计算中, 通常将整个重离子碰撞过程分成许多小的时间间隔(如 $\delta t = 0.5 \text{ fm}/c$), 相邻的两个时间间隔之间, 系统内各粒子的坐标和动量按正则运动方程传播, 这是一个初值问题, 常用下面的 Euler 格式来求解:

$$\mathbf{p}_i(t + \delta t) = \mathbf{p}_i(t) - \delta t \nabla U(\mathbf{r}_i, t + \frac{1}{2} \delta t) \quad (35)$$

$$\mathbf{r}_i(t + \frac{1}{2} \delta t) = \mathbf{r}_i(t - \frac{1}{2} \delta t) + \delta t \frac{\mathbf{p}_i}{\sqrt{p_i^2 + m^2}} \quad (36)$$

如果考虑动量相关势, 则(14)式变为

$$\mathbf{r}_i(t + \frac{1}{2} \delta t) = \mathbf{r}_i(t - \frac{1}{2} \delta t) + \delta t \frac{\mathbf{p}_i}{\sqrt{p_i^2 + m^2}} + \delta t \nabla_p U(\mathbf{r}_i, \mathbf{p}_i, t - \frac{1}{2} \delta t) \quad (37)$$



二、中能重离子碰撞微观输运理论模型

- 输运理论的基本概念
- 中能重离子碰撞输运模型
- BUU和QMD的数值实现



(1) 哈密顿运动方程

尽管从形式上看，我们可以从核多体理论导出BUU方程或QMD方程，但这些方程的直接求解是十分困难的。在实际的应用中还必须采用许多近似的方程。其中最主要的近似是将核子在平均场作用下的时间演化 (*propagation*) 同随机的核子-核子碰撞分离开来考虑、前者对应于*Vlasov*方程，相当于TDHF的半经典极限，后者则对应于(2.20)式的右边部分，它也导致核相空间分布的改变。

在忽略平均场的动量相关的情况下，*Vlasov*方程，即(2.20)式的左边部分为：

$$\frac{\partial \delta}{\partial t} + \frac{\mathbf{p}}{m} \cdot \nabla f - \nabla U \cdot \nabla_{\mathbf{p}} f = 0 \quad (3.1)$$

可以证明*Vlasov*方程等价于经典的哈密顿运动方程：

$$\dot{\mathbf{p}}_i = - \frac{\partial H}{\partial \mathbf{r}_i} = - \nabla U(\mathbf{r}_i) \quad (3.2)$$

$$\dot{\mathbf{r}}_i = \frac{\partial H}{\partial \mathbf{p}_i} = \frac{\mathbf{p}_i}{\sqrt{\mathbf{p}_i^2 + m^2}} \quad (3.3)$$

其中已计入了相对论运动学。



(1) 哈密顿运动方程

如果计入平均场的动量相关(从G矩阵得到的平均场是动量相关的), 则(3.3)及(3.5)应分别为:

$$\dot{r}_i = \frac{p_i}{\sqrt{p_i^2 + m^2}} + \nabla_p U(r_i, p_i) \quad (3.6)$$

$$r_i \left(t + \frac{1}{2} \delta t \right) = r_i \left(t - \frac{1}{2} \delta t \right) + \delta t \frac{p_i(t)}{\sqrt{p_i^2(t) + m^2}} + \delta t \nabla_p U \left(r_i, p_i, t - \frac{1}{2} \delta t \right) \quad (3.7)$$

如果不考虑平均场和核子-核子截面的自治性要求, 我们可以利用参数化的平均场 U 。其中最常用的是Skyrme型参数化:

$$U(\rho) = A(\rho/\rho_0) + B(\rho/\rho_0)^\sigma \quad (3.8)$$

中其 ρ_0 是核物质饱和密度。 A 和 B 是由核物质的饱和性质(饱和密度 ρ_0 和结合能 B/A)决定的可调数。 σ 的大小决定了核物质的不可压缩系数 K 。



(1) 哈密顿运动方程

BUU方程的求解：试验粒子方法 (C. Y. Wong, 黄卓然)

volumes in configuration and momentum space. The continuous distribution $f(\mathbf{r}, \mathbf{p})$ can be replaced by a large number of test particles. Formally, we can write the distribution as:

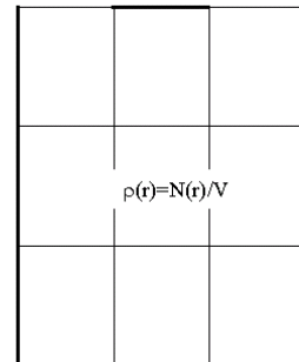
$$f(\mathbf{r}, \mathbf{p}) \cong \frac{1}{\tilde{N}} \sum_i \delta(\mathbf{r} - \mathbf{r}_i) \delta(\mathbf{p} - \mathbf{p}_i) \quad (26)$$

where \mathbf{r}_i and \mathbf{p}_i are coordinates of the individual test particles. We choose these coordinates so that f averaged over a small phase-space volume approximates the desired initial condition, $\int_{\Omega} f d^3r d^3p = \bar{f}\Omega = (1/\tilde{N}) \sum_{i \in \Omega} 1$. To see that the test particles obey classical equations of motion, we take derivatives of eq. (26):

$$\nabla_r f = \frac{1}{\tilde{N}} \sum_i \delta'(\mathbf{r} - \mathbf{r}_i) \delta(\mathbf{p} - \mathbf{p}_i)$$

$$\nabla_p f = \frac{1}{\tilde{N}} \sum_i \delta(\mathbf{r} - \mathbf{r}_i) \delta'(\mathbf{p} - \mathbf{p}_i)$$

$$\frac{\partial f}{\partial t} = \frac{1}{\tilde{N}} \sum_i \left(\delta'(\mathbf{r} - \mathbf{r}_i) \delta(\mathbf{p} - \mathbf{p}_i) \frac{\partial \mathbf{r}_i}{\partial t} + \delta(\mathbf{r} - \mathbf{r}_i) \delta'(\mathbf{p} - \mathbf{p}_i) \frac{\partial \mathbf{p}_i}{\partial t} \right).$$



It is now easy to see that eq. (25) is satisfied if $\mathbf{r}_i, \mathbf{p}_i$ obey Hamilton's equations. The test particle method was first applied to the nuclear Vlasov equation by Wong [31].



(2) 两体碰撞和Pauli阻塞

哈密顿运动方程(3.2)和(3.3)式等价于*V*Isou方程,即只考虑了核子-核子相互作用中的平均场部分,而没有计入两体碰撞。在实际的计算中两体碰撞是在哈密顿运动方程的基础上人为地加进去的。

通常将整个重离子反应过程(例如100fm/c)分成许多小的间隔(例如划分为500个小间隔, $\delta t = 0.2\text{fm}/c$),在相继的两个时刻之间,系统内各粒子的空间坐标和动量坐标按(3.2)和(3.3)式演化,即由(3.4)和(3.5)式给出。而在每一个小的时间间隔内,粒子之间可能发生两体碰撞。所以对每一个时间间隔我们必须检查每一粒子同所有其它粒子的关系,判断他们之间是否发生碰撞以及确定它们碰撞后的动量。

两粒子间发生碰撞的必要条件是,在这一时间间隔 δt 内,两粒子间的最接近距离 d_{min} 必须小于 $\sqrt{\sigma_{tot}(\sqrt{s})}/\pi$ 。其中 $\sigma_{tot}(\sqrt{s})$ 是具有质心系不变能量 \sqrt{s} 的粒子对的总截面,包括弹性(σ_{el})截面和非弹(σ_{inel})截面。显然所取的时间间隔 δt 必须足够小,使得每一粒子在此时间间隔内至多只发生一次碰撞。



(2) 两体碰撞和Pauli阻塞

假如两粒子发生碰撞，那么这一碰撞可以是弹性的，也可以是非弹性的。当束流能量小于150MeV/A时，核子向 Δ 激发的非弹几率非常小，核子间的碰撞只是弹性的，在整个反应过程中系统只包含有核子，在更高的入射能量时，核子可以被激发到 Δ 态。在通常的BUU和QMD计算中，常包括了下列碰撞过程

- (a) $N + N \rightarrow N + N$
 - (b) $N + \Delta \rightarrow N + \Delta$
 - (c) $\Delta + \Delta \rightarrow \Delta + \Delta$
 - (d) $N + N \rightarrow N + \Delta$
 - (e) $N + \Delta \rightarrow N + N$
- } 弹性
- } 非弹

(a), (b)和(c)是弹性散射，(d)表示核子被激发到 Δ 态，(e)则是(d)的逆过程，表明 Δ 粒子退激发为核子。



(2) 两体碰撞和Pauli阻塞

核子-核子的弹性及非弹截面可由实际测量得到，(b)，(c)道的截面(涉及J粒子的弹性散射)被认为和(a)道截面相同，(e)道截面可由(d)道截面经细致平衡(*detailed balance*)原理得到实际计算中常用所谓的 *cugnon* 参数化。对于弹性道(a)，(b)和(c)，总截面为：

$$\begin{aligned} \sigma_{el}(\sqrt{s}) &= 55.0 \text{ mb} & \sqrt{s} < 1.8993 \text{ GeV} & \quad (3.11) \\ &= 20 + \frac{35}{1 + 100(\sqrt{s} - 1.8993)^2} \text{ mb}, & \sqrt{s} > 1.8993 \text{ GeV} & \end{aligned}$$

对于Δ激发道(d)，总截面为：

$$\begin{aligned} \sigma_{NN}(\sqrt{s}) &= 0, & \sqrt{s} < 2.015 \text{ GeV} & \quad (3.12) \\ &= \frac{20(\sqrt{s} - 2.015)^2}{0.015 + (\sqrt{s} - 2.015)^2} & \sqrt{s} > 2.015 \text{ GeV} & \end{aligned}$$



(2) 两体碰撞和Pauli阻塞

至于 Δ 吸收道(e)的总截面则由细致平衡原理得到:

$$\sigma_{N \rightarrow NN}(\sqrt{s}) = (p_f^2/p_i^2) \frac{1}{8} \sigma_{NN \rightarrow N}(\sqrt{s}) \quad (3.13)$$

这样对于每一个粒子对, 我们首先要检查它的质量以确定这是 NN , $N\Delta$ 或 $\Delta\Delta$ 散射, 进一步要计算它的不变质量 \sqrt{s} 以及相应的总截面(弹性截面和非弹性截面之和), 以判断这一粒子对之间是否发生碰撞。

如果两粒子间发生碰撞, 则碰撞后粒子动量大小可由动量守恒得到。为了确定这些粒子动量的方向, 我们还需要知道散射过程的微分截面。对于(a), (b)和(c)的弹性过程, 微分截面被认为是非各向同性的:

$$\frac{d\sigma}{dt} = a e^{bt} \quad (3.14)$$

其中 $t = -2p^2(1 - \cos\theta_s)$, θ_s 是散射角, 参数 b 取为:

$$b(\sqrt{s}) = \frac{6[3.65(\sqrt{s} - 1.866)]^0}{1 + [3.65(\sqrt{s} - 1.866)]^6}$$

对于非弹性道(d)和(e), 最早的cugnon参数化认为它是各向同性的。



(2) 两体碰撞和Pauli阻塞

对于给定的微截面,我们可用Monte-Carlo方法来确定散射角 θ_s 。先任取一个介于(0, 1)间的随机数 x_1 , 由此及微分截面 $\frac{d\sigma}{dt}$ 确定 t_1 :

$$\int_{t_0}^{t_1} a e^{bt} dt / \int_{t_0}^0 a e^{bt} dt = x_1$$

其中 $t_0 = -2p^2$ 。散射角 θ_s 则由 $\cos\theta_s = 1 - \frac{t_1}{t_0}$ 得到。方位角 ϕ_s 则可在(0, 2π)间任意选取。如果微分截面是各向同性的,那么散射角 θ_s 也可从 $\cos\theta_s = 1 - 2x$ (x 为随机数)任意选取。通过这样的步骤我们可以确定两粒子碰撞后的动量大小和方向($\mathbf{p}_1 + \mathbf{p}_2 \rightarrow \mathbf{p}_3 + \mathbf{p}_4$)。



(2) 两体碰撞和Pauli阻塞

进一步我们还必须考虑Pauli阻塞效应。显然由能动量守恒及给定的微分截面我们确定了散射后两粒子的动量 \mathbf{p}_3 和 \mathbf{p}_4 。另外我们也知道它们的位置坐标 \mathbf{r}_3 和 \mathbf{r}_4 。假设每个粒子在坐标空间及动量空间占有一定的体积。我们计算此体积被其它粒子占有的百分比 P_1 和 P_2 。显然此两粒子末态的Pauli阻塞的几率是

$$P_{block} = \min\{1, P_1 P_2\} \quad (3.15)$$

相应的允许散射的几率为 $1 - P_{block}$ ，将此几率和一个任意选取的随机数 $x \in (0, 1)$ 相比较，我们可以判断这一次碰撞是否被Pauli阻塞。如果碰撞是Pauli阻塞的，我们就不改变这一对粒子的初始动量，即它们的动量仍为 \mathbf{p}_1 和 \mathbf{p}_2 。

泡利阻塞效应的一种考虑方法是：核子发生碰撞后，在相空间中以核子为中心构造一个相体积为 $h^3/2$ 的球(考虑了自旋自由度， h 为普朗克常数)，然后考察此球被其它的和它具有相同同位旋的核子所占据的几率。产生一个随机数 ξ ，若 ξ 小于该几率，则碰撞被阻塞。



(2) 两体碰撞和Pauli阻塞

最初的Cugnon参数化有两个不足之处。首先它不区分 pp 散射和 np 散射。(3.11)和(3.12)只是对 pp 散射实验数据的拟合。在低能核子-核子散射过程中,由于同位旋效应, np 散射截面比 $pp(nn)$ 散射截面要大得多。其中 Δ 粒子的激发和吸收被认为在核子-核子质心系中是各向同性的。在高中能核子-核子散射过程中, Δ 的激发和吸收主要是 p 波,因而是非各向同性的。最近Cugnon提出了新的关于核子-核子截面的参数化,首先它将 $pp(nn)$ 散射和 np 散射分开处理,分别拟合 pp 散射和 np 散射的实验数据,其次在新的Cugnon参数化中, Δ 粒子的激发和吸收是非各向同性的。我们称这样的参数化为同位旋相关Cugnon参数化^[46]。



(2) 两体碰撞和Pauli阻塞

可以采用两种核子-核子碰撞截面的参数化形式。其中一种是 Cugnon 给出的同位旋不相关的核子-核子碰撞截面的形式 $\sigma_{\text{Cug}}^{[22]}$ ，另一种是实验提取的同位旋相关的核子-核子碰撞截面的形式 $\sigma_{\text{exp}}^{[23]}$ 。在入射能量小于 300 MeV/u 时，采用实验提取的同位旋相关的核子-核子碰撞截面的形式，n-p 碰撞截面大约是 n-n 和 p-p 碰撞截面的 3 倍。其具体形式为

$$\sigma_{pn} = \begin{cases} -\frac{5067.4}{E^2} + \frac{9069.2}{E} + 6.9466(\text{mb}), & E \leq 40(\text{MeV}) \\ \frac{239380}{E^2} + \frac{1802.0}{E} + 27.147(\text{mb}), & 40 < E \leq 400(\text{MeV}) \\ 34.5(\text{mb}), & 400 < E \leq 800(\text{MeV}) \end{cases} \quad (39)$$

$$\sigma_{nn}(\sigma_{pp}) = \begin{cases} -\frac{1174.8}{E^2} + \frac{3088.5}{E} + 5.3107(\text{mb}), & E \leq 40(\text{MeV}) \\ \frac{93074}{E^2} - \frac{11.148}{E} + 22.429(\text{mb}), & 40 < E \leq 310(\text{MeV}) \\ \frac{887.37}{E} + 0.05331E + 3.5475(\text{mb}), & 310 < E \leq 800(\text{MeV}) \end{cases} \quad (40)$$

其中 E 为实验室系中核子的入射能量。上述截面包括弹散与非弹散部分，但非弹散截面未考虑 π 介子产生。



(3) 初始化和稳定性

下面我们以QMD计算中的初始化为例对这一问题再作些深入的讨论。6维空间的初始化分两步进行。首先是在坐标空间的初始化。对为 A 个核子选择它们的中心位置 r_0 的初始值。通常认为核子以相同的几率分布于半径 $r = 1.12A^{1/3} \text{fm}$ 的球内。每个核子在此球内的坐标由Monte-Carlo方法确定，即提取三个随机数 $x_1, x_2, x_3 \in (0, 1)$ ，核子坐标为：

$$r = R(x_1)^{1/3} = 1.112A^{1/3}(x_1)^{1/3} \text{fm}$$

$$\cos\theta = 1 - 2x_2$$

$$\phi = 2\pi x_3$$

核子在直角坐标中的位置分别为 $r\sin\theta\cos\phi$ ， $r\sin\theta\sin\phi$ 和 $r\cos\theta$ 。当然由于测不准关系的限制，两粒子间的空间距离和动量空间的距离都不允许太小。在选择（用Monte-Carlo方法）核子在坐标空间的位置时，一般要求两核子间的最小距离 r_{min} 为 1.5fm 。也就是说，当用随机方法将到第 i 个核子的坐标后，我们必须检查它和所有前 $i-1$ 个核子的关系，如果出现 $r_{min} > r_{ij}$ (r_{ij} 表示两核子间的距离)的情况，则得重新提取随机数，为第 i 个粒子选择新的坐标。



(3) 初始化和稳定性

第二步是在动量空间的初始化。首先要确定核子的定域费米动量。在 *Thomas-Fermi* 近似下核子的费米动量由下列关系给出 $p_F(r_{i0}) = \sqrt{2mU(r_{i0})}$ 。其中 $U(r_{i0})$ 是粒子 i 的势能。核子的实际动量被认为随机地分布于 0 与费米动量 p_F 之间，即选取随机数 x_1, x_2 和 $x_3 \in (0, 1)$ ，则核子动量的球坐标为：

$$p_r = p_F (x_1)^{1/3}$$

$$\cos\theta = 1 - 2x_2$$

$$\varphi = 2\pi x_3$$

而核子动量在直角坐标的分量为 $p_r \sin\theta \cos\varphi$, $p_r \sin\theta \sin\varphi$ 及 $p_r \cos\theta$ ，同样由于泡利原理的限制，两核子在相空间的坐标不能无限靠近。一般要求两核子在相空间的距离 $(r_{i0} - r_{j0})^2 (p_{i0} - p_{j0})^2$ 不少于 7.84×10^{-2} 。如果这一条件不满足，则必须选取新的随机数。



(3) 初始化和稳定性

这样的初始化能给出合理的结合能及均方根半径。图3.3给出了关于核结合能的计算结果，包括由Li到Au五个核。其中的黑点为模拟结果，已对12次独立的模拟作了平均。实线是经验的Weizsäcker质量公式的结果，显然数值模拟(初始化)能很好地符合结合能的要求。对均方根半径也有类似的结论。

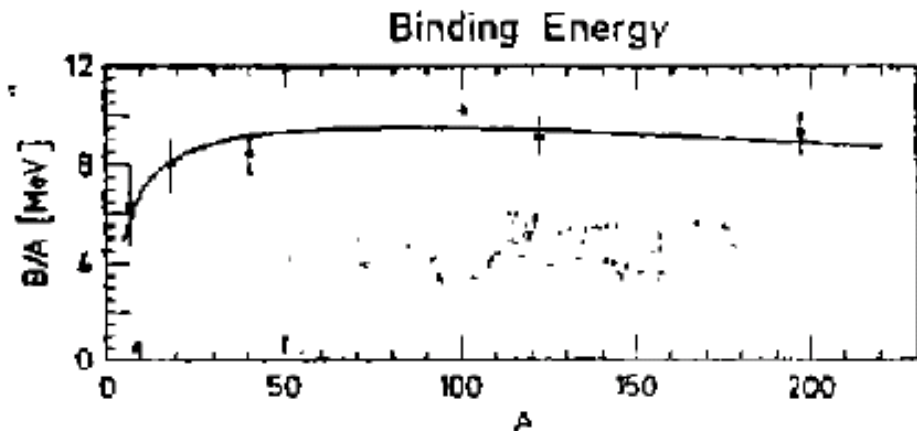


图3.3 每核子结合能 B/A 同核子数 A 的关系。点表示QMD中初始化的结果，实线则来自经验的Weizsäcker公式



(3) 初始化和稳定性

对于初始化的另一个重要的要求是其稳定性，特别地当用QMD方法研究多重散裂问题时，核的稳定性要求大于 $200\text{fm}/c$ 。我们在图3.4给出了从Li到Au五个核的均方根半径的时间演化，对每一个核均给出了12次独立的初始化的结果。从图中可以看到，对重核，均方根半径围绕某个平均值作小的波动。没有核子被蒸发掉。对轻核稳定性差一些。在 $200\text{fm}/c$ 的时间间隔内有一、二个核子被蒸发掉。因为 *Thomas-Fermi* 近似对轻核并不非常适用。

BUU计算中的初始化和QMD计算中的初始化基本相同。只是在BUU计算中我们必须为 NA 个试验粒子选择初始空间坐标及初始动量坐标。为了更形象地表明核的稳定性，我们在图3.5和图3.6中给出 ^{40}Ca 和 ^{98}Nb 两个静态核在坐标空间($x-z$ 平面)及动量空间(p_x-p_z 平面)的时间演化。显然在相当长的时间内核在坐标空间和动量空间均保持了其稳定性。



(3) 初始化和稳定性

QMD

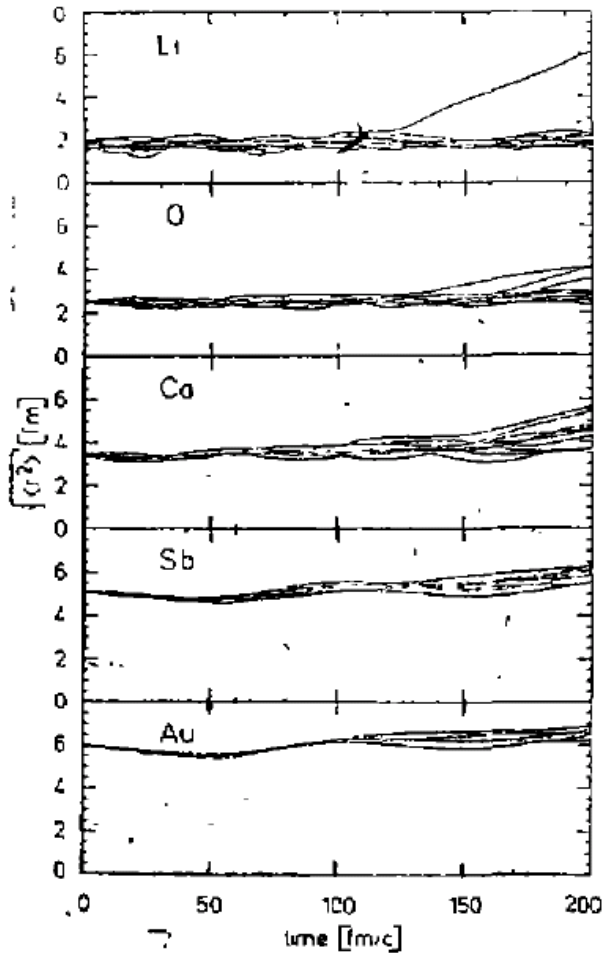


图3.4 均方根半径 $\sqrt{\langle r^2 \rangle}$ 的时间演化，不同的曲线对应于不同的模拟

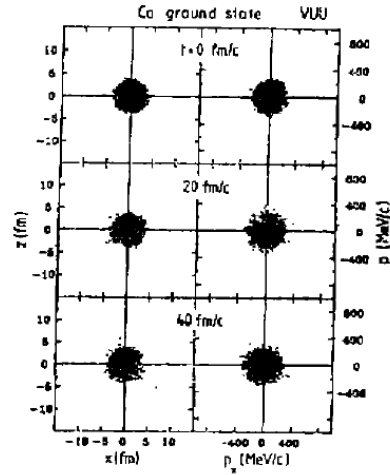


图3.5 BUU计算中 ^{40}Ca 在坐标空间(x-z平面)及动量空间(p_x - p_z 平面)的时间演化

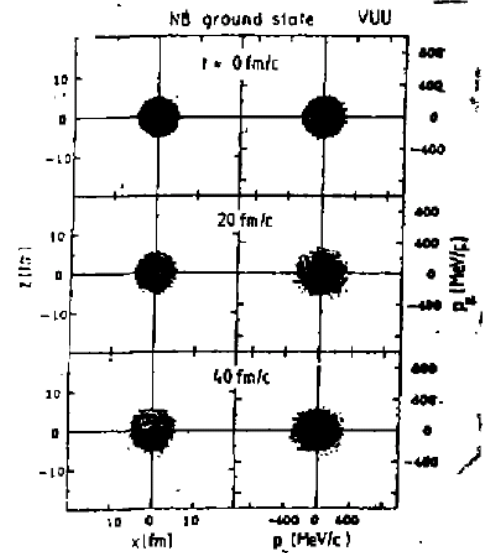


图3.6 类似于图3.5，但对 ^{93}Nb 核



(3) 初始化和稳定性

必须指出的是,正是由于初始核稳定性的限制, QMD一直无法用于研究低能重离子反应($E_{lab} \leq 30 \text{ MeV/A}$), 特别是无法研究融合(*fusion*) 反应以及重离子反应机制由低能向中高能演化。最近一些作者将所谓的(*Cooling*)方法同*Monte-Carlo*方法相结合, 提出了靶核与子弹核初始化的一种新方法。这样得到的核能在2000fm/c的时间尺度上保持其稳定性, 从而QMD方法能被用于研究低能重离子反应, 特别是可以研究核反应机制随入射能量的变化^[67-70]。

这一方法的基本思想是, 首先利用*Monte-Carlo*方法选择核子的空间坐标和动量坐标, 此时核结合能可能是大于零的, 然后通过两体碰撞, 使核的结合能逐渐变小, 一直到由于*Pauli*原理的限制, 任意两核子间不再发生碰撞为止, 这就是所谓的*Cooling*原理。



(3) 初始化和稳定性

作为例子我们在图3.7中给出了 ^{16}O 的结合能在Cooling方法中由正值向负值的演化过程,在Cooling的初始阶段只考虑两体碰撞,在前100fm/c,核很快被冷却。这以后两体Cooling机制的作用逐渐变小,必须同时计入单体Cooling机制。大约在1200fm/c时核结合能为 -8MeV 左右。至此我们得到真正的可用于QMD演化的初始核。为了表明这样制备的初始核的稳定性,我们在图3.8中给出了 ^{16}O 和 ^{40}Ca 均方根半径的时间演化。显然在整个4000fm/c的时间间隔内,核的均方根半径基本保持常数。

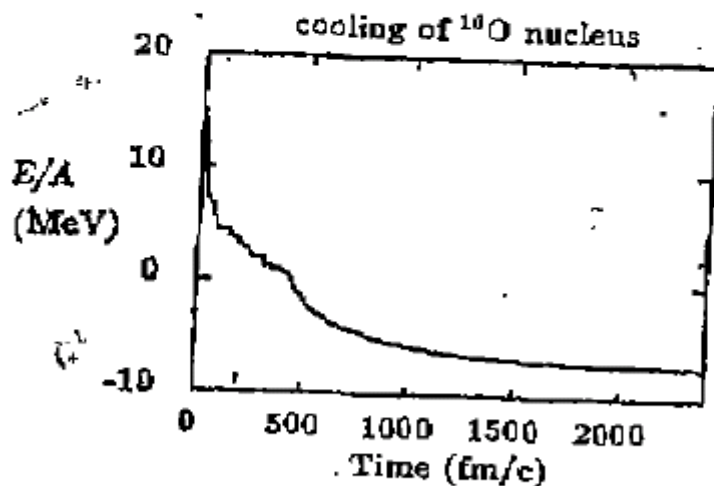


图3.7 Cooling方法中 ^{16}O 结合能随时间的演化

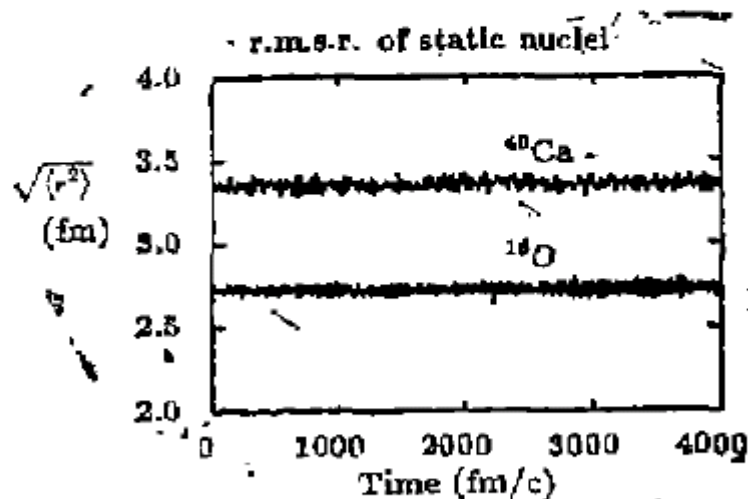
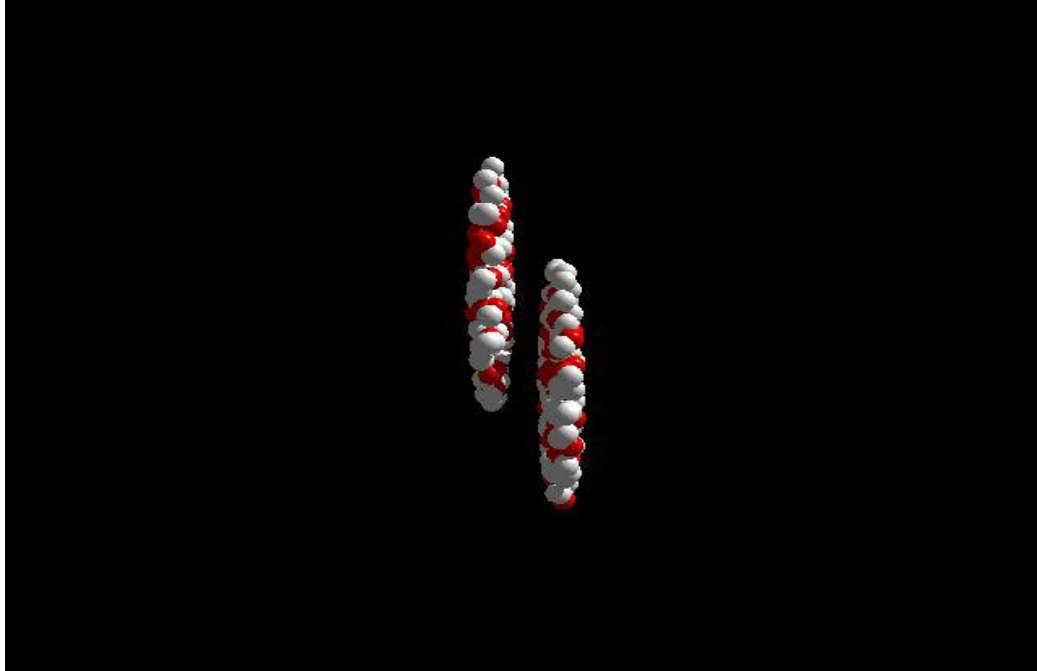


图3.8 采用Cooling方法后 ^{16}O 及 ^{40}Ca 均方根半径随时间的演化



Transport Models



Transport Models for HIC's at intermediate energies:

N-body approaches

CMD, QMD, IQMD, IDQMD, ImQMD, ImIQMD, AMD, FMD

One-body approaches

BUU/IBUU, BNV, LV, IBL

Relativistic covariant approaches

RBUU, RVUU, RQMD...

Broad applications of transport models

in astrophysics, plasma physics, electron transport in semiconductor and nanostructures, particle and nuclear physics, nuclear stockpile stewardship



PHYSICAL REVIEW C 93, 044609 (2016)

Understanding transport simulations of heavy-ion collisions at 100A and 400A MeV: Comparison of heavy-ion transport codes under controlled conditions

Jun Xu,^{1,*} Lie-Wen Chen,^{2,†} ManYee Betty Tsang,^{3,‡} Hermann Wolter,^{4,§} Ying-Xun Zhang,^{5,||} Joerg Aichelin,⁶ Maria Colonna,⁷ Dan Cozma,⁸ Pawel Danielewicz,³ Zhao-Qing Feng,⁹ Arnaud Le Fèvre,¹⁰ Theodoros Gaitanos,¹¹ Christoph Hartnack,⁶ Kyungil Kim,¹² Youngman Kim,¹² Che-Ming Ko,¹³ Bao-An Li,¹⁴ Qing-Feng Li,¹⁵ Zhu-Xia Li,⁵ Paolo Napolitani,¹⁶ Akira Ono,¹⁷ Massimo Papa,¹⁸ Taesoo Song,¹⁹ Jun Su,²⁰ Jun-Long Tian,²¹ Ning Wang,²² Yong-Jia Wang,¹⁵ Janus Weil,¹⁹ Wen-Jie Xie,²³ Feng-Shou Zhang,²⁴ and Guo-Qiang Zhang¹



Transport 2014, Shanghai, Jan. 8-12, 2014.



Understanding transport simulations of heavy-ion collisions at 100A and 400A MeV: Comparison of heavy-ion transport codes under controlled conditions

Jun Xu,^{1,*} Lie-Wen Chen,^{2,†} ManYee Betty Tsang,^{3,‡} Hermann Wolter,^{4,§} Ying-Xun Zhang,^{5,||} Joerg Aichelin,⁶ Maria Colonna,⁷ Dan Cozma,⁸ Pawel Danielewicz,³ Zhao-Qing Feng,⁹ Arnaud Le Fèvre,¹⁰ Theodoros Gaitanos,¹¹ Christoph Hartnack,⁶ Kyungil Kim,¹² Youngman Kim,¹² Che-Ming Ko,¹³ Bao-An Li,¹⁴ Qing-Feng Li,¹⁵ Zhu-Xia Li,⁵ Paolo Napolitani,¹⁶ Akira Ono,¹⁷ Massimo Papa,¹⁸ Taesoo Song,¹⁹ Jun Su,²⁰ Jun-Long Tian,²¹ Ning Wang,²² Yong-Jia Wang,¹⁵ Janus Weil,¹⁹ Wen-Jie Xie,²³ Feng-Shou Zhang,²⁴ and Guo-Qiang Zhang¹

TABLE I. The names, code authors and correspondents, and representative references of nine BUU-type and nine QMD-type models participating in the transport-code-comparison project. The intended beam-energy range for each code is given in GeV.

BUU type	Code correspondents	Energy range	Reference	QMD type	Code correspondents	Energy range	Reference
BLOB	P. Napolitani, M. Colonna	0.01–0.5	[19]	AMD	A. Ono	0.01–0.3	[28]
GIBUU-RMF	J. Weil	0.05–40	[20]	IQMD-BNU	J. Su, F. S. Zhang	0.05–2	[29]
GIBUU-Skyrme	J. Weil	0.05–40	[20]	IQMD	C. Hartnack, J. Aichelin	0.05–2	[30–32]
IBL	W. J. Xie, F. S. Zhang	0.05–2	[21]	CoMD	M. Papa	0.01–0.3	[33,34]
IBUU	J. Xu, L. W. Chen, B. A. Li	0.05–2	[11,22]	ImQMD-CIAE	Y. X. Zhang, Z. X. Li	0.02–0.4	[35]
pBUU	P. Danielewicz	0.01–12	[23,24]	IQMD-IMP	Z. Q. Feng	0.01–10	[36]
RBUU	K. Kim, Y. Kim, T. Gaitanos	0.05–2	[25]	IQMD-SINAP	G. Q. Zhang	0.05–2	[37]
RVUU	T. Song, G. Q. Li, C. M. Ko	0.05–2	[26]	TuQMD	D. Cozma	0.1–2	[38]
SMF	M. Colonna, P. Napolitani	0.01–0.5	[27]	UrQMD	Y. J. Wang, Q. F. Li	0.05–200	[39,40]

9 BUU-type codes and 9 QMD-type codes

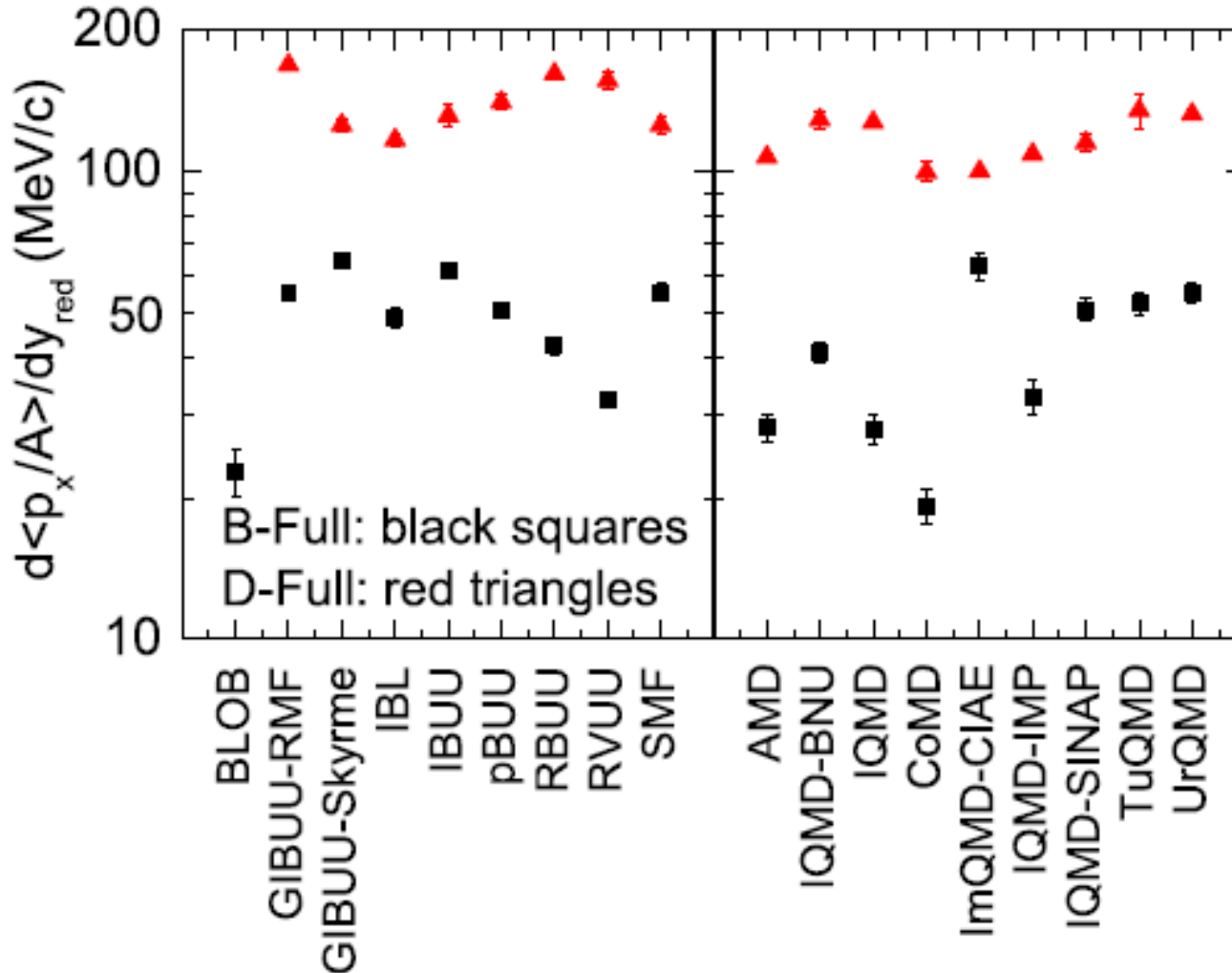


重离子碰撞微观运输模型概览

9 BUU-type codes and 9 QMD-type codes

B-full mode (100A MeV) and D-full mode (400A MeV) at $b = 7$ fm

Au+Au



Strong model dependence exists at lower energies !!!



Transport Models for Heavy-Ion Collisions

PHYSICAL REVIEW C **93**, 044609 (2016)

Understanding transport simulations of heavy-ion collisions at 100A and 400A MeV: Comparison of heavy-ion transport codes under controlled conditions

Jun Xu,^{1,*} Lie-Wen Chen,^{2,†} ManYee Betty Tsang,^{3,‡} Hermann Wolter,^{4,§} Ying-Xun Zhang,^{5,||} Joerg Aichelin,⁶
Maria Colonna,⁷ Dan Cozma,⁸ Pawel Danielewicz,³ Zhao-Qing Feng,⁹ Arnaud Le Fèvre,¹⁰ Theodoros Gaitanos,¹¹

Christoph H
Paolo Napolitani

PHYSICAL REVIEW C **97**, 034625 (2018)

Comparison of heavy-ion transport simulations: Collision integral in a box

Ying-Xun Zhang,^{1,2,*} Yong-Jia Wang,^{3,†} Maria Colonna,^{4,‡} Pawel Danielewicz,^{5,§} Akira Ono,^{6,||} Manyee Betty Tsang,^{5,¶}
Hermann Wolter,^{7,#} Jun Xu,^{8,**} Lie-Wen Chen,⁹ Dan Cozma,¹⁰ Zhao-Qing Feng,¹¹ Subal Das Gupta,¹² Natsumi Ikeno,¹³
Che-Ming Ko,¹⁴ B...
Akira Ohnishi,¹⁹ Dmy...

PHYSICAL REVIEW C **100**, 044617 (2019)

Comparison of heavy-ion transport simulations: Collision integral with pions and Δ resonances in a box

Akira Ono,^{1,*} Jun Xu,^{2,3,†} Maria Colonna,⁴ Pawel Danielewicz,⁵ Che Ming Ko,⁶ Manyee Betty Tsang,⁵ Yong-Jia Wang,⁷
Hermann Wolter,⁸ Ying-Xun Zhang,^{9,10} Lie-Wen Chen,¹¹ Dan Cozma,¹² Hannah Elfner,^{13,14,15} Zhao-Qing Feng,¹⁶

Comparison of Heavy-Ion Transport Simulations: Mean-field Dynamics in a Box [arXiv:2106.12287 \(PRC, accepted\)](https://arxiv.org/abs/2106.12287)

Maria Colonna,^{1,*} Ying-Xun Zhang,^{2,3,†} Yong-Jia Wang,^{4,‡} Dan Cozma,⁵ Pawel Danielewicz,^{6,§} Che Ming Ko,⁷
Akira Ono,^{8,¶} Manyee Betty Tsang,^{6,**} Rui Wang,^{9,10} Hermann Wolter,^{11,††} Jun Xu,^{12,13,‡‡} Zhen Zhang,¹⁴
Lie-Wen Chen,¹⁵ Hui-Gan Cheng,¹⁶ Hannah Elfner,^{17,18,19} Zhao-Qing Feng,²⁰ Myungkuk Kim,²¹ Youngman
Kim,²² Sangyong Jeon,²³ Chang-Hwan Lee,²⁴ Bao-An Li,²⁵ Qing-Feng Li,^{4,26} Zhu-Xia Li,² Swagata Mallik,²⁷
Dmytro Oliinychenko,^{28,29} Jun Su,¹⁴ Taesoo Song,^{17,30} Agnieszka Sorensen,³¹ and Feng-Shou Zhang^{32,33}

- ❑ Model dependence?
- ❑ How to improve the accuracy/precision of the simulations?
- ❑

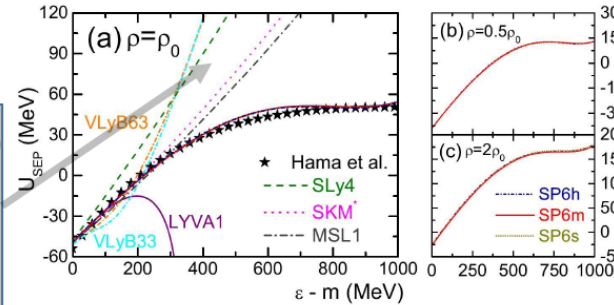
Transport Code
Comparison Project!



Skyrme Pseudopotential for Heavy-Ion Collisions

Skyrme pseudopotential

$$v_{Sk} = t_0^{(0)}(1 + x_0^{(0)}\hat{P}_\sigma) + \frac{1}{6}t_3^{(0)}(1 + x_3^{(0)}\hat{P}_\sigma)\rho^\alpha(\vec{R}) \\ + \frac{1}{2}t_1^{(2)}(1 + x_1^{(2)}\hat{P}_\sigma)[\vec{k}'^2 + \vec{k}^2] \\ + t_2^{(2)}(1 + x_2^{(2)}\hat{P}_\sigma)\vec{k}' \cdot \vec{k}$$



R. Wang, L.-W. Chen, and Y. Zhou, PRC98, 054618 (2018)

N3LO local nuclear
energy density functional

B.G. Carlsson et al PRC78,044326 (2008)

Corresponding N3LO
Skyrme pseudopotential

F. Raimondi et al PRC83,054311 (2011)

4th and 6th order of momentum

$$+ \frac{1}{4}t_1^{(4)}(1 + x_1^{(4)}\hat{P}_\sigma)[(\vec{k}'^2 + \vec{k}^2)^2 + 4(\vec{k}' \cdot \vec{k})^2] + t_2^{(4)}(1 + x_2^{(4)}\hat{P}_\sigma)(\vec{k}' \cdot \vec{k})(\vec{k}'^2 + \vec{k}^2) \\ + \frac{1}{2}t_1^{(6)}(1 + x_1^{(6)}\hat{P}_\sigma)(\vec{k}'^2 + \vec{k}^2)^2[(\vec{k}'^2 + \vec{k}^2)^2 + 12(\vec{k}' \cdot \vec{k})^2] \\ + t_2^{(6)}(1 + x_2^{(6)}\hat{P}_\sigma)(\vec{k}' \cdot \vec{k})[3(\vec{k}'^2 + \vec{k}^2)^2 + 4(\vec{k}' \cdot \vec{k})^2]$$

plus spin-orbit and
tensor terms
an overall $\delta(\vec{r}_1 - \vec{r}_2)$
is implicit

R. Wang (王睿), LWC,
and Y. Zhou (周颖),
PRC98, 054618 (2018)

**Can fit the experimental
nucleon optical model
potential up to ~1 GeV !**

**Suitable interactions for
HICs at CEE/CSR
energies !**

**Also for nuclear
structures and neutron
stars !**



Lattice Hamiltonian Method

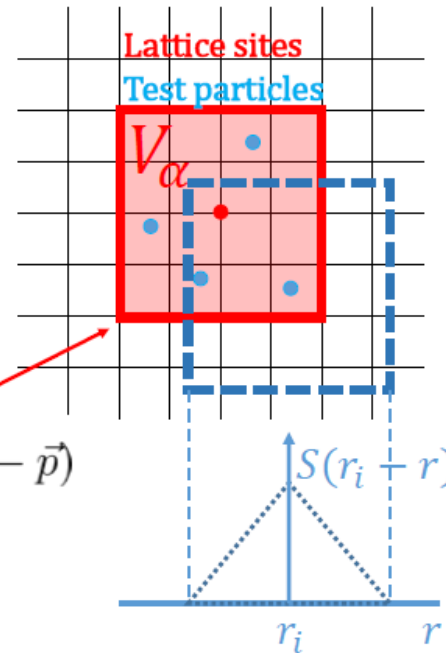
The lattice Hamiltonian method

To study nuclear giant resonance in transport model, we need **long time evolution**

suitable

The lattice Hamiltonian method of solving BUU equation conserves the total energy

Conserve energy precisely!



$$f(\vec{r}_\alpha, \vec{p}) = \frac{1}{2} \frac{1}{N_E / (2\pi\hbar)^3} \sum_{i \in V_\alpha} S(\vec{r}_i - \vec{r}) \delta(\vec{p}_i - \vec{p})$$

$$\rho(\vec{r}_\alpha) = 2 \int f(\vec{r}_\alpha, \vec{p}) \frac{d\vec{p}}{(2\pi\hbar)^3} = \frac{1}{N_E} \sum_{i \in V_\alpha} S(\vec{r}_i - \vec{r})$$

$$H \approx \sum_i \frac{p_i^2}{2m} + N_{TP} \Delta V \sum_\alpha \left\{ \mathcal{H}^{\text{local}}[\rho(r_\alpha)] + \mathcal{H}^{\text{DD}}[\rho(r_\alpha)] + \mathcal{H}^{\text{Cou}}[\rho(r_\alpha)] + \mathcal{H}^{\text{grad}}(\vec{r}_\alpha) + \mathcal{H}^{\text{MD}}(\vec{r}_\alpha) \right\}$$

R.J. Lenk and V.R. Pandharipande, PRC39,2242 (1989)



Stochastic Collision Approach

Stochastic collision in LH method

For phase space volume $(\vec{p}_1 \pm \Delta^3 p_1)$ and $(\vec{p}_2 \pm \Delta^3 p_2)$ at \vec{r}_α

$$\Delta N_{22}^{\text{coll}}(\vec{r}_\alpha) = \frac{\Delta^3 p_1}{(2\pi\hbar)^3} \left| \frac{df(\vec{r}_\alpha, \vec{p}_1)}{dt} \right|_{\vec{p}_2}^{\text{coll}} l^3 \Delta t$$

$$\left| \frac{df(\vec{r}_\alpha, \vec{p}_1)}{dt} \right|_{\vec{p}_2}^{\text{coll}} = \frac{\Delta^3 p_1}{(2\pi\hbar)^3} f(\vec{r}_\alpha, \vec{p}_1) f(\vec{r}_\alpha, \vec{p}_2)$$

$$\times \int \frac{d\vec{p}_3}{(2\pi\hbar)^3} \frac{d\vec{p}_4}{(2\pi\hbar)^3} |\mathcal{M}_{12 \rightarrow 34}|^2 (2\pi)^4 \delta^4(\vec{p}_1 + \vec{p}_2 - \vec{p}_3 - \vec{p}_4)$$

$$= \frac{\Delta^3 p_1}{(2\pi\hbar)^3} f(\vec{r}_\alpha, \vec{p}_1) f(\vec{r}_\alpha, \vec{p}_2) v_{\text{rel}} \sigma_{\text{NN}}^* \quad \text{by definition}$$

In lattice Hamiltonian method $f(\vec{r}_\alpha, \vec{p}_i) = \frac{\Delta N_i S(\vec{r}_i - \vec{r}_\alpha)}{\frac{1}{(2\pi\hbar)^3} \Delta^3 p_i}$

$$P_{22} = \frac{\Delta N_{22}^{\text{coll}}(\vec{r}_\alpha)}{\Delta N_1 \Delta N_2} = v_{\text{rel}} \frac{\sigma_{\text{NN}}^*}{N_{\text{E}}} S(\vec{r}_1 - \vec{r}_\alpha) S(\vec{r}_2 - \vec{r}_\alpha) l^3 \Delta t$$

More reliable than the commonly used geometric method when **the mean free path MFP of a test nucleon is not much larger than the interaction length between two test nucleons** or when the **NN scattering cross section is very large!**

See, e.g.,
P. Danielewicz and G.F. Bertsch,
NPA 533, 712 (1991);
Z. Xu and C. Greiner,
PRC71, 064901 (2005)

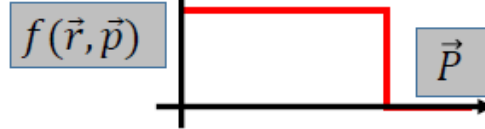
Initialization in Lattice Hamiltonian Method

Initialization of test particles

Thomas-Fermi initialization

$$E = \int \mathcal{H}(r, \rho_\tau(r), \nabla \rho_\tau(r), \nabla^2 \rho_\tau(r) \dots) dr$$

$$\frac{\partial H}{\partial \rho} - \nabla \frac{\partial H}{\partial (\nabla \rho)} + \nabla^2 \frac{\partial H}{\partial (\nabla^2 \rho)} = 0$$



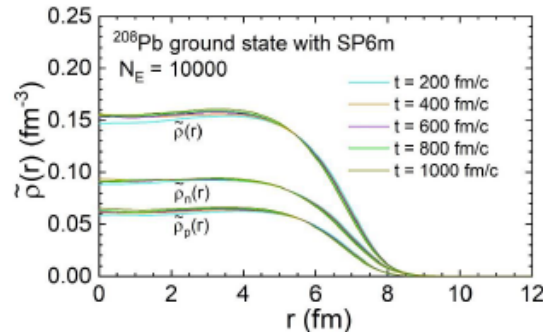
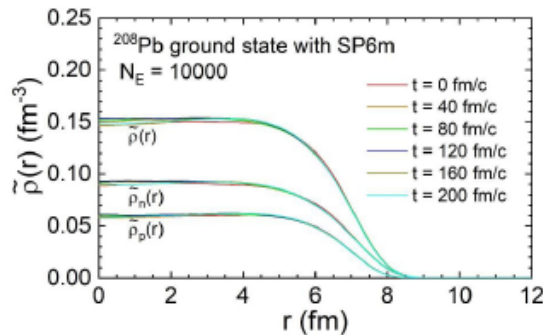
$$\frac{1}{2m} \{p_\tau^F[\rho(r)]\}^2 + U_\tau \{p_\tau^F[\rho(r)], r\} = \mu_\tau$$

Very stable ground state of the initialized nuclei!

R. Wang (王睿), LWC, and Z. Zhang (张振), PRC99, 044607 (2019)

The **GPU** parallel computing with large enough test particle number (up to **~100000** !)

The density profile in lattice Hamiltonian method



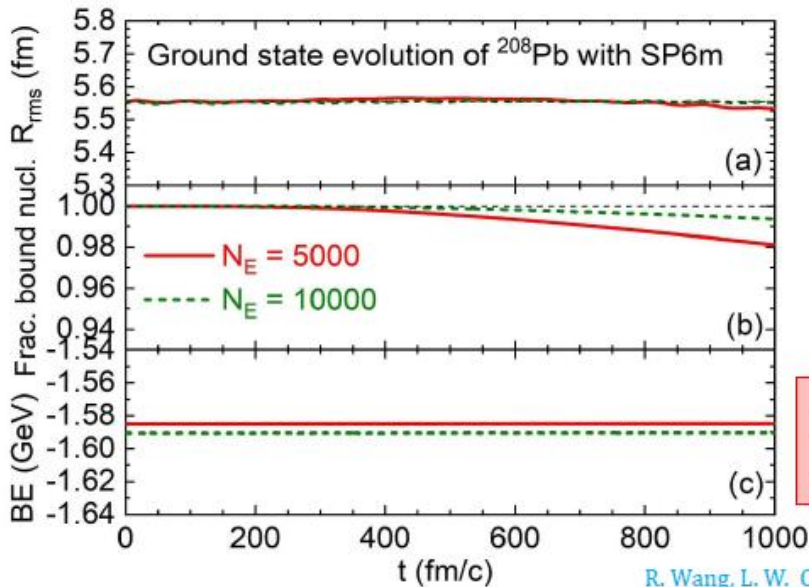
R. Wang, L. W. Chen, and Z. Zhang, PRC99, 044609 (2019)



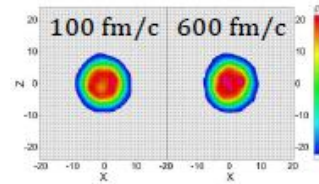
Initialization in Lattice Hamiltonian Method

Ground state LHV Calculations

The rms radius, fraction of bound nucleons, binding energy of ground state evolution



R. Wang, L. W. Chen, and Z. Zhang, PRC99, 044609 (2019)



Free test nucleons are those whose **form factor do not overlap** with that of other test nucleons

$$\langle r^2 \rangle = N_{\text{nucl}}^{-1} \int_{\text{bound}} d^3r^2 \rho(r)$$

At 1000 fm/c, only about 2% of test nucleons evaporated from the nucleus for $N_E = 5000$ case

Very stable ground state of the initialized nuclei!

R. Wang (王睿), LWC, and Z. Zhang (张振), PRC99, 044607 (2019)

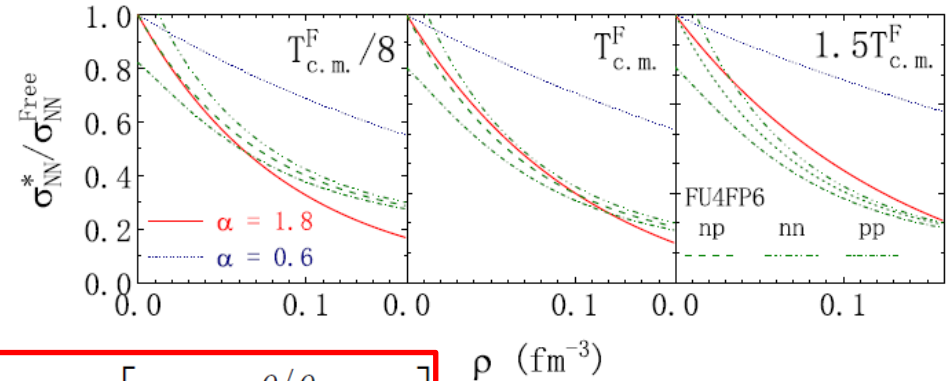
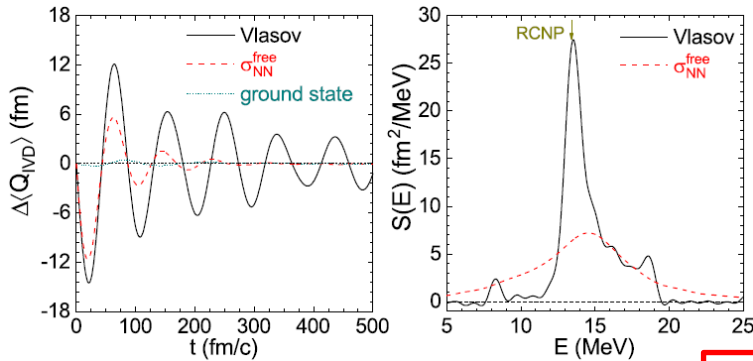
The **GPU** parallel computing with large enough test particle number (up to **~100000** !)



Lattice Boltzmann-Uehling-Uhlenbeck Equation

Constraining the in-medium NN cross sections from the width of IVGDR

R. Wang (王睿), Z. Zhang (张振), LWC, C.M. Ko, and Y.G. Ma, PLB807, 135532 (2020)



$$\sigma_{NN}^* = \sigma_{NN}^{\text{free}} \exp \left[-\alpha \frac{\rho / \rho_{\text{nuc}}}{1 + (T_{\text{c.m.}} / T_0)^2} \right]$$

T-Matrix Approach:

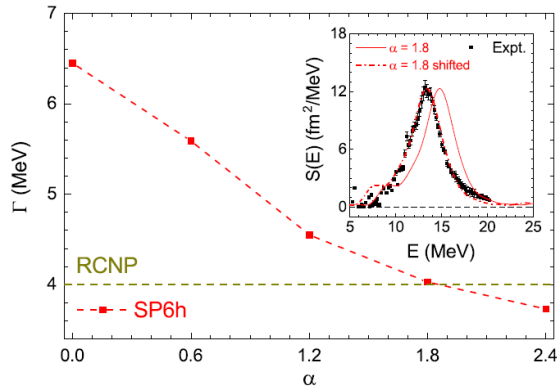
T. Alm, G. Röpke, and M. Schmidt, PRC50, 31 (1994)

FU4FP6 from nucleon induced reaction cross section:

L. Ou and X.Y. He, CPC43, 044103 (2019)

□ The width of IVGDR is sensitive to in-medium NN cross sections

□ Strong medium correction ($\alpha=1.8$) is obtained from RCNP data





三、中能重离子碰撞与核物质对称能

- 核物质的对称能
- 对称能与重离子碰撞



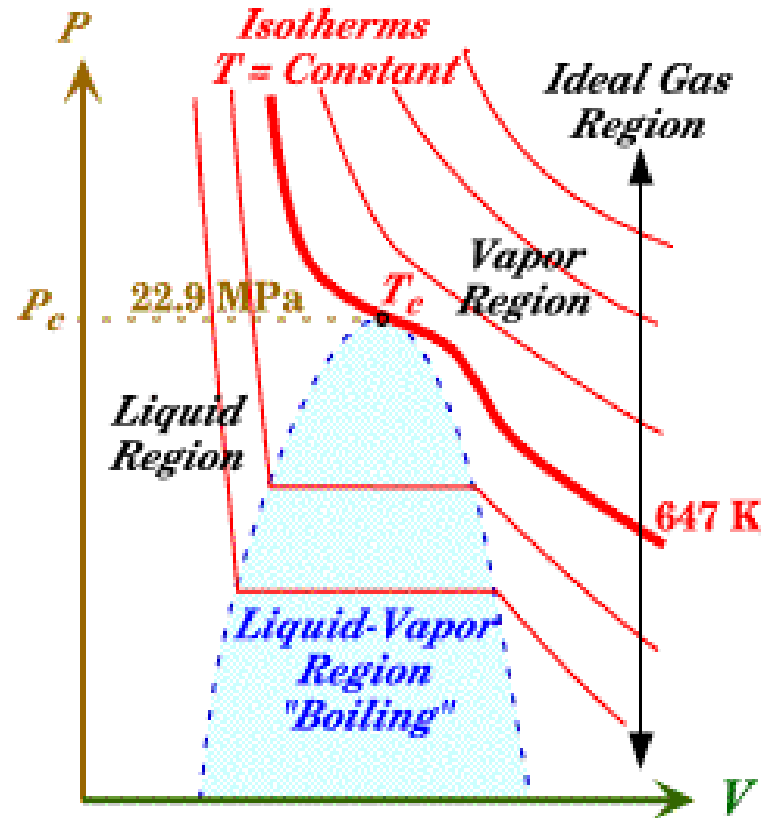
物质的状态方程

状态方程(EOS-Equation of State): a relationship among several state variables

van der Waals EOS:
$$\left[p + a\left(\frac{n}{V}\right)^2 \right] (V - nb) = nRT$$



The Nobel Prize in Physics 1910 was awarded to Johannes Diderik van der Waals *"for his work on the equation of state for gases and liquids"*.



- The EOS depends on the interactions and properties of the particles in the matter.
- It describes how the state of the matter changes under different conditions



有限核的对称能

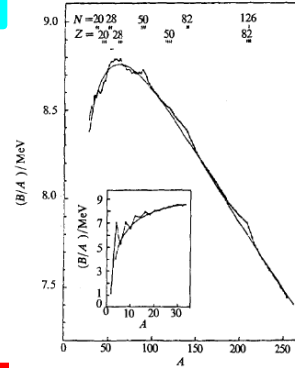
原子核的结合能 - 液滴模型

(Liquid-drop model: **Bethe-Weizsäcker mass formula-1935**)

$$a_v A - a_s A^{2/3} - a_4 \frac{(N - Z)^2}{A} - a_c \frac{Z(Z - 1)}{A^{1/3}} + a_p \frac{\Delta(N, Z)}{A^{1/2}}$$

$$S_v \frac{(N_v - Z_v)^2}{A} + S_s \frac{(N_s - Z_s)^2}{A^{2/3}}$$

Symmetry energy term
(对称能项)



$$a_v A - a_s A^{2/3} - \frac{S_v}{1 + y_s A^{-1/3}} \frac{(N - Z)^2}{A} - a_c \frac{Z(Z - 1)}{A^{1/3}} + a_p \frac{\Delta(N, Z)}{A^{1/2}}$$

Symmetry energy including surface diffusion effects ($y_s = S_v/S_s$)

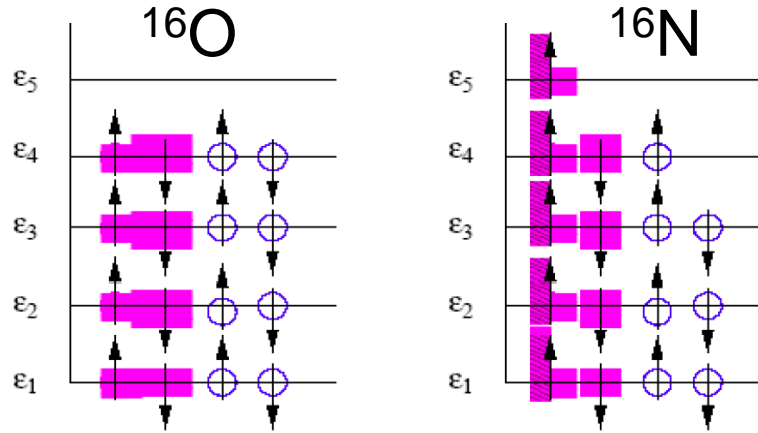


有限核的对称能

$$a_4(N-Z)^2 / A$$

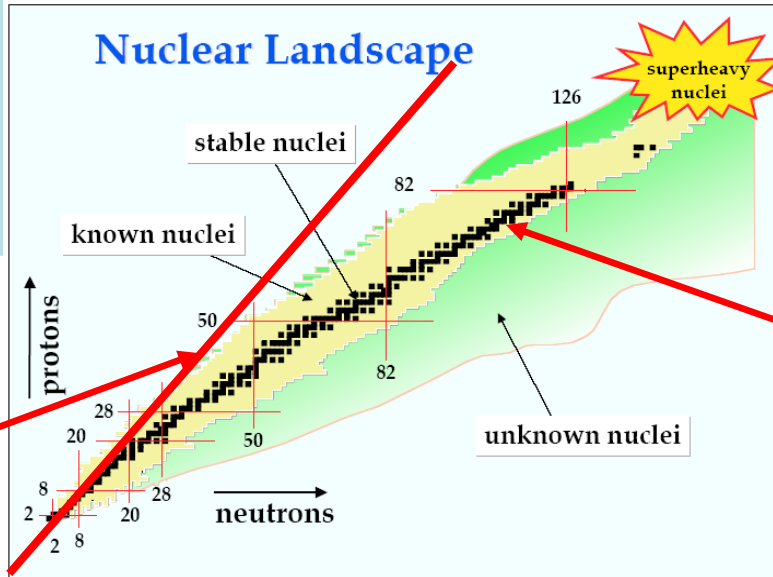
泡利不相容原理

⊙ 质子 ⊚ 中子



对称能：
使中子数和质子数
趋于对称

库仑能：
使中子数和质子数
偏离对称



$N = Z$

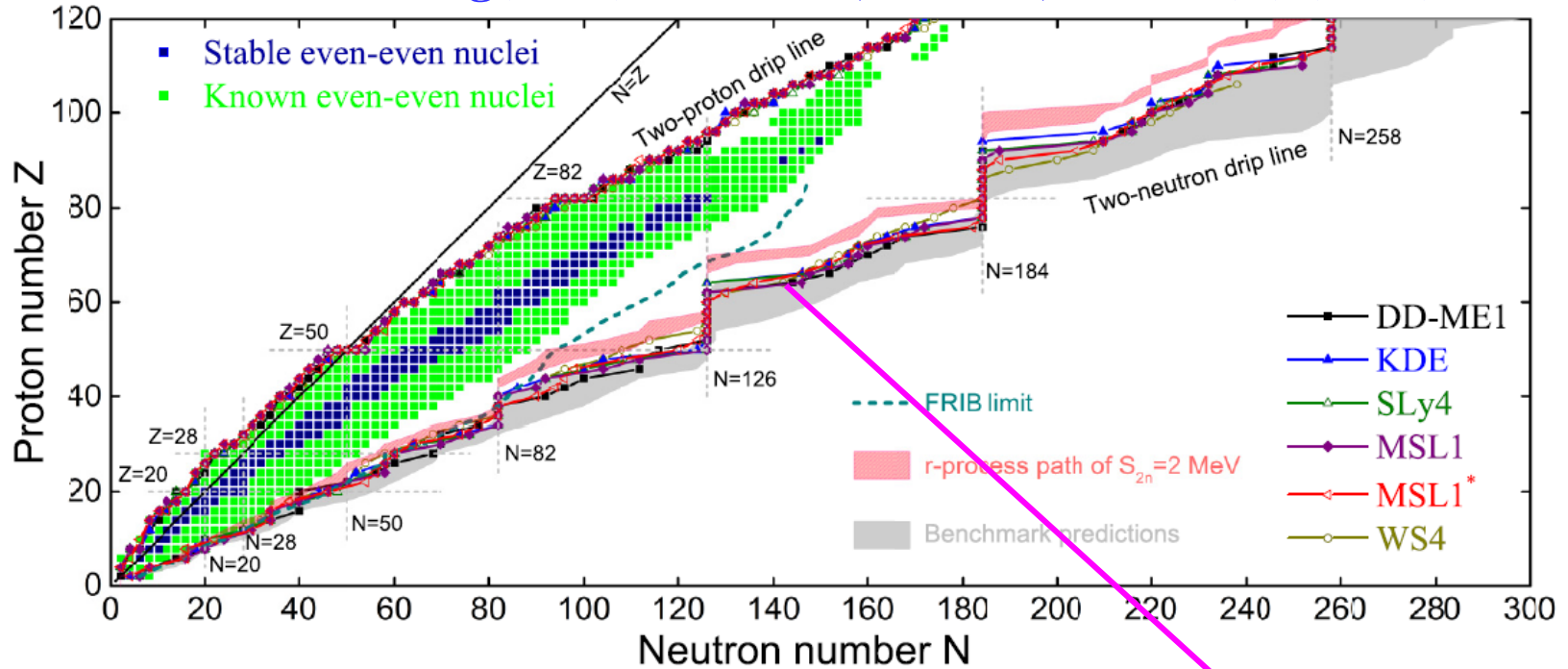
$N > Z$

The Esym is very important for the global behaviors of N/P driplines! R. Wang (王睿) /LWC, PRC92, 031303(R) (2015)



有限核的对称能

Rui Wang(王睿) and LWC, PRC92, 031303(R) (2015)



their even-even neighbors [22]. Accordingly, we estimate the total number of bound nuclei to be 6794, 6895, 7115, and 6659 for KDE, SLy4, MSL1, and MSL1*, respectively, leading to a precise estimate of 6866 ± 166 (only 3191 have been discovered experimentally [47]). Although the above

对称能对原子核的中子滴线位置起到了决定性的作用！



核物质的状态方程及对称能

EOS of Isospin Asymmetric Nuclear Matter (Parabolic law)

$$E(\rho, \delta) = E(\rho, 0) + E_{\text{sym}}(\rho)\delta^2 + O(\delta^4), \quad \delta = (\rho_n - \rho_p) / \rho$$

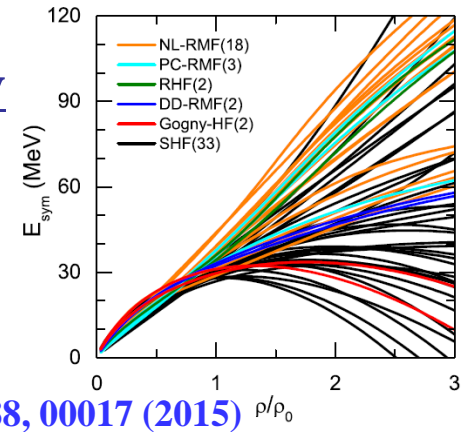
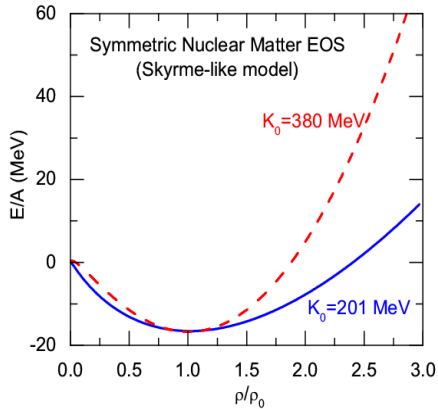
Symmetric Nuclear Matter
(relatively well-determined)

Isospin asymmetry
Symmetry energy term (poorly known)

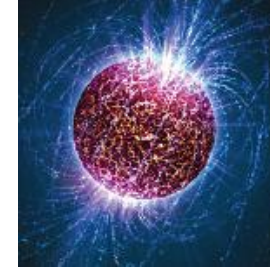
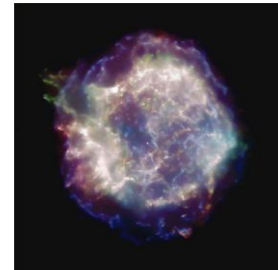
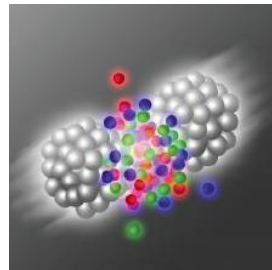
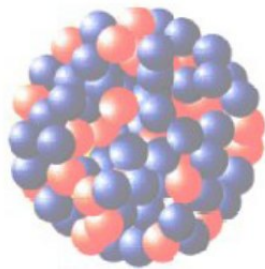
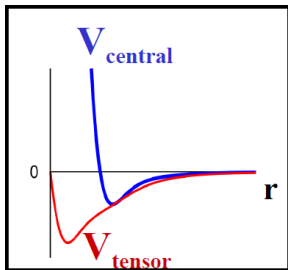
Nuclear Matter Symmetry Energy

$$E_{\text{sym}}(\rho) \equiv \frac{1}{2} \frac{\partial^2 E(\rho, \delta)}{\partial \delta^2}$$

饱和密度: $\rho_0 \approx 0.16 \text{ fm}^{-3}$



LWC, EPJ Web of Conf. 88, 00017 (2015) ρ/ρ_0



Nature of the nuclear force?

Structure and stability of nuclei?

Dynamics of heavy ion collisions?

Mechanism of supernova explosion?

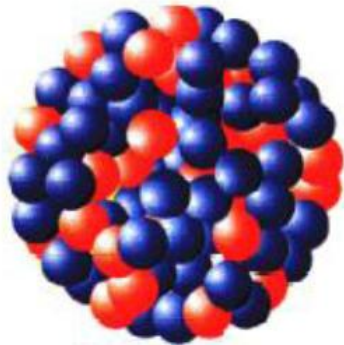
Nature of compact stars?

GW from binary NS merger?



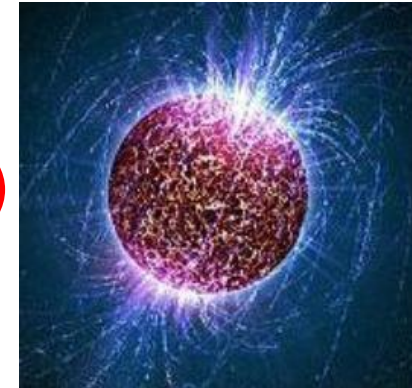
为什么研究对称能?

**Nuclear Physics
on the Earth**



**Physics at fm scale
(~10 fm)**

**Astrophysics and Cosmology
in Heaven**



**Physics at km scale
(~10 km)**

**Symmetry
Energy**

**Size different by
18 orders !!!**

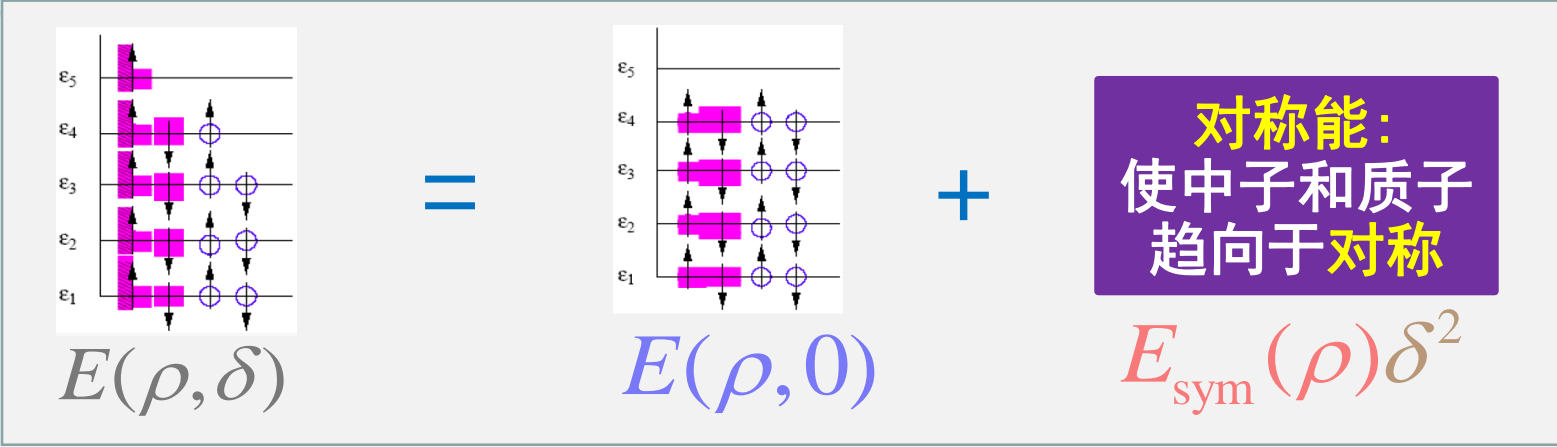


为什么研究对称能？



$$\rho = \rho_n + \rho_p$$

$$\delta = \frac{\rho_n - \rho_p}{\rho_n + \rho_p}$$



非对称核物质状态方程

很不确定

对称核物质状态方程

已经比较清楚

对称能

核物质状态方程
同位旋相关部分
很不确定

对称能是回答两个以下重大科学问题的关键量

- 中子星和致密核物质的性质是什么？
- 宇宙中的元素是怎样产生的？

The Frontiers of Nuclear Science
A LONG RANGE PLAN

《美国核科学前沿长期规划》

The Nuclear Science Advisory Committee

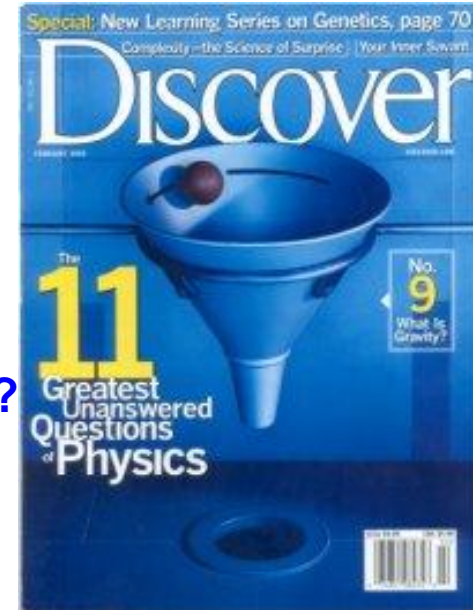
◆ 确定对称能已成为一些核物理大科学装置的重要物理目标，比如：中国兰州CSR、日本RIBF/RIKEN、美国FRIB/MSU和德国FAIR/GSI



为什么研究对称能？

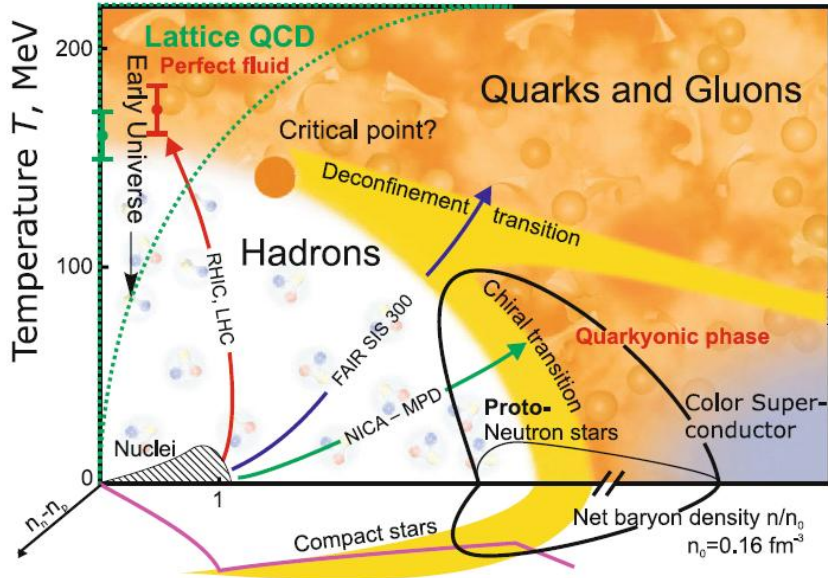
本世纪11个最重要的物理问题 (美国《发现》2002)

1. What is dark matter
2. What is dark energy
3. How were the heavy elements from iron to uranium made?
从铁到铀等重元素是如何形成的？ -高同位旋、高密度
4. Do neutrinos have mass?
5. Where do ultrahigh-energy particles come from?
6. Is a new theory of light and matter needed to explain what happens at very high energies and temperatures?
7. Are there new states of matter at ultrahigh temperatures and densities?
极端高温、高密条件下会出现新物态吗？ -高温、高密度
8. Are protons unstable?
9. What is gravity?
10. Are there extra dimensions?
11. How did the universe begin?





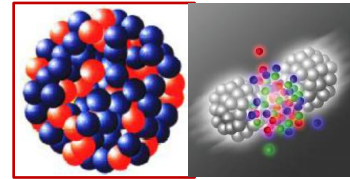
V.E. Fortov, *Extreme States of Matter – on Earth and in the Cosmos*, Springer-Verlag, 2011



Holy Grail of Nuclear Physics

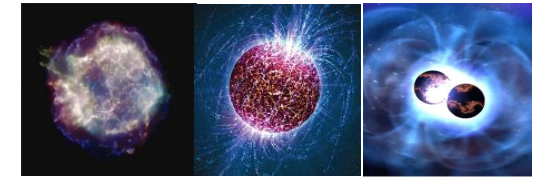


Probing QCD phase diagram in Nuclei and Heavy Ion Collisions in terrestrial labs and in NS Merger, SN, and Nstar in heaven?



Nuclei

HIC



SN

NStar

NS Merger

- Small baryon chemical potential: **Smooth Crossover Transition**
- Large baryon chemical potential: **First-order Phase Transition**
- QCD **Critical Endpoint**: where the first-order phase transition ends

Esym - Large isospin at low T and high densities!
Quark Matter Symmetry Energy?

M. Di Toro et al., NPA775 (2006);
P.C. Chu (初鹏程)/LWC, ApJ780 (2014); LWC, 《原子核物理评论》 34, 20 (2017) [arXiv:1708.04433]



核物质对称能: 多体理论方法

The nuclear matter EOS cannot be measured experimentally, its determination thus depends on theoretical approaches

- **Microscopic Many-Body Approaches**

- Non-relativistic Brueckner-Bethe-Goldstone (BBG) Theory

- Relativistic Dirac-Brueckner-Hartree-Fock (DBHF) approach

- Self-Consistent Green's Function (SCGF) Theory

- Variational Many-Body (VMB) approach

- Green's Function Monte Carlo Calculation

- $V_{\text{low}k}$ + Renormalization Group

- Nuclear Lattice Approach

- **Effective Field Theory**

- Density Functional Theory (DFT)

- Chiral Perturbation Theory (ChPT)

- QCD-based theory

- **Phenomenological Approaches**

- Relativistic mean-field (RMF) theory

- Quark Meson Coupling (QMC) Model

- Relativistic Hartree-Fock (RHF)

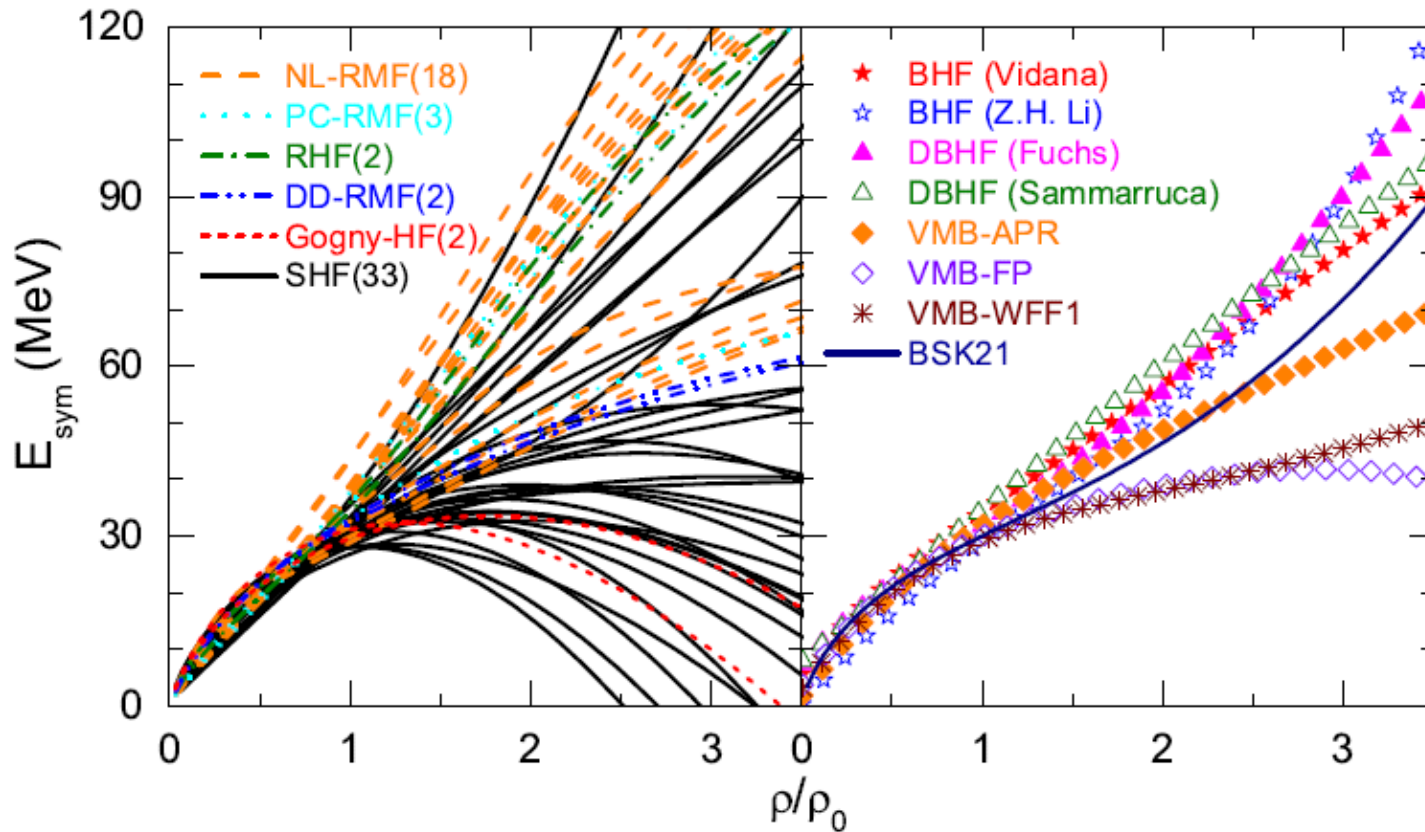
- Non-relativistic Hartree-Fock (Skyrme-Hartree-Fock)

- Thomas-Fermi (TF) approximations



核物质对称能: 多体理论方法

L.W. Chen, Nucl. Phys. Rev. (原子核物理评论) 34, 20 (2017) [arXiv:1708.04433]





核物质对称能：实验探针

Promising Probes of the $E_{\text{sym}}(\rho)$ in Nuclear Reactions (an incomplete list !)

At sub-saturation densities (亚饱和密度行为)

- Sizes of n-skins of unstable nuclei from total reaction cross sections
- **Proton-nucleus elastic scattering in inverse kinematics**
- Parity violating electron scattering studies of the n-skin in ^{208}Pb
- **n/p ratio of FAST, pre-equilibrium nucleons**
- **Isospin fractionation and isoscaling in nuclear multifragmentation**
- **Isospin diffusion/transport**
- Neutron-proton differential flow
- **Neutron-proton correlation functions at low relative momenta**
- $t/{}^3\text{He}$ ratio
- **Hard photon production**

Towards high densities reachable at CSR/Lanzhou, FAIR/GSI, RIKEN, GANIL and, FRIB/MSU (高密度行为)

- **π^-/π^+ ratio, K^+/K^0 ratio?**
- Neutron-proton differential transverse flow
- **n/p ratio at mid-rapidity**
- Nucleon elliptical flow at high transverse momenta
- **n/p ratio of squeeze-out emission**

B.A. Li, L.W. Chen, C.M. Ko
Phys. Rep. 464, 113(2008)
Citations: 1020+



An incomplete list

- Cooling Storage Ring (**CSR**) Facility at HIRFL/Lanzhou in China (2008)
up to 500 MeV/A for ^{238}U (~1 GeV/A for C)
<http://www.impcas.ac.cn/zhuye/en/htm/247.htm>
- Radioactive Ion Beam Factory (**RIBF**) at RIKEN in Japan (2007)
<http://www.riken.jp/engn/index.html>
- Texas A&M Facility for Rare Exotic Beams -T-REX (2013)
<http://cyclotron.tamu.edu>
- Facility for Antiproton and Ion Research (**FAIR**)/GSI in Germany (2022?)
up to 2 GeV/A for ^{132}Sn (**NUSTAR** - NUClear STructure, Astrophysics and Reactions)
http://www.gsi.de/fair/index_e.html
- **SPIRAL2**/GANIL in France (2013)
<http://pro.ganil-spiral2.eu/spiral2>
- Selective Production of Exotic Species (**SPES**)/INFN in Italy (2015)
<http://web.infn.it/spes>
- Facility for Rare Isotope Beams (**FRIB**)/MSU in USA (2022?)
up to 400(200) MeV/A for ^{132}Sn
<http://www.frib.msu.edu/>
- The Korean Rare Isotope Accelerator (KoRIA-**RAON**(**RISP Accelerator Complex**)) (2021?)
up to 250 MeV/A for ^{132}Sn , up to 109 pps

.....



三、中能重离子碰撞与核物质对称能

- 核物质的对称能
- 对称能与重离子碰撞

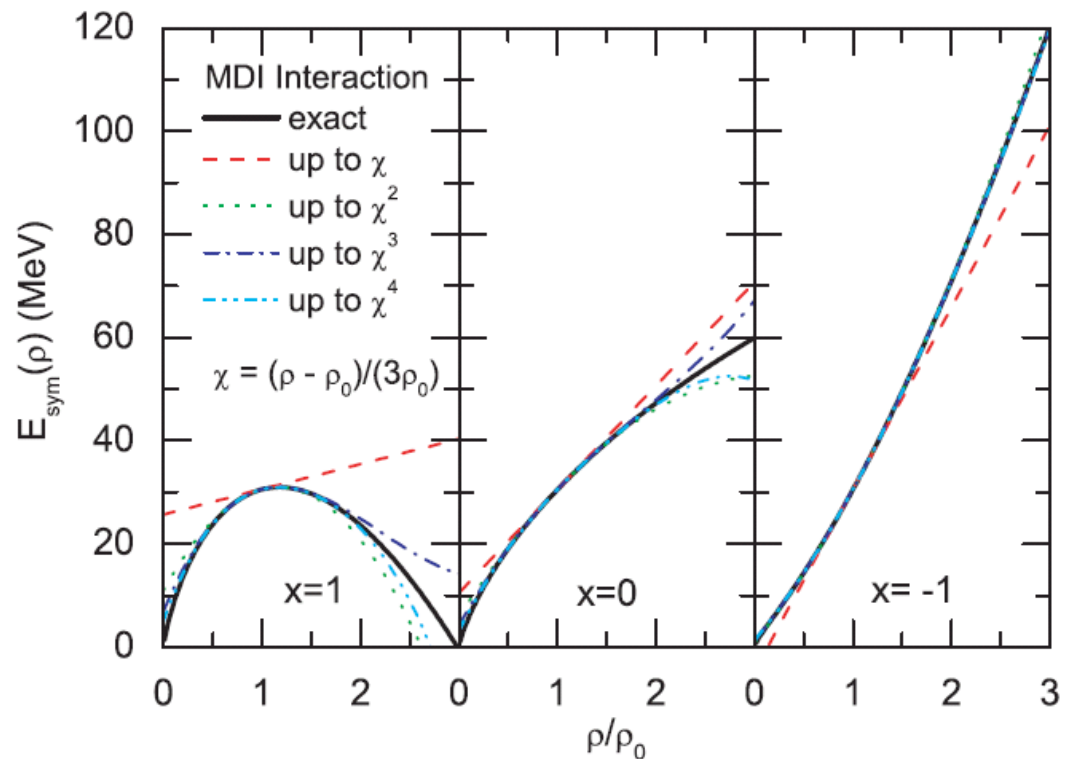
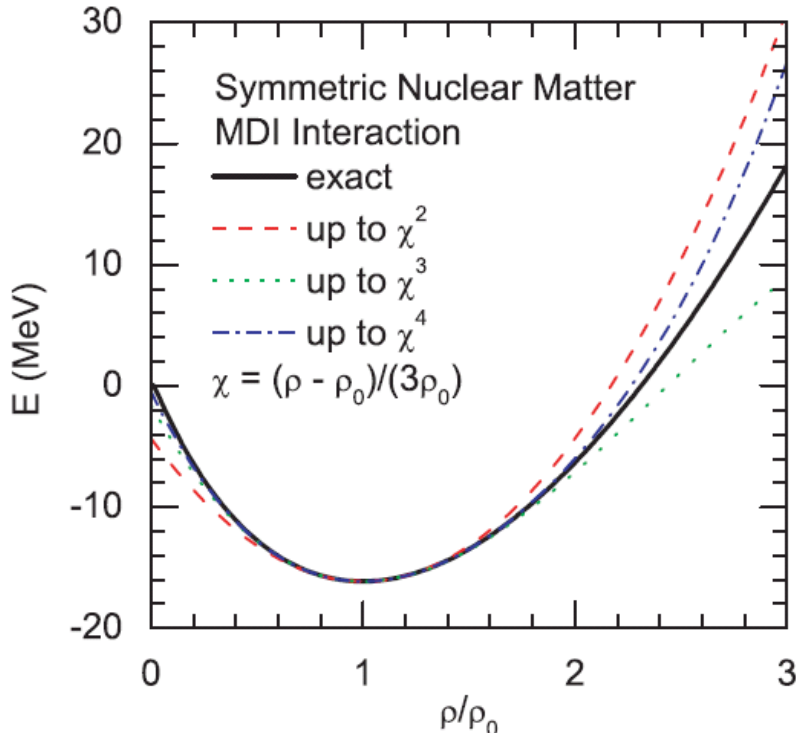


重离子碰撞：对称核物质的状态方程

Why Heavy-Ion Collisions?

It is very difficult to obtain information on the nuclear matter EOS at higher densities from nuclear properties around normal density which can be extracted from nuclear structure of finite nuclei and nuclear excitation!

LW Chen et al., PRC80, 014322 (2009) $E_{\text{sym}}(\rho) = E_{\text{sym}}(\rho_0) + L\chi + \frac{K_{\text{sym}}}{2!}\chi^2 + \frac{J_{\text{sym}}}{3!}\chi^3 + \frac{I_{\text{sym}}}{4!}\chi^4 + O(\chi^5)$



$$E_0(\rho) = E_0(\rho_0) + L_0\chi + \frac{K_0}{2!}\chi^2 + \frac{J_0}{3!}\chi^3 + \frac{I_0}{4!}\chi^4 + O(\chi^5)$$



Isospin-dependent BUU (IBUU) model

Phase-space distributions $f(\vec{r}, \vec{p}, t)$ satisfy the Boltzmann equation

$$\frac{\partial f(\vec{r}, \vec{p}, t)}{\partial t} + \vec{\nabla}_p \varepsilon \cdot \vec{\nabla}_r f - \vec{\nabla}_r \varepsilon \cdot \vec{\nabla}_p f = I_c(f, \sigma_{NN})$$

- Solve the Boltzmann equation using test particle method
- Isospin-dependent initialization
- Isospin- (momentum-) dependent **mean field potential**

$$V = V_0 + \frac{1}{2}(1 - \tau_z)V_C + V_{\text{sym}}$$



- Isospin-dependent **N-N cross sections**
 - a. Experimental free space N-N cross section σ_{exp}
 - b. In-medium N-N cross section from the Dirac-Brueckner approach based on Bonn A potential $\sigma_{\text{in-medium}}$
 - c. Mean-field consistent cross section due to m^*
- Isospin-dependent **Pauli Blocking**



Transport model: IBUU04

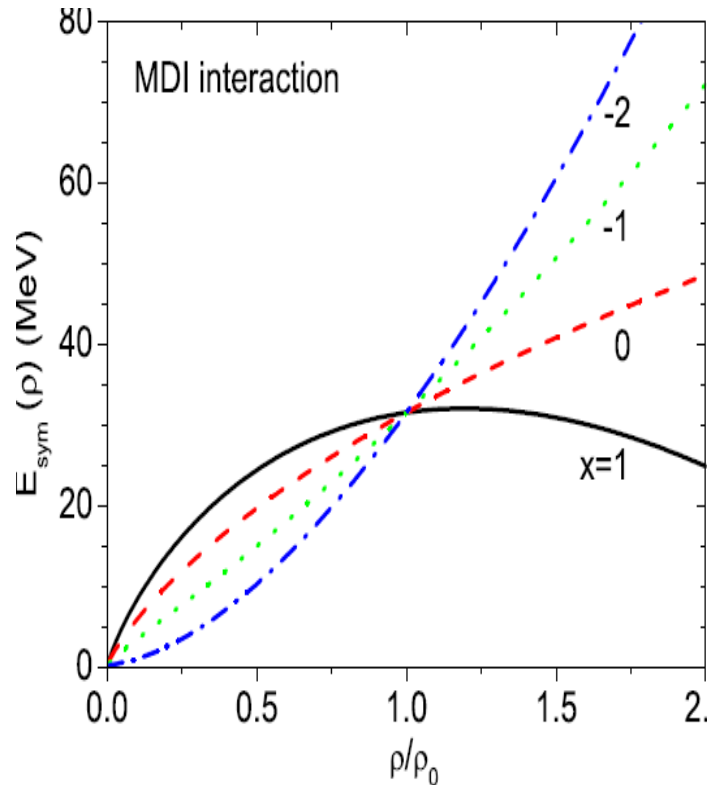
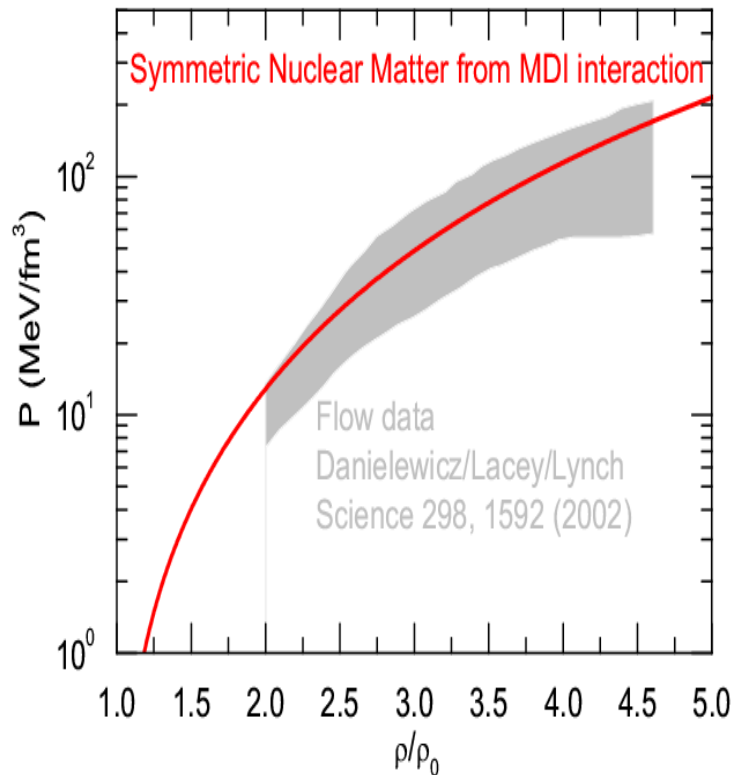
Isospin- and momentum-dependent potential (MDI)

Das/Das Gupta/Gale/Li,
PRC67,034611 (2003)

$$U(\rho, \delta, \vec{p}, \tau, x) = A_u(x) \frac{\rho_{\tau'}}{\rho_0} + A_l(x) \frac{\rho_{\tau}}{\rho_0} + B \left(\frac{\rho}{\rho_0} \right)^{\sigma} (1 - x \delta^2) - 8\tau x \frac{B}{\sigma + 1} \frac{\rho^{\sigma-1}}{\rho_0^{\sigma}} \delta \rho_{\tau'}$$

$$+ \frac{2C_{\tau, \tau}}{\rho_0} \int d^3 p' \frac{f_{\tau}(\vec{r}, \vec{p}')}{1 + (\vec{p} - \vec{p}')^2 / \Lambda^2} + \frac{2C_{\tau, \tau'}}{\rho_0} \int d^3 p' \frac{f_{\tau'}(\vec{r}, \vec{p}')}{1 + (\vec{p} - \vec{p}')^2 / \Lambda^2}$$

$$A_u(x) = -95.98 - x \frac{2B}{\sigma + 1}, \quad A_l(x) = -120.57 + x \frac{2B}{\sigma + 1}$$



MDI Interaction
(: Gogny)

$\rho_0 = 0.16 \text{ fm}^{-3}$
 $E(\rho_0) / A = -16 \text{ MeV}$
 $E_{\text{sym}}(\rho_0) = 31.6 \text{ MeV}$
 $K_0 = 211 \text{ MeV}$
 $m^* / m = 0.68$

Chen/Ko/Li,
PRL94,032701 (2005)

Li/Chen,
PRC72, 064611 (2005)



In-medium Nucleon-nucleon cross sections: Effective mass scaling model

● Neglecting medium effects on the transition matrix

● Medium effects: effective mass on the incoming current in initial state and level density of the final state

$$\sigma_{medium} / \sigma_{free} \approx \left(\frac{\mu_{NN}^*}{\mu_{NN}} \right)^2$$

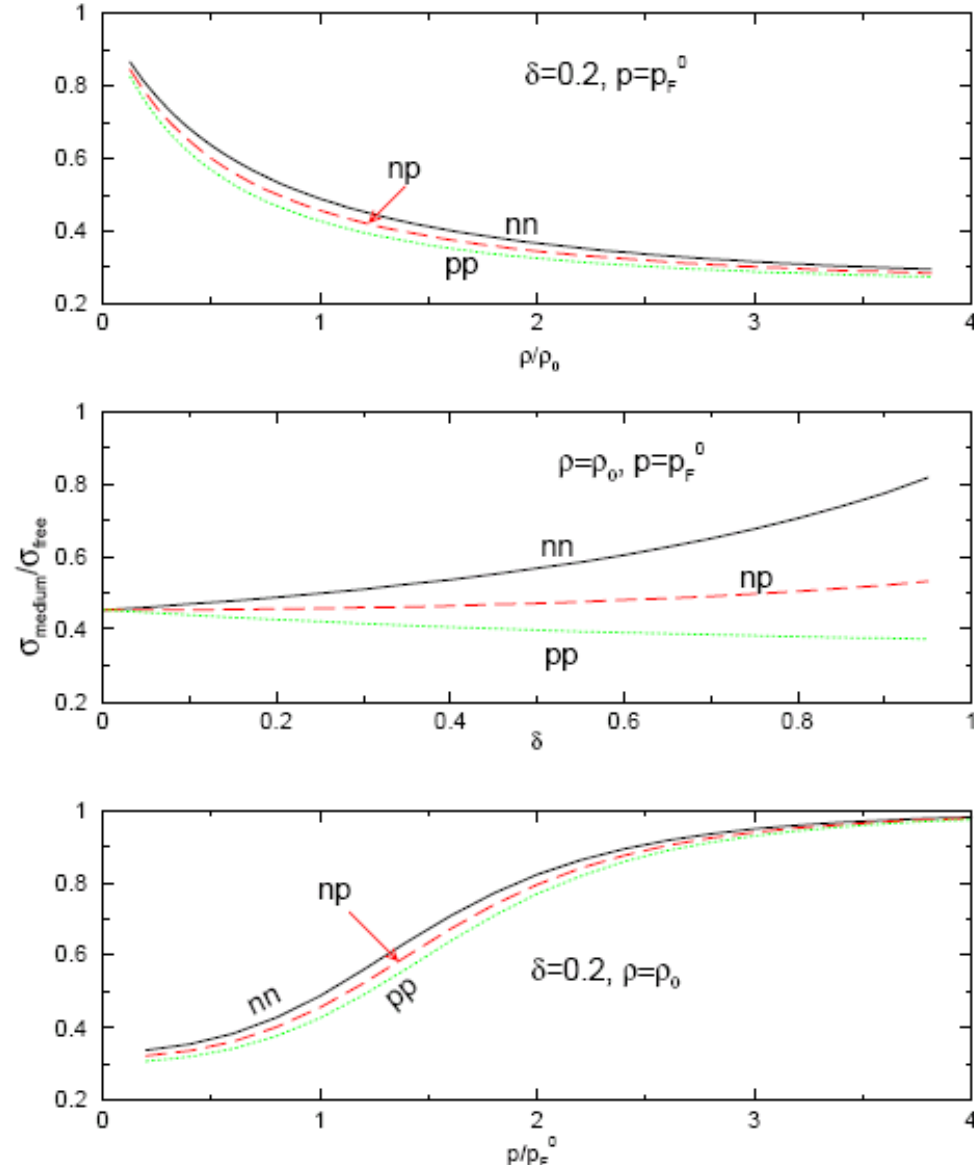
μ_{NN}^* is the reduced mass of the colliding pair NN in medium

J.W. Negele and K. Yazaki, PRL 47, 71 (1981)
V.R. Pandharipande and S.C. Pieper, PRC 45, 791 (1992)
M. Kohno et al., PRC 57, 3495 (1998)
D. Persram and C. Gale, PRC65, 064611 (2002).

1. In-medium cross sections are reduced
2. nn and pp cross sections are splitted due to the neutron-proton effective mass splitting in neutron-rich matter

Li/Chen, PRC72 (2005)064611

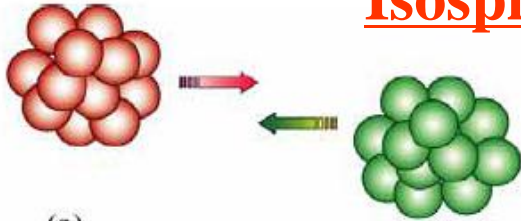
$\sigma_{medium} / \sigma_{free}$ in neutron-rich matter



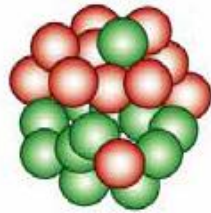


对称能探针：同位旋弥散

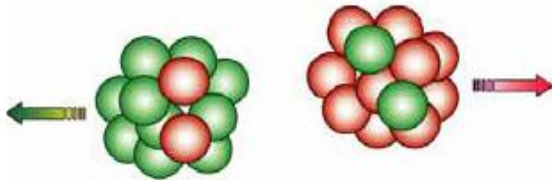
Isospin Diffusion/Transport



(a)



(b)



(c)

Particle Flux:

$$\Gamma_i = n_i (\underline{v}_i - \underline{v}),$$

Isospin Flow:

$$\Gamma_I = \Gamma_n - \Gamma_p = -n D_I \frac{\partial \delta}{\partial \mathbf{r}}.$$

Isospin diffusion coefficient D_I depends on the symmetry potential

L. Shi and P. Danielewicz,

Phys. Rev. C **68**, 017601 (2003).

How to measure
Isospin Diffusion?

F. Rami et al. (FOPI/GSI) **PRL84, 1120 (2000)**

A measure of isospin transport in the reaction A+B using any isospin tracer X

$$R_X = \frac{2X^{A+B} - X^{A+A} - X^{B+B}}{X^{A+A} - X^{B+B}}$$

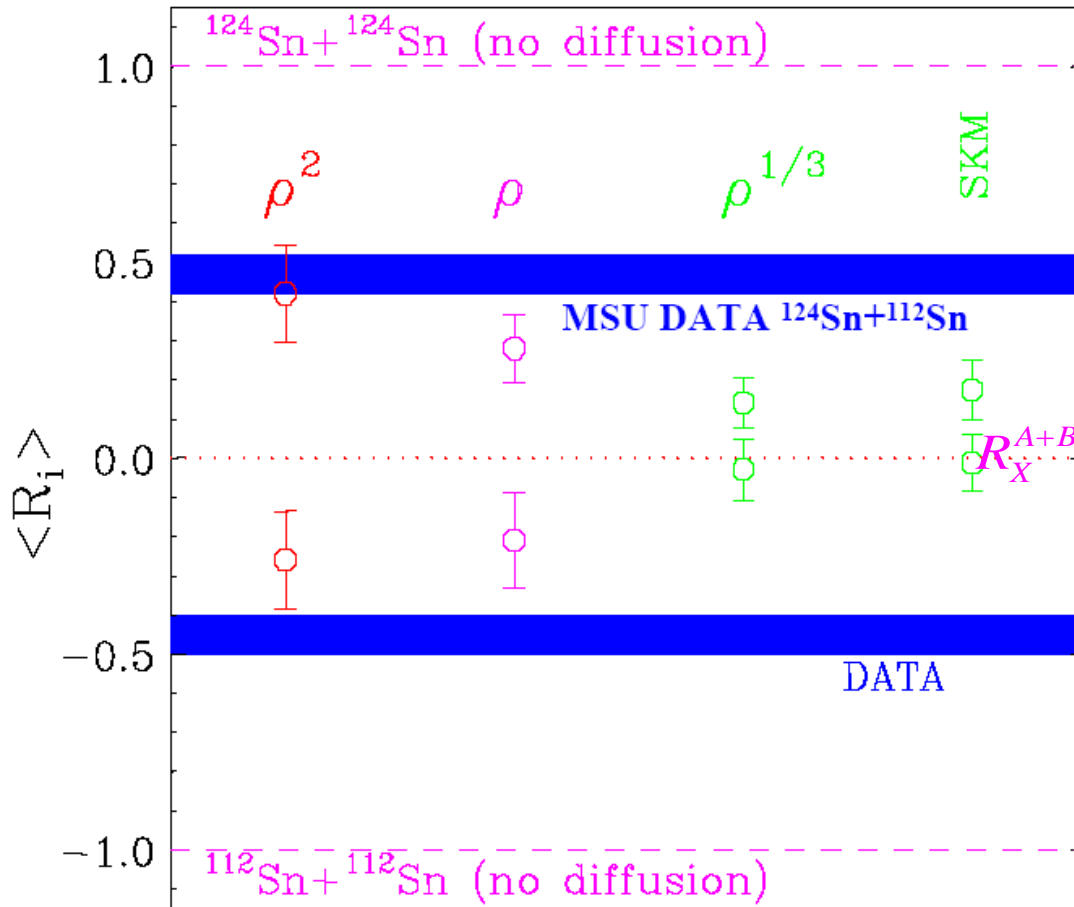
A+A, B+B, A+B

X: isospin tracer



对称能探针：同位旋弥散

Isospin diffusion in $^{124}\text{Sn}+^{112}\text{Sn}$ @ $E/A=50$ MeV and $b=6$ fm



Data favors a stiff symmetry

terms near

$$E_{\text{sym}}^{\text{int}}(\rho) \propto (\rho)^2$$

M.B. Tsang et al.

PRL 92, 062701

(2004)

≈ 0 If complete isospin mixing/ equilibrium

→ 0 (Stronger);

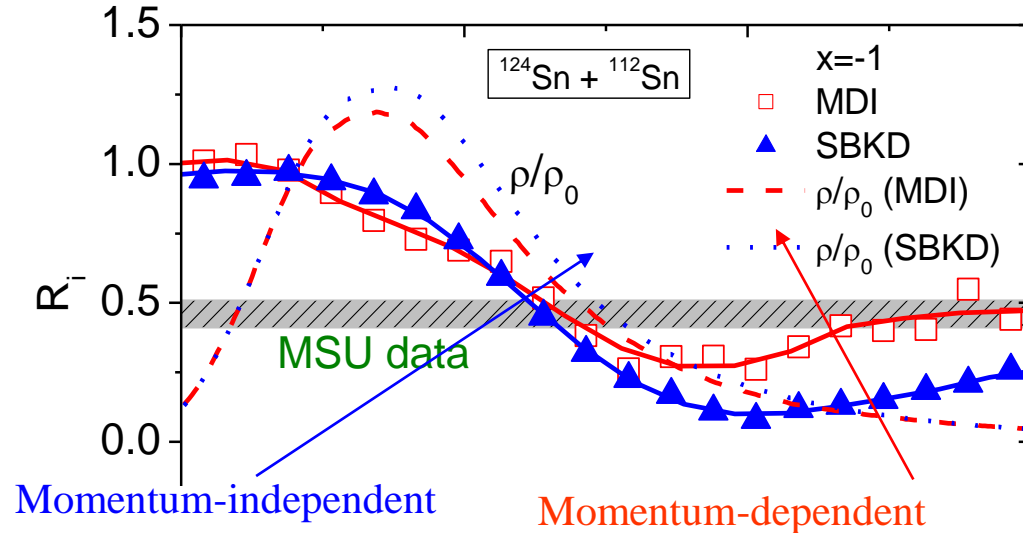
→ ± 1 (Weaker)

The theoretical analysis (BUU) did NOT include Momentum Dependence for nuclear potential !



对称能探针：同位旋弥散

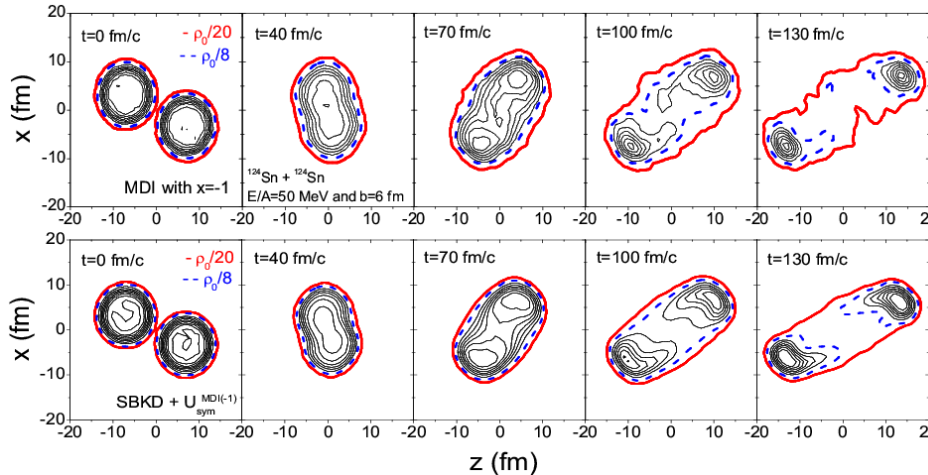
Comparing momentum-dependent IBUU04 calculations with data on isospin transport



Chen/Ko/Li,
PRL94, (2005) 032701

Citations: 437+

All have the same
 $E_{\text{sym}}(\rho) = 31.6 (\rho/\rho_0)^{1.05}$

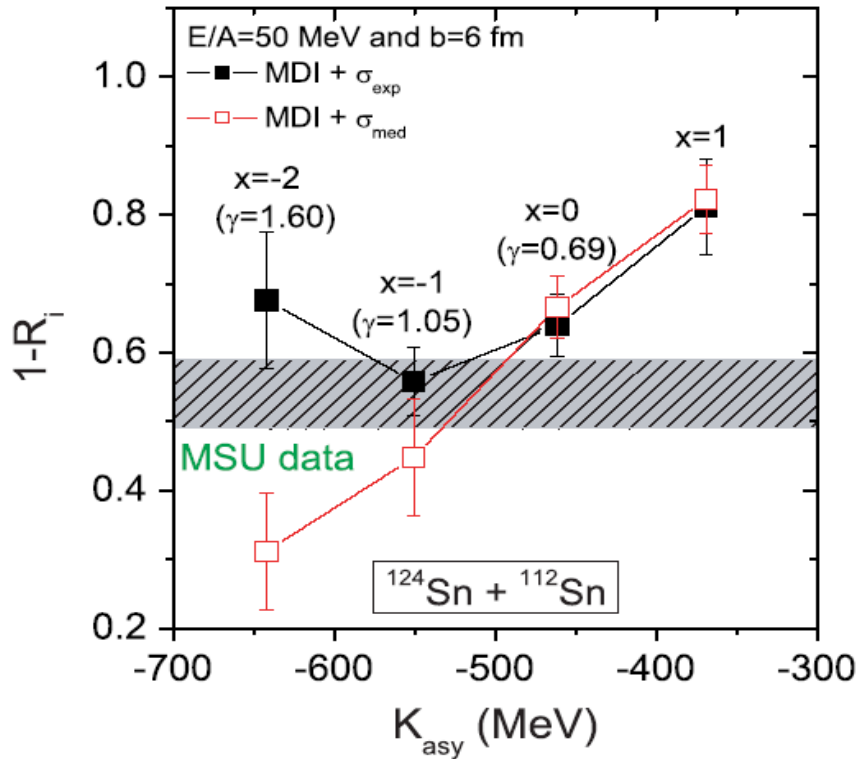




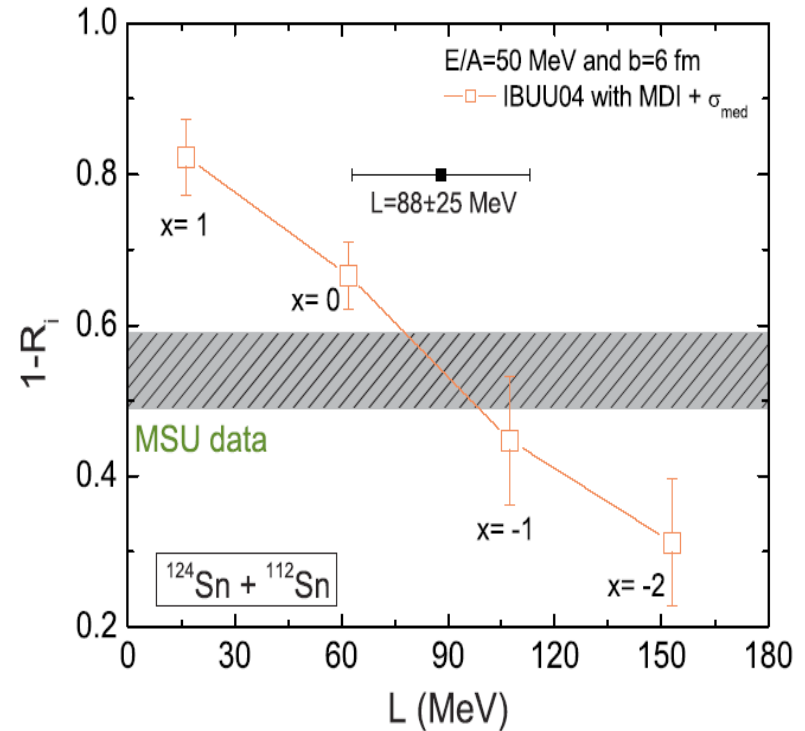
对称能探针：同位旋弥散

Symmetry energy, isospin diffusion, in-medium cross section

Li/Chen, PRC72, 064611(2005)



Chen/Ko/Li, PRC72,064309 (2005)



Fit the symmetry energy with

$$E_{sym}(\rho) = 31.6(\rho / \rho_0)^\gamma \text{ MeV}$$

(From $0 \leq \rho \leq \rho_0$), we obtain:

$\gamma = 1.05$ for $x = -1$ and $\gamma = 0.69$ for $x = 0$

Isospin Diffusion Data →

$K_{asy} = -500 \pm 50$ MeV

$L = 86 \pm 25$ MeV

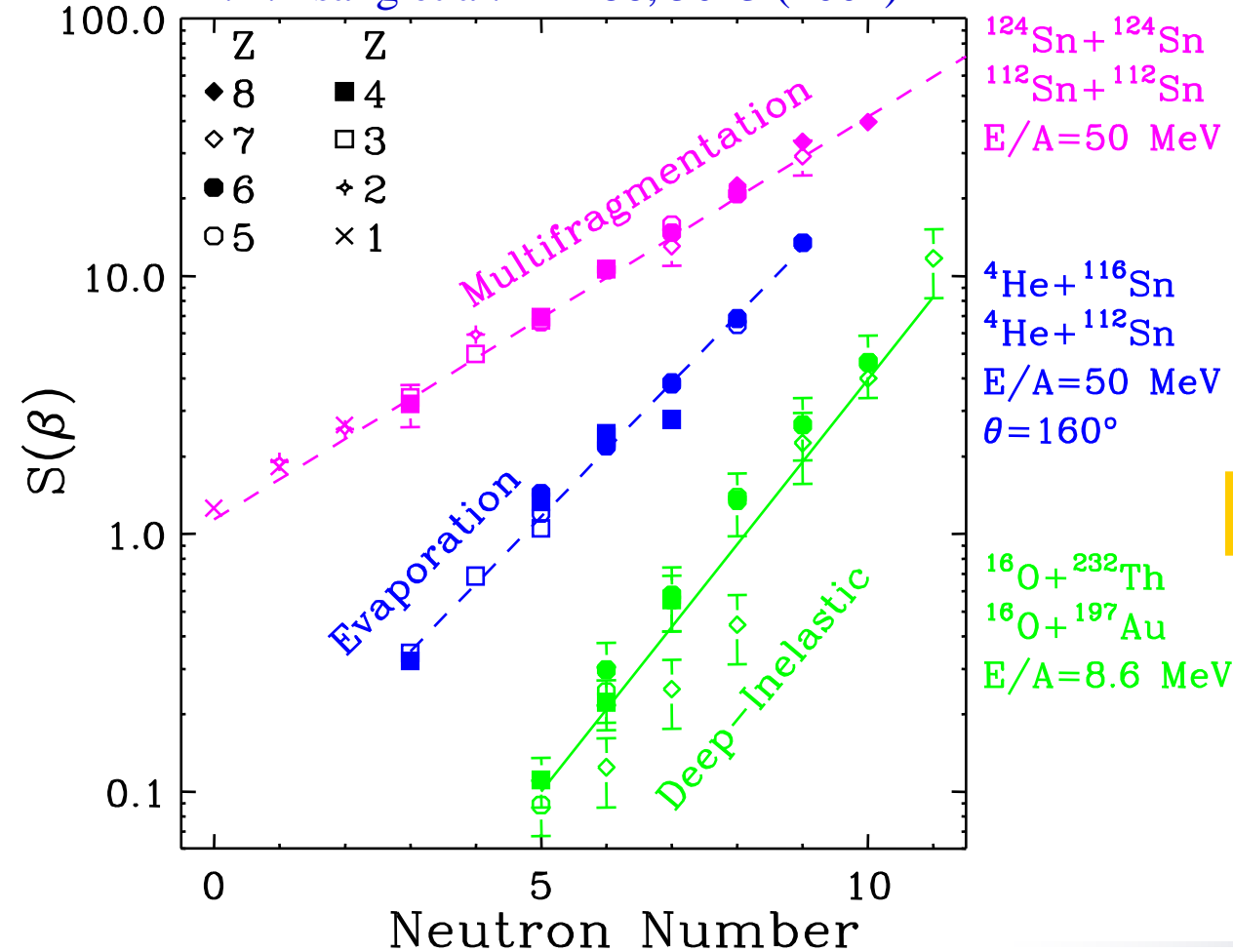


对称能探针：同位旋标度

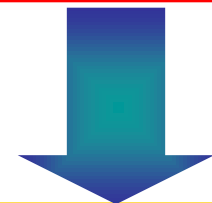
Isoscaling in HIC's

Isoscaling observed in many reactions

M.B. Tsang et al. PRL86, 5023 (2001)



$$Y_2 / Y_1 \propto e^{(N\Delta\mu_n + Z\Delta\mu_p) / T}$$



$$Y_2(N, Z) / Y_1(N, Z) \propto e^{\alpha N + \beta Z}$$

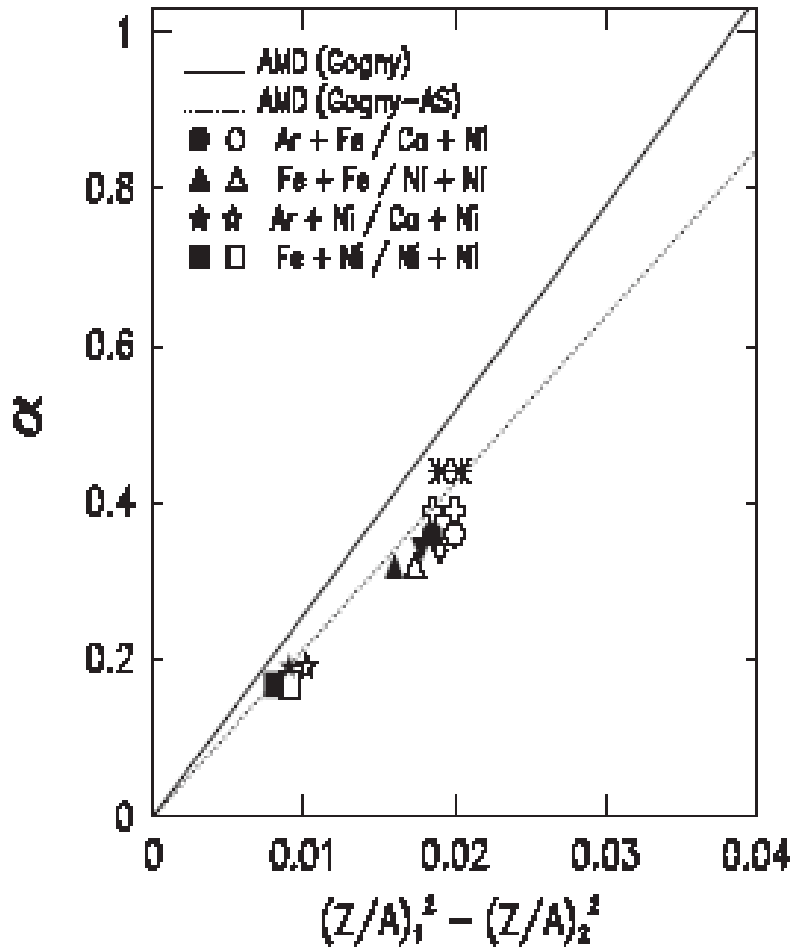


$$\alpha = \frac{4C_{\text{sym}}}{T} \left[(Z/A)_1^2 - (Z/A)_2^2 \right]$$

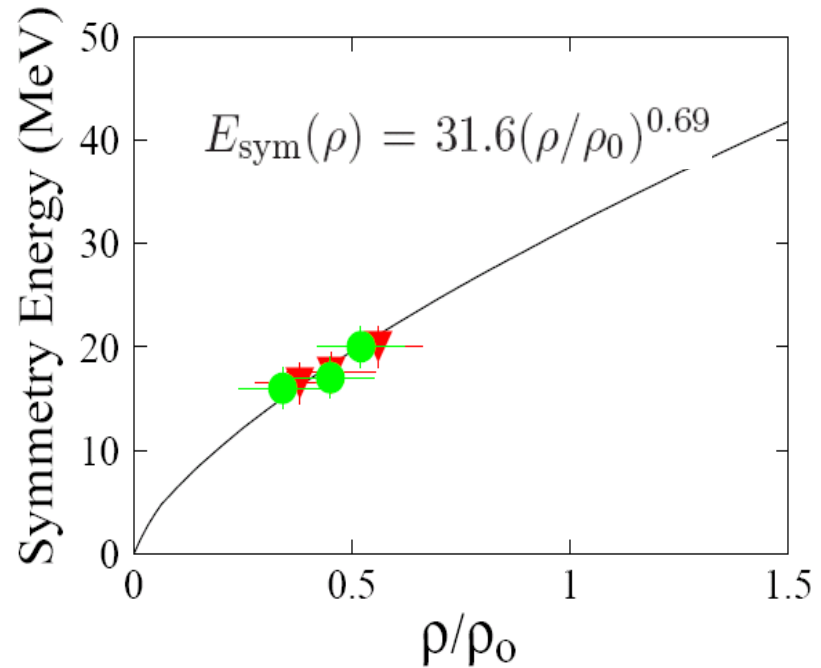


对称能探针：同位旋标度

Constraining Symmetry Energy by Isocaling: TAMU Data



Shetty et al.
PRC75(07);PRC76(07)

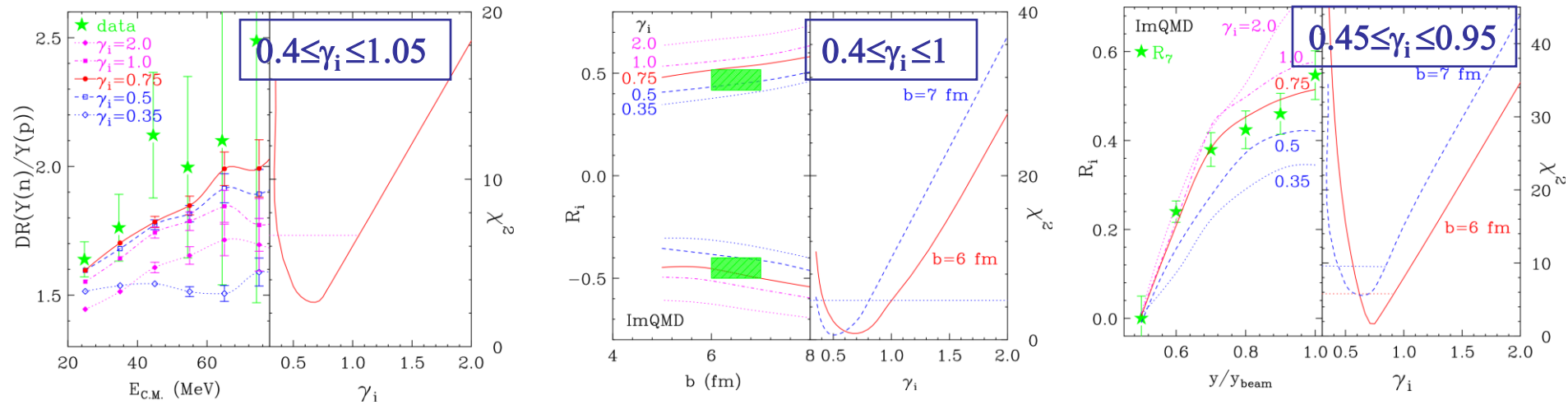


Consistent with isospin diffusion data!



ImQMD: n/p ratios and two isospin diffusion measurements

Tsang/Zhang/Danielewicz/Famiano/Li/Lynch/Steiner, PRL 102, 122701 (2009)



Consistent constraints from the χ^2 analysis of three observables

$$S = 12.5(\rho/\rho_0)^{2/3} + 17.6(\rho/\rho_0)^{\gamma_i}$$

$$0.4 \leq \gamma_i \leq 1.05$$

$$\text{IBUU04} : S \sim 31.6(\rho/\rho_0)^\gamma$$

$$0.69 \leq \gamma \leq 1.05$$



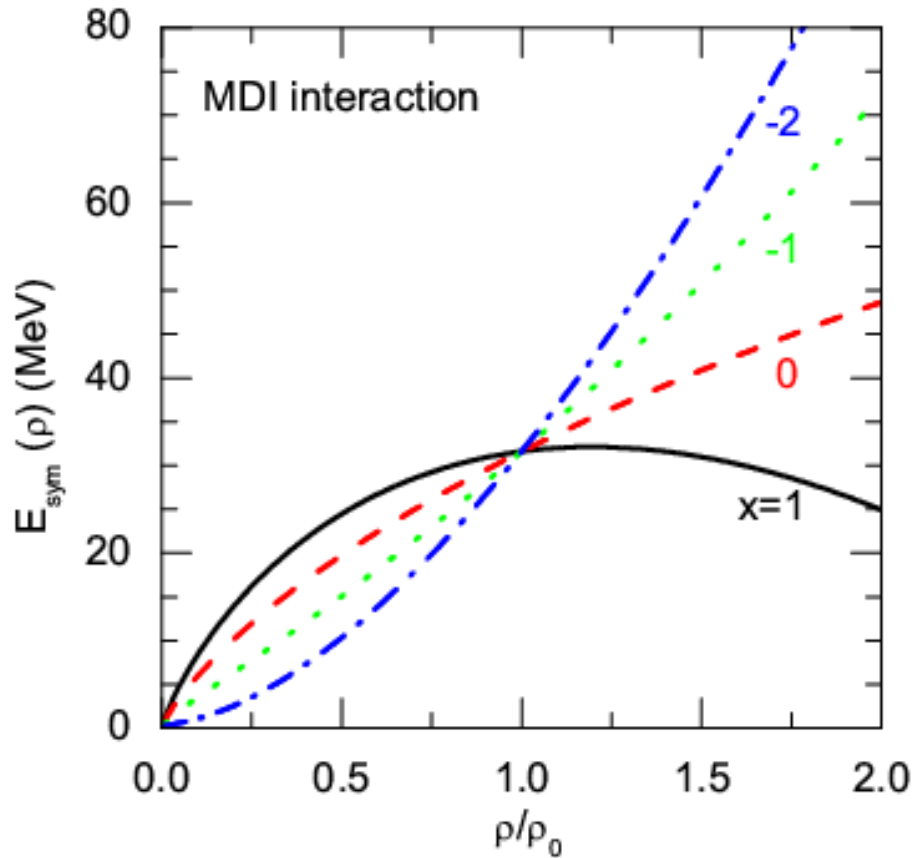
对称能的亚饱和密度行为

Symmetry energy constrained at **sub**-saturation densities

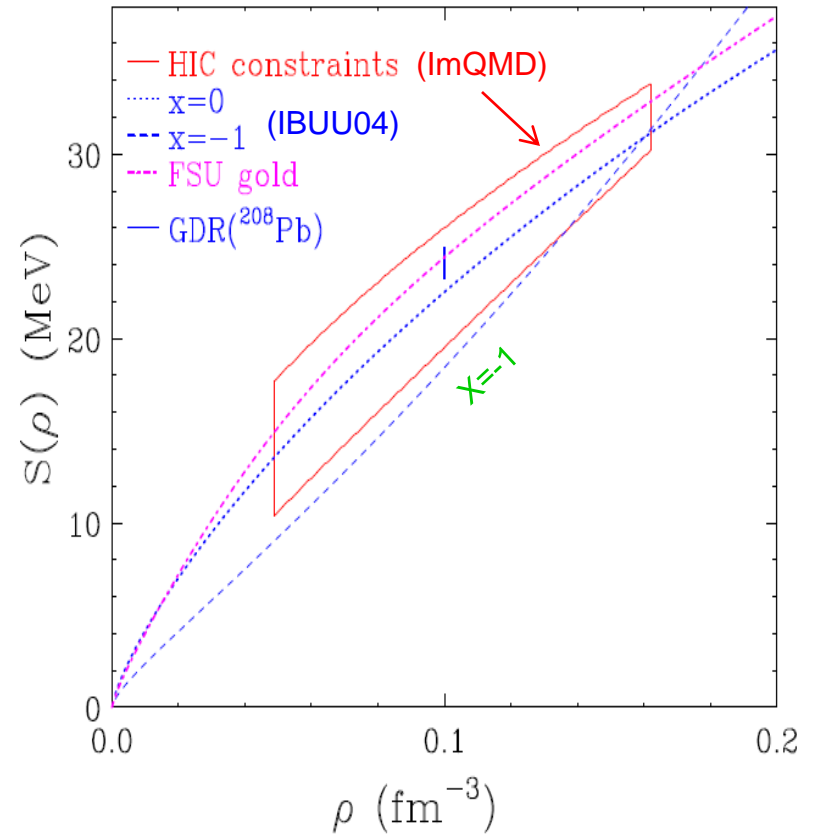
$$31.6(\rho / \rho_0)^{0.69} \leq E_{sym}(\rho) \leq 31.6(\rho / \rho_0)^{1.05} \quad (\text{亚饱和密度: } 0.2-0.3 < \rho/\rho_0 < 1.2)$$

between the $x = 0$ and $x = -1$ lines, agrees extremely well with the **APR**

Chen/Ko/Li, PRL 94, 032701 (2005)

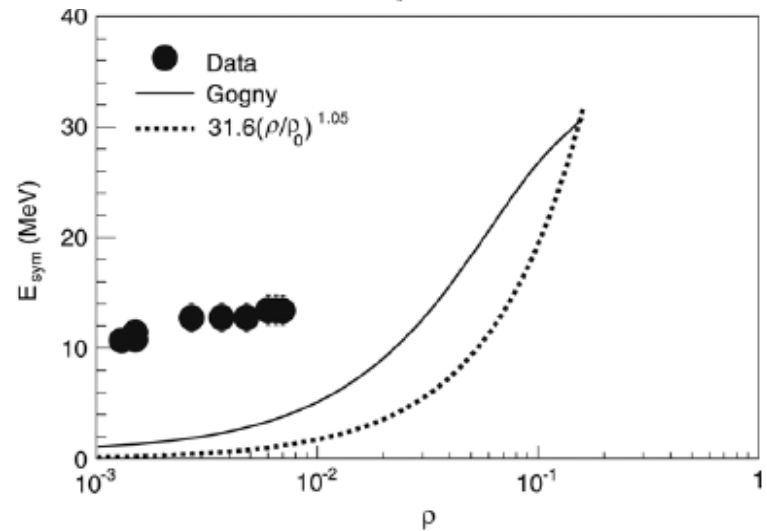
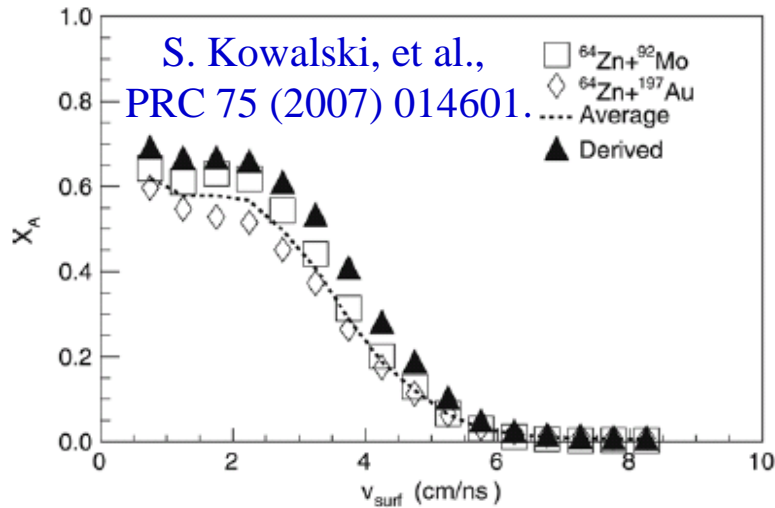
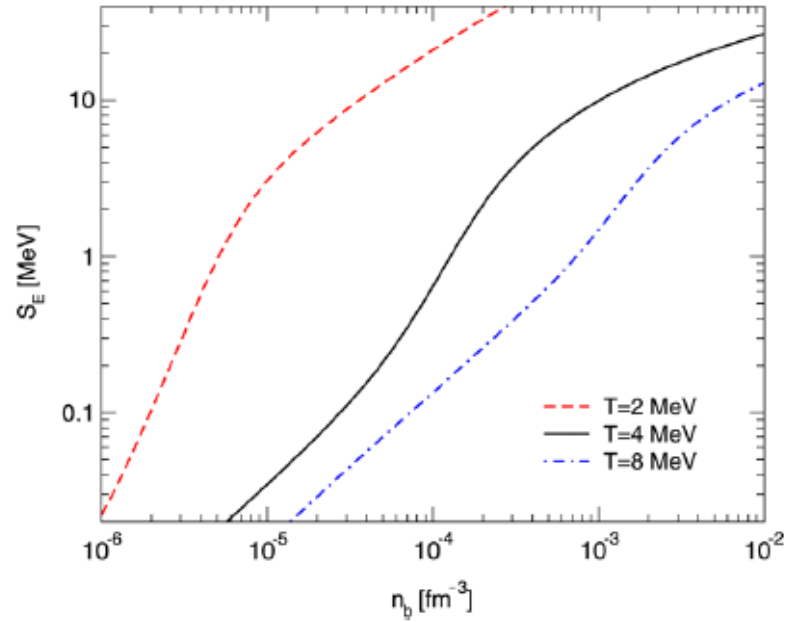
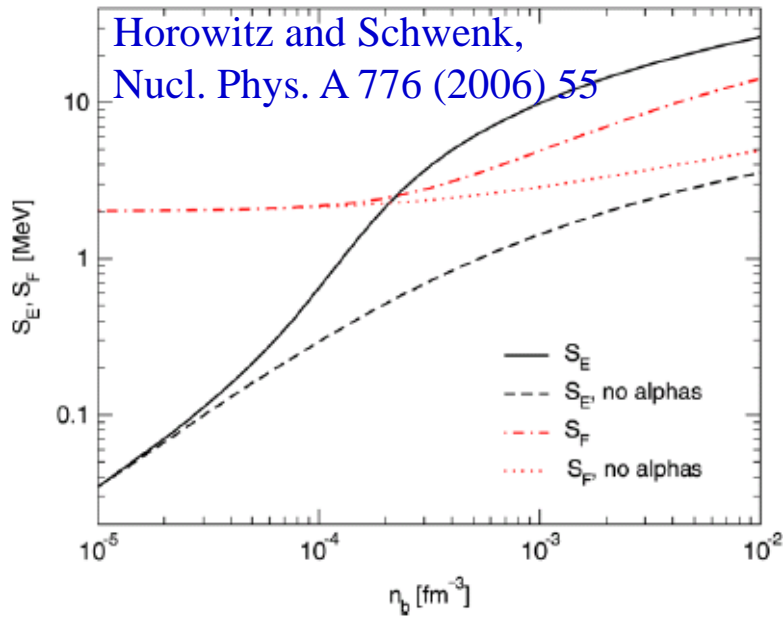


Tsang et al., PRL 102, 122701 (2009)





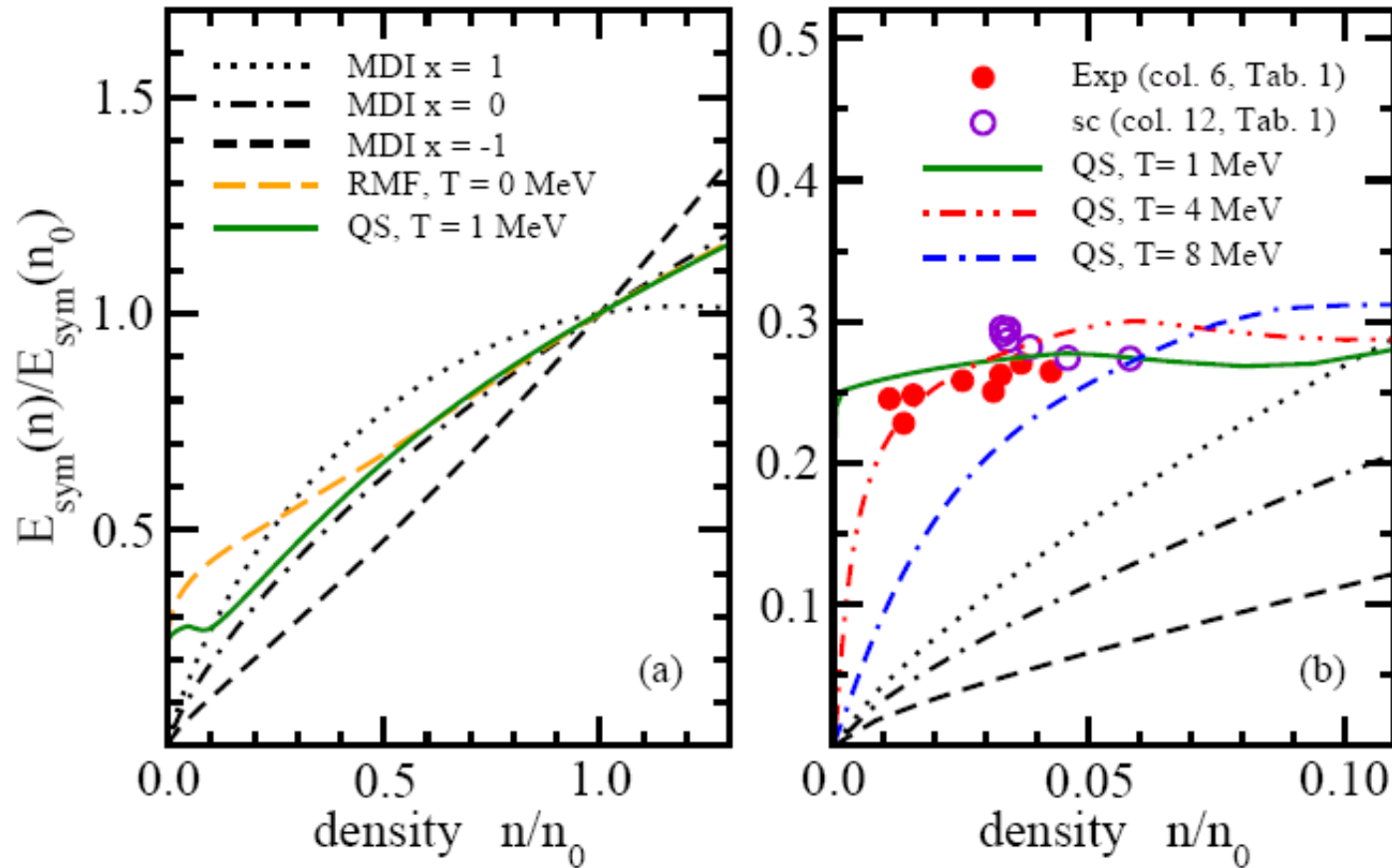
极端低密时的对称能：结团效应





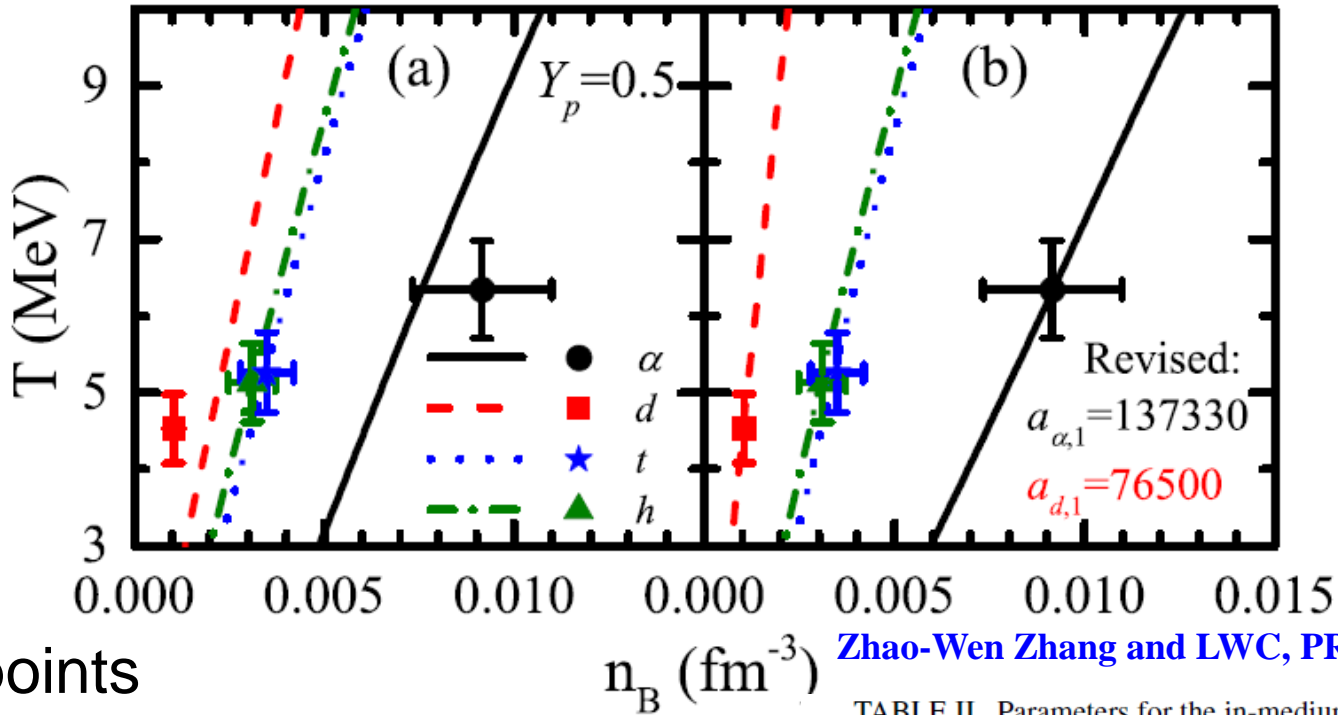
Symmetry Energy of Dilute Warm Nuclear Matter

J. B. Natowitz,¹ G. Röpke,² S. Typel,^{3,4} D. Blaschke,^{5,6} A. Bonasera,^{1,7} K. Hagel,¹ T. Klähn,^{5,8} S. Kowalski,¹ L. Qin,¹ S. Shlomo,¹ R. Wada,¹ and H. H. Wolter⁹





极端低密时的对称能：结团效应



Zhao-Wen Zhang and LWC, PRC95, 064330 (2017)

Mott points

The binding energy of clusters depend on T and n_B
Mott Point: Binding energy vanish

TABLE II. Parameters for the in-medium cluster binding energy shifts. The values are taken from Ref. [11] and the values of $a_{\alpha,1}$ and $a_{d,1}$ in the parentheses are the revised values in the present work to fit the experimental Mott densities [47].

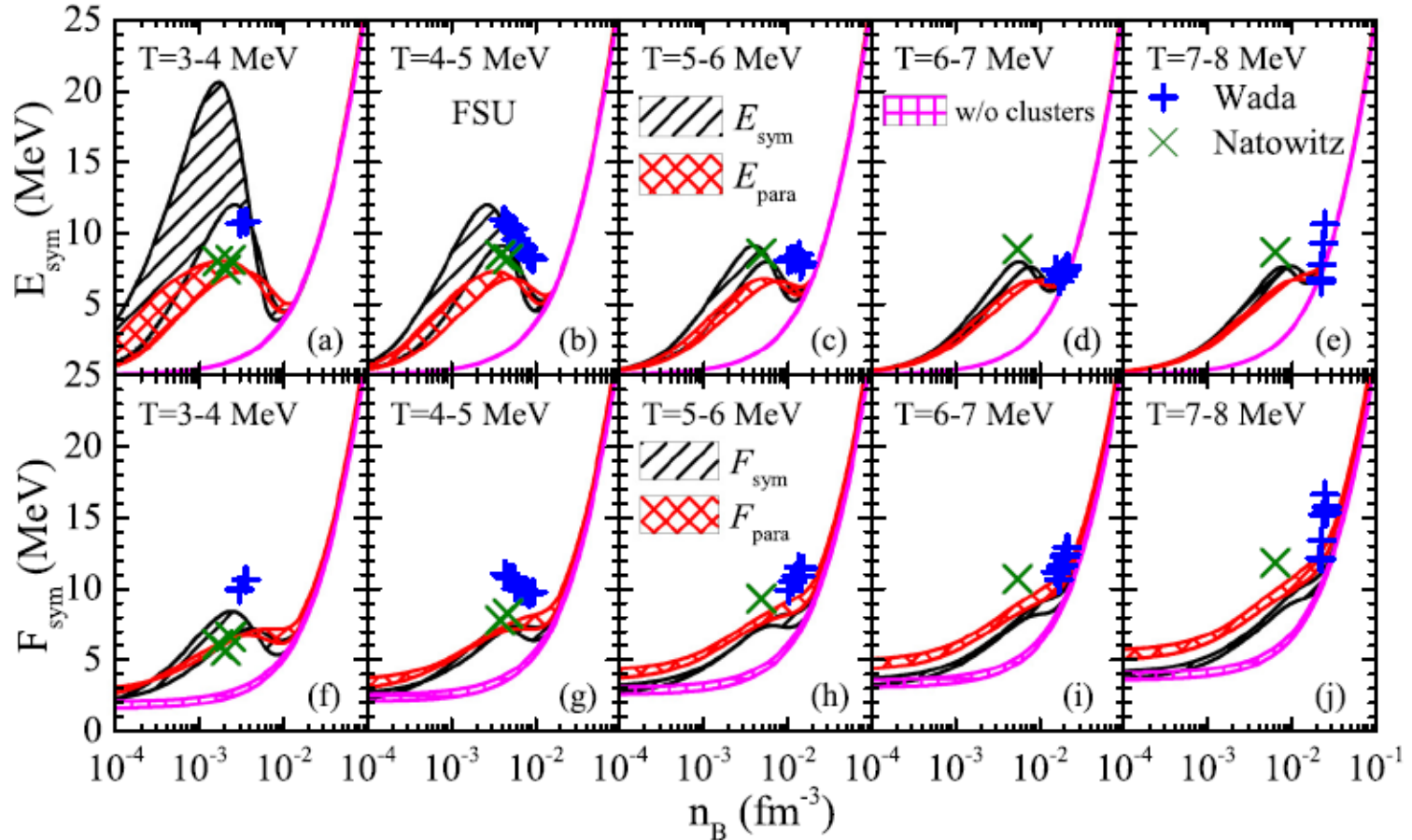
Cluster i	$a_{i,1}$ ($\text{MeV}^{5/2} \text{fm}^3$)	$a_{i,2}$ (MeV)	$a_{i,3}$ (MeV)	B_i^0 (MeV)
α	164371 (137330)	10.6701		28.29566
d	38386.4 (76500)	22.5204	0.2223	2.224566
t	69516.2	7.49232		8.481798
h	58442.5	6.07718		7.718043

Data of Mott points:
K. Hagel et al., Phys. Rev. Lett. 108, 062702 (2012)



极端低密时的对称能：结团效应

Zhao-Wen Zhang and LWC, PRC95, 064330 (2017)



● Experimental data can be reasonably reproduced

Data:

J.B. Natowitz, *et al.* Phys. Rev. Lett., 104, 202501 (2010), R. Wada *et al.*, Phys. Rev. C 85, 064618 (2012)



Light Cluster Production and Coalescence Model

The coalescence model

$$1 + 2 + \dots + M \rightarrow C$$

$$N_C = g_C \int \prod_{i=1}^M p_i \cdot d\sigma_i \frac{d^3 p_i}{(2\pi)^3 E_i} f_i(x_i; p_i) \rho_C^W(x_1, \dots, x_M; p_1, \dots, p_M)$$

$d\sigma_i$: The element of a spacelike hypersurface at freeze-out

ρ_C^W : Coalescence probability (Wigner phase-space density)

- Depends on constituents' **space-time structure** at freeze-out
- Neglecting the **binding energy effect** ($T \gg E_{\text{binding}}$),
Coalescence probability: Wigner phase-space density in the rest-frame of the cluster.
- **Rare process** has been assumed (the coalescence process can be treated **perturbatively**).

Higher energy collisions and higher energy cluster production!



对称能探针：轻粒子产生

Wigner phase-space density for Deuteron

Wigner transformation

$$\rho_d^W(\mathbf{r}, \mathbf{k}) = \int d^3 R e^{-ik \cdot \mathbf{r}} \phi(\mathbf{r} + \mathbf{R}/2) \phi^*(\mathbf{r} - \mathbf{R}/2)$$

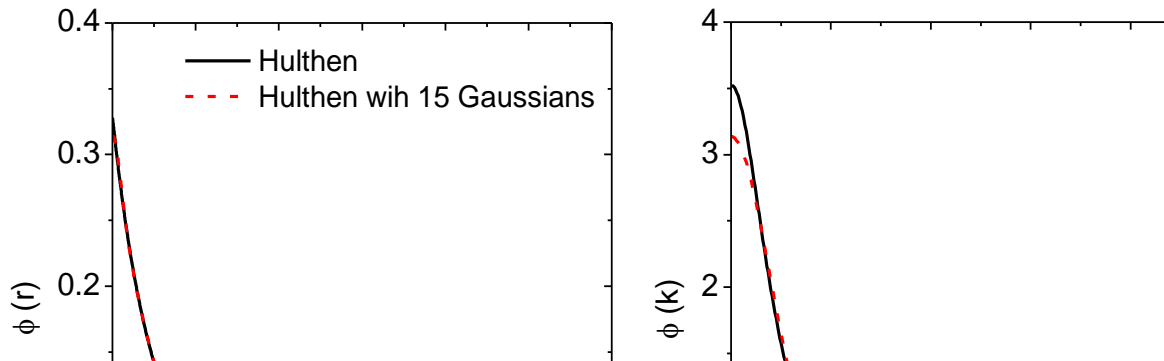
Hulthen wave function

$$\phi(r) = \sqrt{\frac{\alpha\beta(\alpha + \beta)}{2\pi(\alpha - \beta)^2}} \frac{e^{-\alpha r} - e^{-\beta r}}{r} \approx \sum_{i=1}^{15} c_i \left(\frac{2\omega_i}{\pi}\right)^{3/4} e^{-\omega_i r^2}$$

$$\alpha = 0.23 \text{ fm}^{-1}$$

$$\beta = 1.61 \text{ fm}^{-1}$$

$$\sqrt{\langle r^2 \rangle} = 1.89 \text{ fm}$$





Wigner phase-space density for $t/{}^3\text{He}$

Assume nucleon wave function in $t/{}^3\text{He}$ can be described by the harmonic oscillator wave function, i.e.,

$$\psi(\mathbf{r}) = \left(\frac{m\omega}{2\pi}\right)^{3/4} \exp\left(-\frac{1}{2}m\omega r^2\right)$$

with ω the harmonic oscillator frequency

$t/{}^3\text{He}$ Wigner phase-space density and root-mean-square radius:

$$\rho_{t/{}^3\text{He}}^W(\boldsymbol{\rho}, \boldsymbol{\lambda}; \mathbf{k}_\rho, \mathbf{k}_\lambda) = 8^2 \exp(-\rho^2 / \sigma_1^2 - \lambda^2 / \sigma_2^2 - \sigma_1^2 k_\rho^2 - \sigma_2^2 k_\lambda^2)$$

$$\langle r_{t/{}^3\text{He}}^2 \rangle = \frac{1}{2\omega} \frac{m_1^2(m_2 + m_3) + m_2^2(m_3 + m_1) + m_3^2(m_1 + m_2)}{(m_1 + m_2 + m_3)m_1m_2m_3} \quad (\text{t: 1.61 fm; } {}^3\text{He: 1.74 fm})$$

$$\boldsymbol{\rho} = \frac{1}{\sqrt{2}}(\mathbf{r}_1 - \mathbf{r}_2), \quad \boldsymbol{\lambda} = \sqrt{\frac{3}{2}}\left(\frac{m_1}{m_1 + m_2}\mathbf{r}_1 + \frac{m_2}{m_1 + m_2}\mathbf{r}_2 - \mathbf{r}_3\right) \quad (\text{Jacobi Transformation})$$

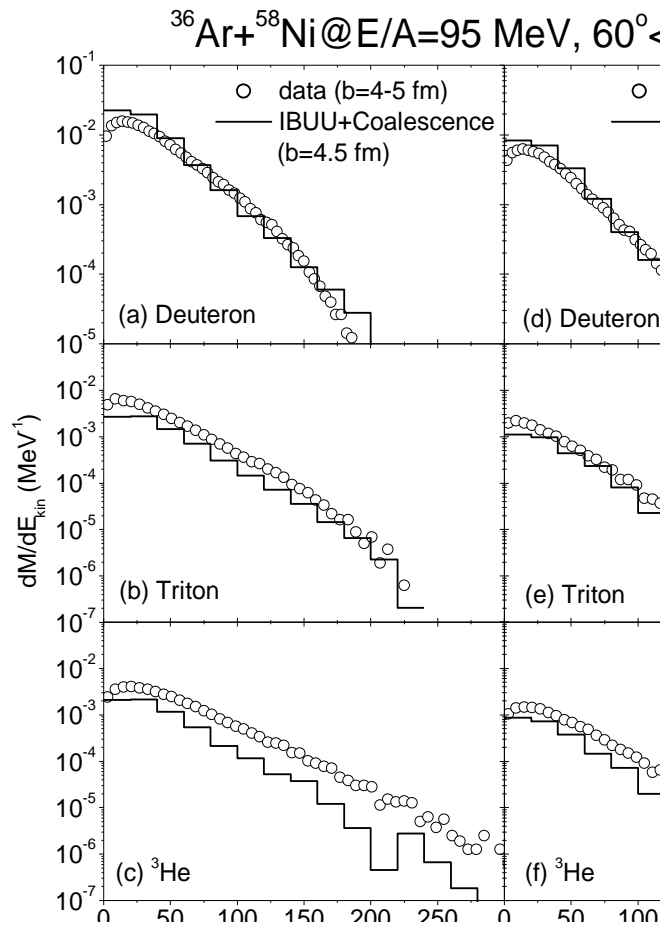
$$\mathbf{k}_\rho = \frac{\sqrt{2}}{m_1 + m_2}(m_2\mathbf{k}_1 - m_1\mathbf{k}_2), \quad \mathbf{k}_\lambda = \frac{\sqrt{6}}{2(m_1 + m_2 + m_3)}(m_3\mathbf{k}_1 + m_3\mathbf{k}_2 - (m_1 + m_2)\mathbf{k}_3)$$

$$\sigma_1^2 = (\mu_1\omega)^{-1} \quad \text{and} \quad \sigma_2^2 = (\mu_2\omega)^{-1} \quad \text{with}$$

$$\mu_1 = 2\left(\frac{1}{m_1} + \frac{1}{m_2}\right)^{-1} \quad \text{and} \quad \mu_2 = \frac{3}{2}\left(\frac{1}{m_1 + m_2} + \frac{1}{m_3}\right)^{-1}$$



Isospin symmetric collisions at $E/A \approx 100$ MeV



Try Coalescence model at intermediate energies!

- Deuteron energy spectra reproduced
- Low energy tritons slightly underestimated
- Inverse slope parameter of ^3He underestimated; probably due to neglect of
 - larger binding effect
 - stronger Coulomb effect
 - wave function

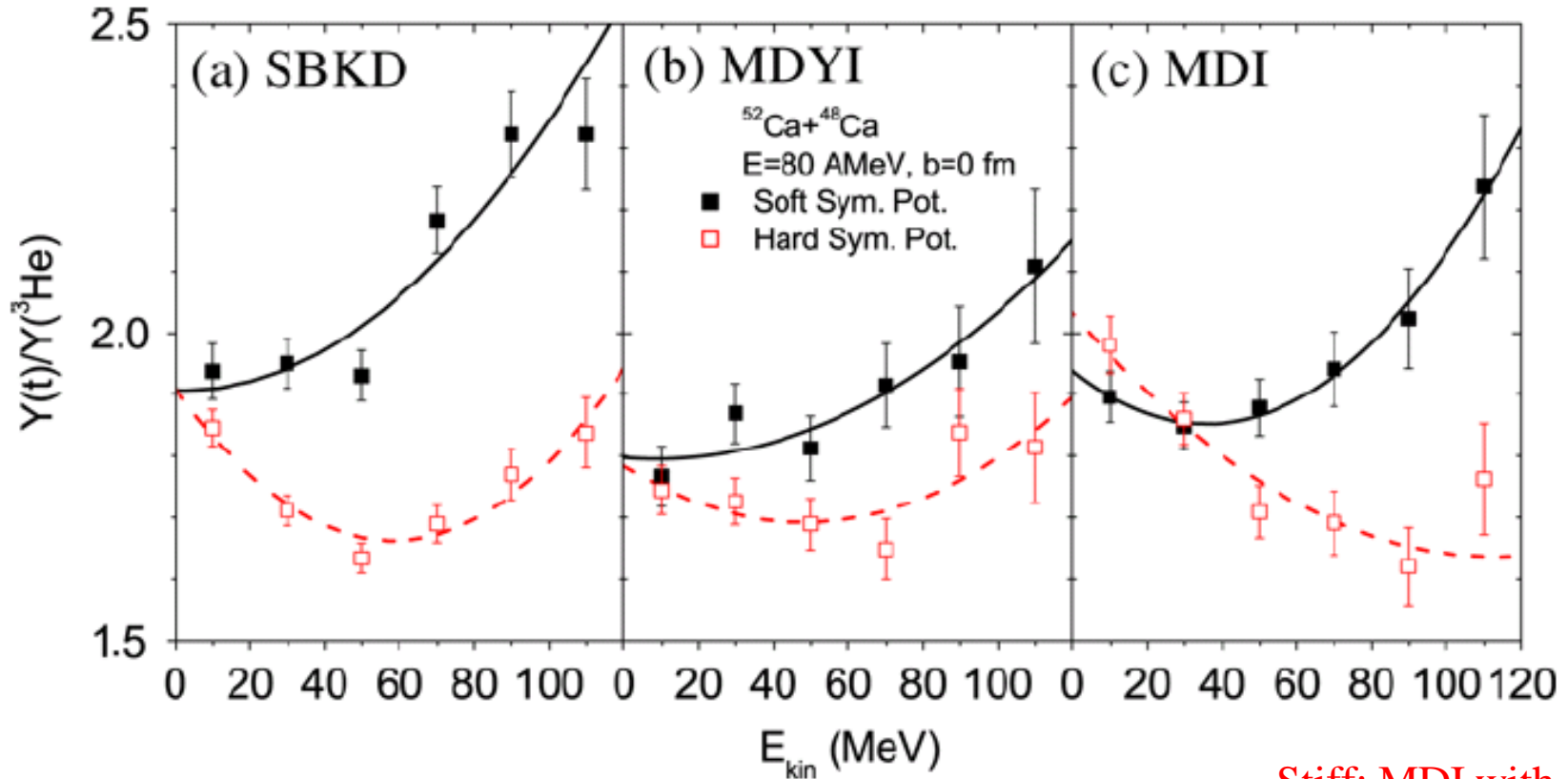
Chen/Ko/Li, NPA729, 809 (2003)

Data are taken from INDRA Collaboration (P. Pawlowski, EPJA9)



对称能探针：轻粒子产生

Symmetry Energy Effects on $t/{}^3\text{He}$ ratio



Stiff: MDI with $x = -2$

Soft: MDI with $x = 1$

Stiffer symmetry energy gives smaller $t/{}^3\text{He}$ ratio



对称能探针：轻粒子产生

Effects of momentum-dependence of nuclear potential

$t/{}^3\text{He}$ ratio

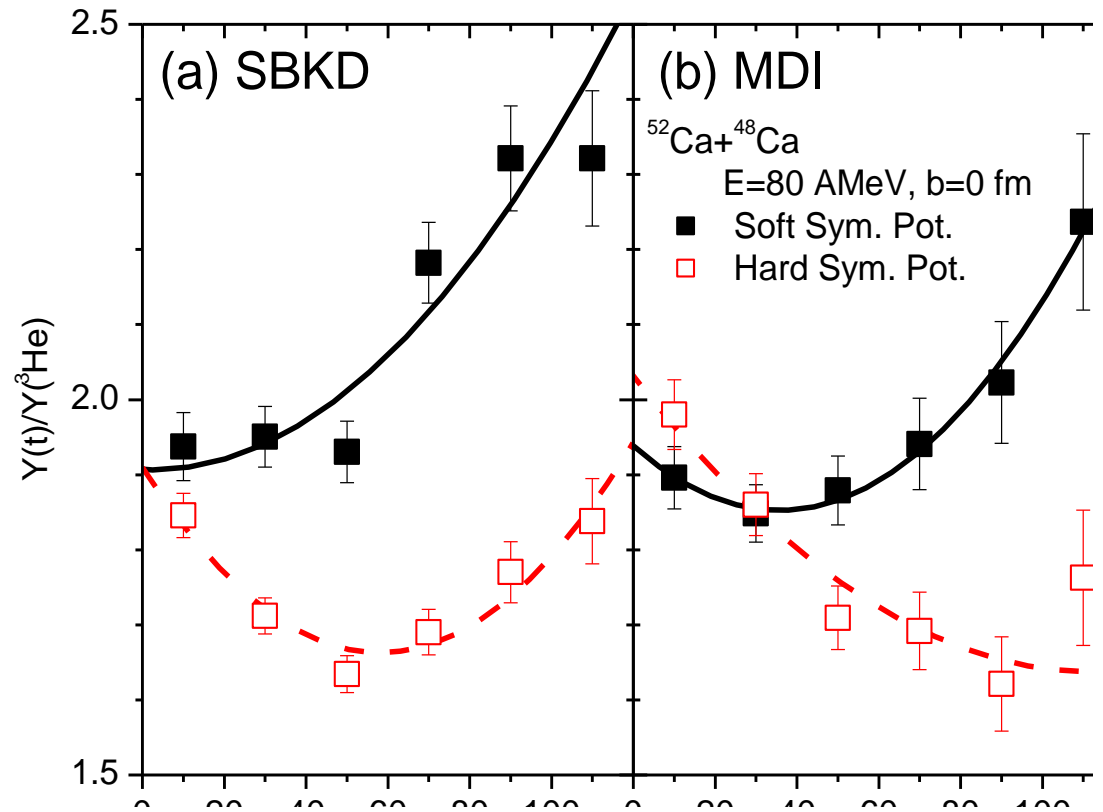
Chen/Ko/Li,
PRC69, 054606 (2004)

Stiff Symmetry Energy:

MDI with $x = -2$

Soft Symmetry Energy:

MDI with $x = 1$



Still sensitive to the symmetry energy



Two-Nucleon Correlation Functions

How to detect the space-time structure of nucleon emission experimentally?

The two-particle correlation function is obtained by convoluting the emission function $g(\mathbf{p}, x)$, i.e., the probability of emitting a particle with momentum \mathbf{p} from space-time point $x=(\mathbf{r}, t)$, with the relative wave function of the two particle, i.e.,

$$C(\mathbf{P}, \mathbf{q}) = \frac{\int d^4 x_1 d^4 x_2 g(\mathbf{P}/2, x_1) g(\mathbf{P}/2, x_2) |\phi(\mathbf{q}, \mathbf{r})|^2}{\int d^4 x_1 g(\mathbf{P}/2, x_1) \int d^4 x_2 g(\mathbf{P}/2, x_2)}$$

$$\mathbf{P} = \mathbf{p}_1 + \mathbf{p}_2, \quad \mathbf{q} = (\mathbf{p}_1 - \mathbf{p}_2)/2$$

$\phi(\mathbf{q}, \mathbf{r})$ is the relative two-particle wavefunction

The two-particle correlation function is a sensitive probe to the space-time structure of particle emission source by final state interaction and quantum statistical effects ($\phi(\mathbf{q}, \mathbf{r})$)

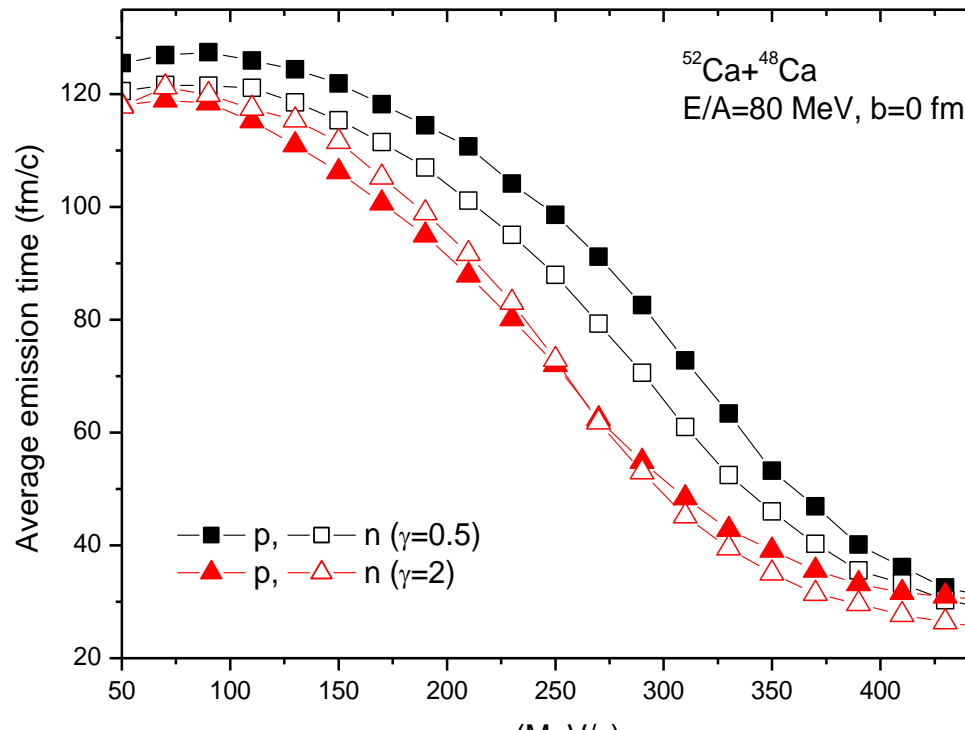
Correlation After Burner (Crab):

including final-state nuclear and Coulomb interactions (S. Pratt, NPA 566, 103 (1994))



Space-time structure of nucleon emission

Emission times from IBUU

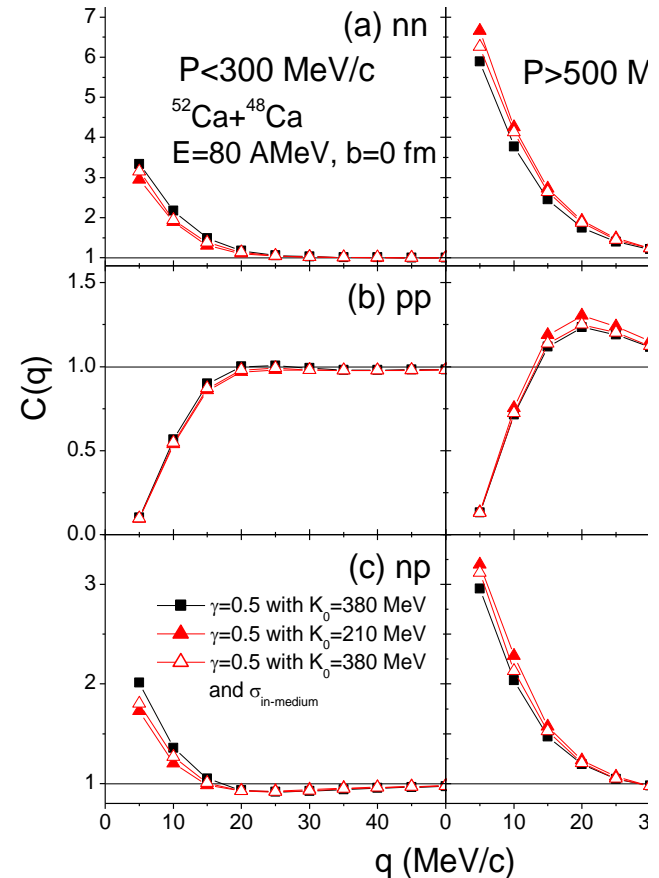
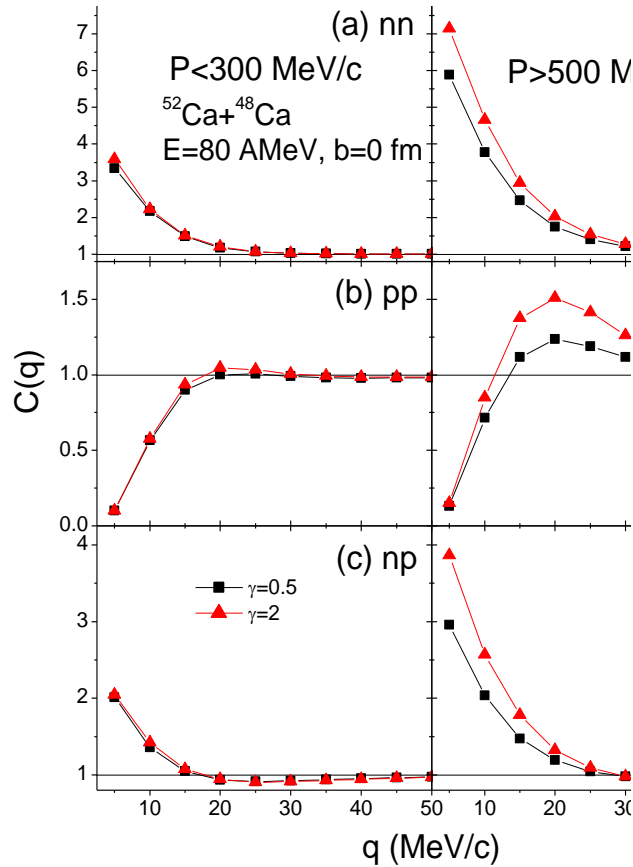


Chen/Ko/Li,
PRL90, 162701 (2003)

- High momentum nucleons emitted earlier than low momentum ones
- Earlier emissions for stiffer symmetry energy
- Larger separation in neutron and proton emission times for softer symmetry energy



Symmetry Energy Effects on Two-Nucleon Correlation Functions



Pairs with P > 500 MeV:

n-n CF: 20%
p-p CF: 20%
n-p CF: 30%

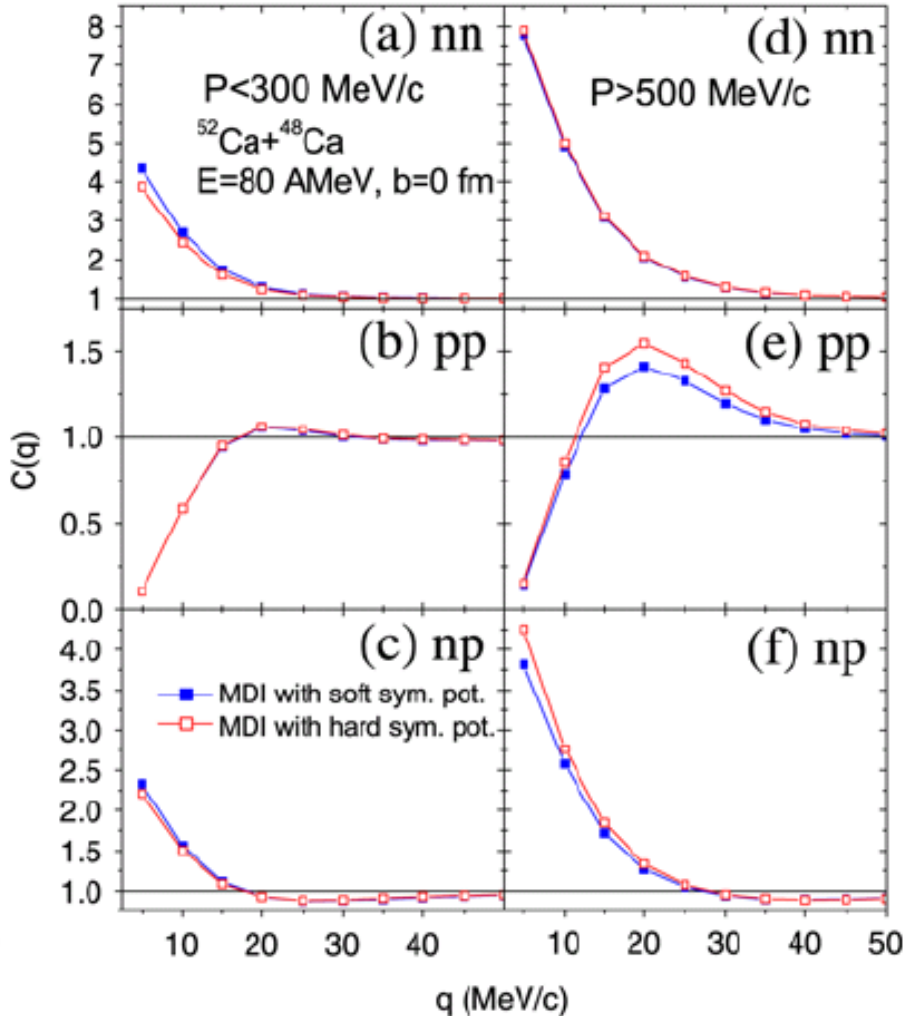
Chen/Ko/Li,
PRL90, 162701 (2003)

Effects are very small for
both **isoscalar potential** and
N-N cross sections



Effects of momentum-dependence of nuclear potential

Chen/Ko/Li, PRC69, 054606 (2004)



MDI

Das, Das Gupta, Gale and Li
PRC67, (2003)

Stiff Symmetry Energy: MDI with $x = -2$

Soft Symmetry Energy: MDI with $x = 1$

Pairs with $P > 500$ MeV:

n-p CF: 11%

The isospin effects on two-particle correlation functions are really observed in recent experimental data !!!

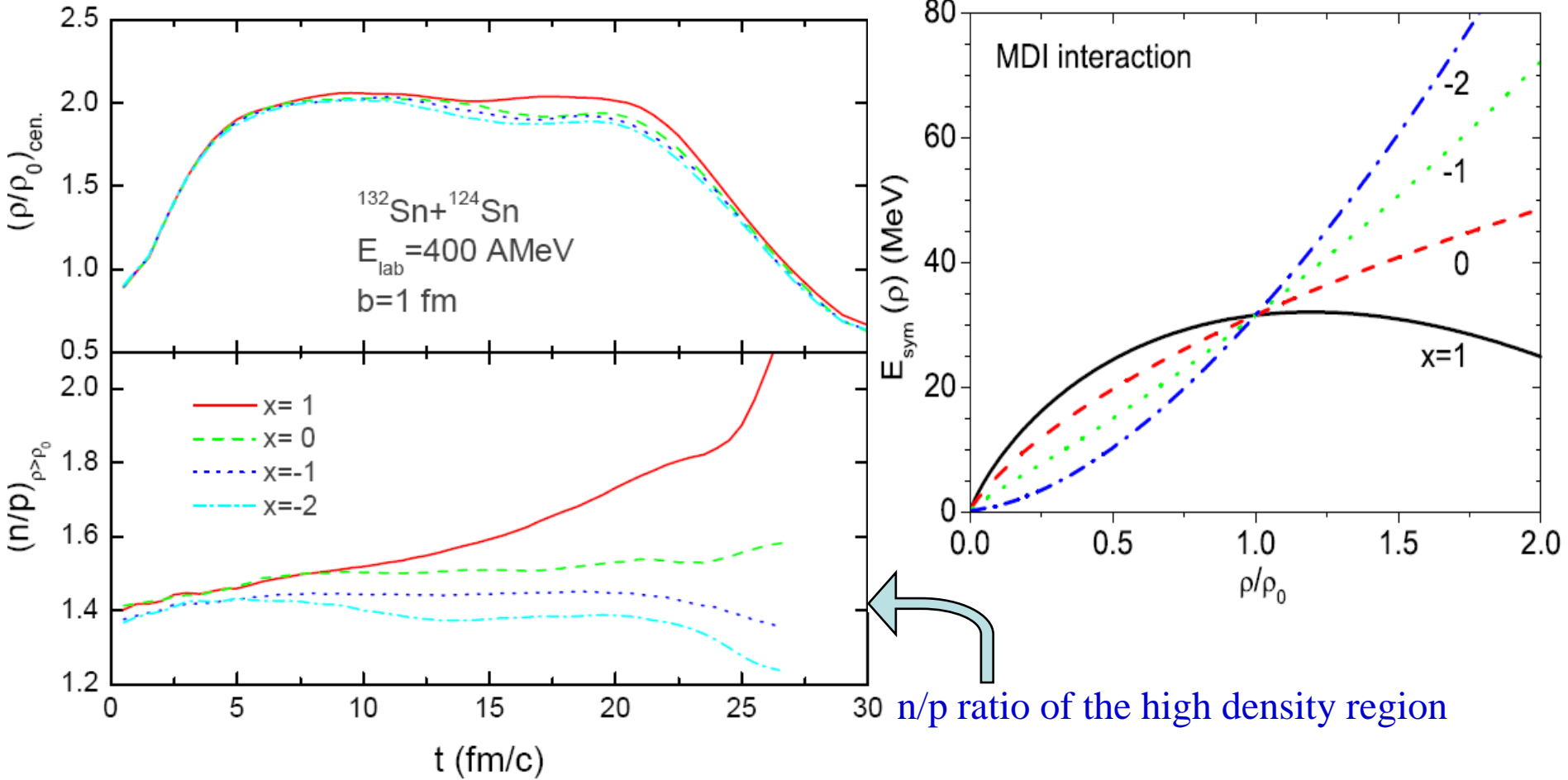
R. Ghetti et al., PRC69 (2004) 031605

肖志刚等, PLB, (2006)



重离子碰撞：对称能的高密行为

Heavy-Ion Collisions at Higher Energies



Isospin fractionation!

Li/Yong/Zuo, PRC **71**, 014608 (2005)



粒子产生阈能

$$\pi : \quad \approx 289 \text{ MeV} \quad (NN \rightarrow NN\pi)$$

$$K^+ / \Lambda / \Sigma : \quad \approx 1583 \text{ MeV} \quad (NN \rightarrow NYK^+)$$

$$K^- : \quad \approx 2513 \text{ MeV} \quad (NN \rightarrow NNK^+ K^-)$$

$$\Xi : \quad \approx 3740 \text{ MeV} \quad (NN \rightarrow N\Xi K^+ K^+)$$

实验发现在低于阈能时，重离子碰撞中仍能产生以上粒子，称为**阈下产生**。重离子碰撞中粒子的阈下产生为研究高温高密核介质中强子的性质以及核介质的性质提供了实验基础。



a) $\Delta(1232)$ resonance model

in first chance NN scatterings:

(neglect rescattering and reabsorption)

$$\frac{\pi^-}{\pi^+} = \frac{5N^2 + NZ}{5Z^2 + NZ} \approx \left(\frac{N}{Z}\right)^2$$

R. Stock, Phys. Rep. 135 (1986) 259.

	π^+	π^0	π^-
nn	0	1	5
pp	5	1	0
np(pn)	1	4	1

b) Thermal model:

(G.F. Bertsch, *Nature* 283 (1980) 281; A. Bonasera and G.F. Bertsch, *PLB*195 (1987) 521)

$$\frac{\pi^-}{\pi^+} \propto \exp[(\mu_n - \mu_p) / kT]$$

$$\mu_n - \mu_p = (V_{asy}^n - V_{asy}^p)\delta - V_{Coul} + kT \left\{ \ln \frac{\rho_n}{\rho_p} + \sum_m \frac{m+1}{m} b_m \left(\frac{1}{2} \lambda_T^3\right)^m (\rho_n^m - \rho_p^m) \right\}$$

H.R. Jaqaman, A.Z. Mekjian and L. Zamick, PRC (1983) 2782.

c) Transport models (more realistic approach):

see, e.g., *Bao-An Li, Phys. Rev. Lett.* 88 (2002) 192701.



对称能高密探针: pion比率

A Soft or Stiff E_{sym} at supra-saturation densities ???

pion ratio (FOPI): ImIQMD, Feng/Jin, PLB683, 140(2010)

n/p v2 (FOPI):

Russotto/Trautmann/Li et al., (UrQMD)

PLB697, 471(2011) $(\rho/\rho_0)^\gamma$ with $\gamma = 0.9 \pm 0.4$

PRC94, 034608 (2016) $\gamma = 0.72 \pm 0.19$

Pion Medium Effects?

Threshold effects?

Δ resonances?

Xu/Ko/Oh

PRC81, 024910(2010)

Xu/Chen/Ko/Li/Ma

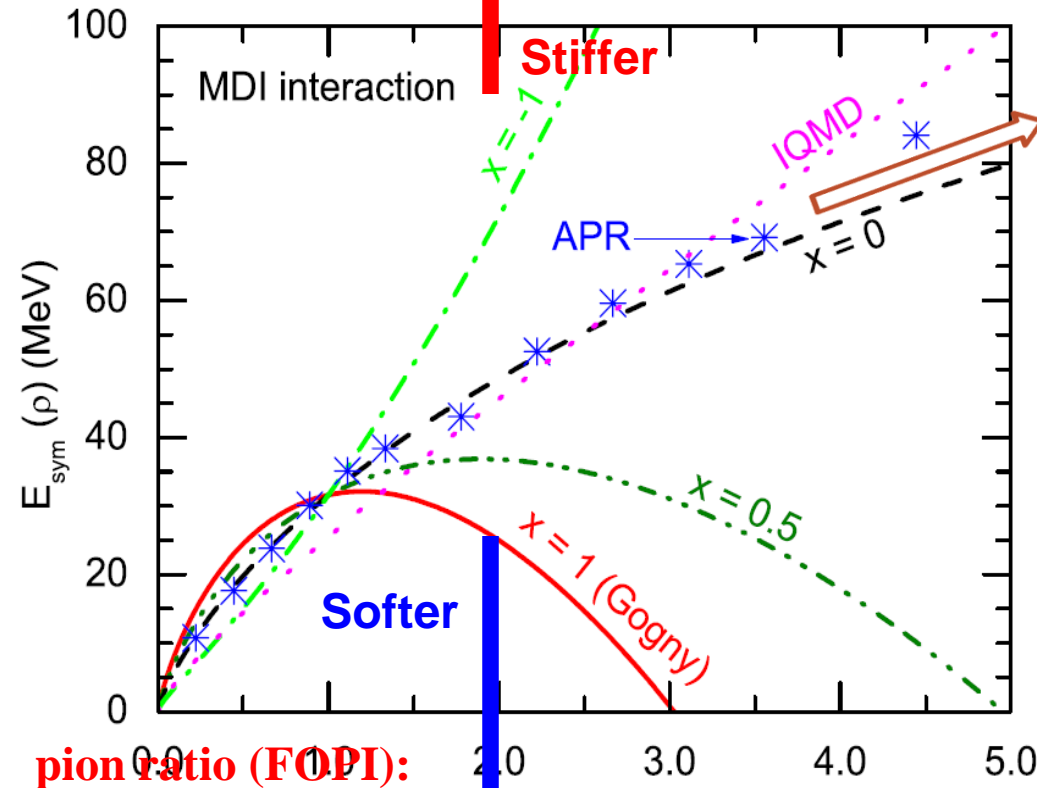
PRC87, 067601(2013)

Hong/Danielewicz,

PRC90, 024605 (2014)

Song/Ko, PRC91, 014901 (2015)

Z. Zhang/Ko, PRC95, 064604 (2017)



pion ratio (FOPI):

IBUU04, Xiao/Li/Chen/Yong/Zhang,

PRL102,062502(2009)

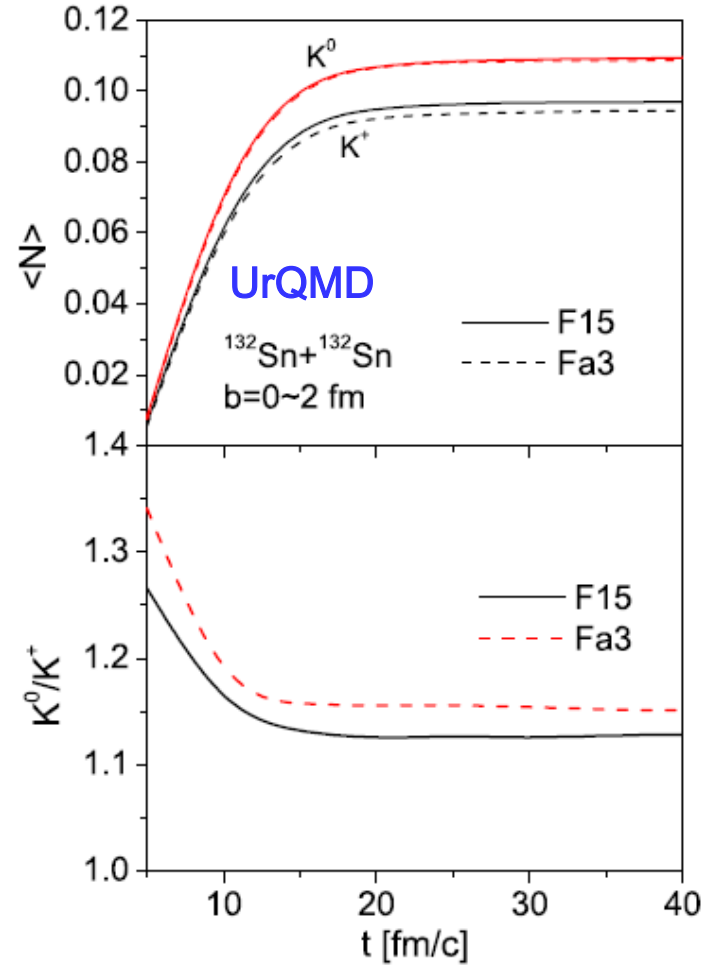
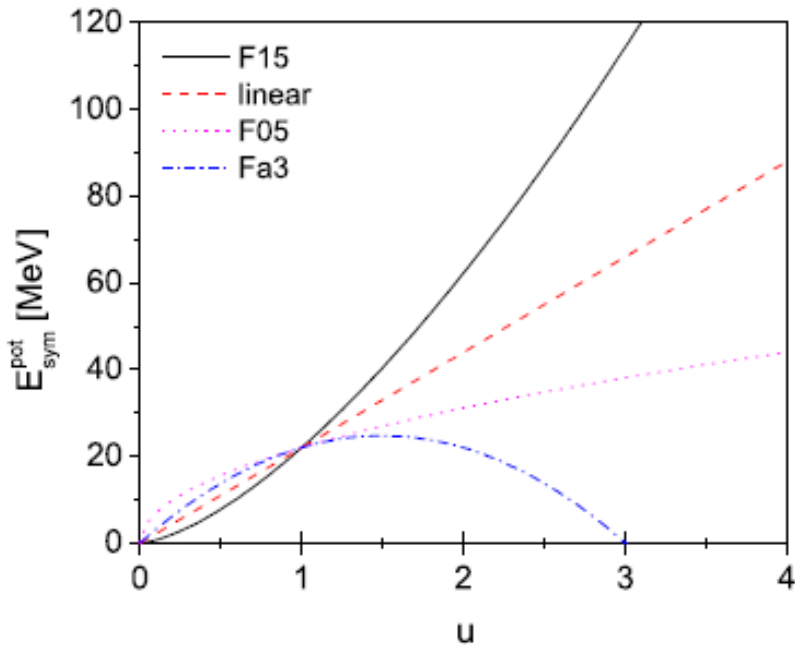
ImIBL, Xie/Su/Zhu/Zhang, PLB718,1510(2013)



对称能高密探针:Kaon比率

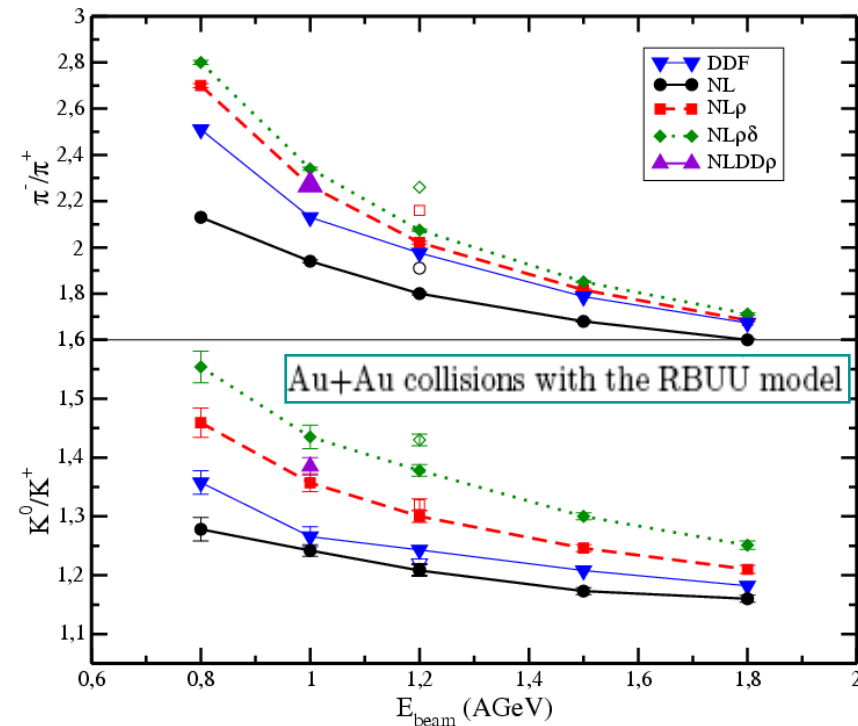
Aichelin/Ko, PRL55, 2661 (1985): Subthreshold kaon yield is a sensitive probe of the EOS of nuclear matter at high densities

Q.F. Li, Z.X. Li, S. Soff, R.K. Gupta, M. Bleicher, and H. Stoecker, JPG31, 1359 (2005)

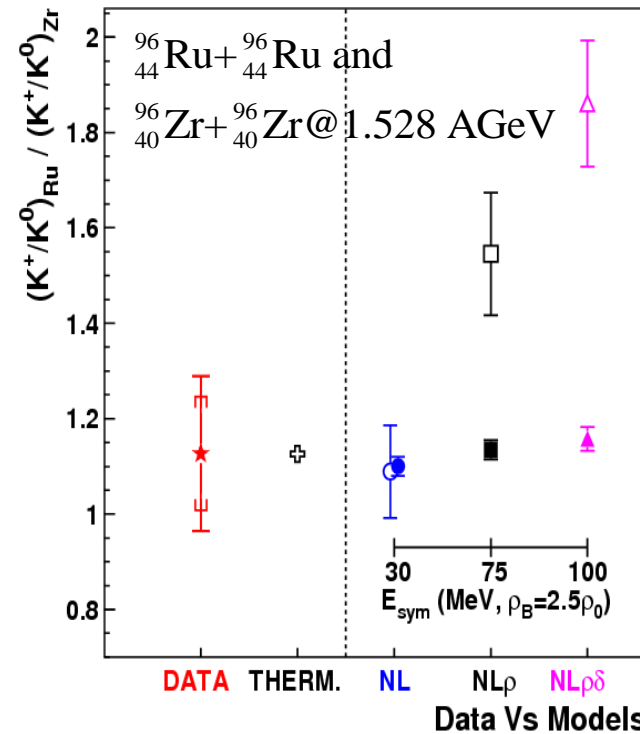


Aichelin/Ko, PRL55, 2661 (1985): Subthreshold kaon yield is a sensitive probe of the EOS of nuclear matter at high densities

Theory: Famiano et al., PRL97, 052701 (2006) Exp.: Lopez et al. FOPI, PRC75, 011901(R) (2007)



Subthreshold K^0/K^+ yield may be a sensitive probe of the symmetry energy at high densities

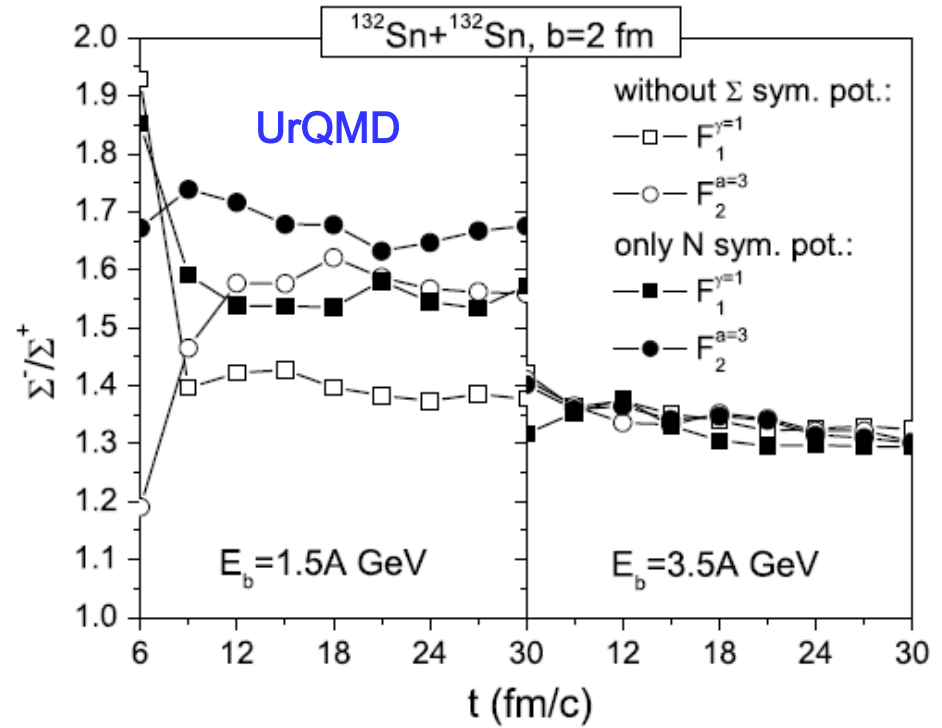
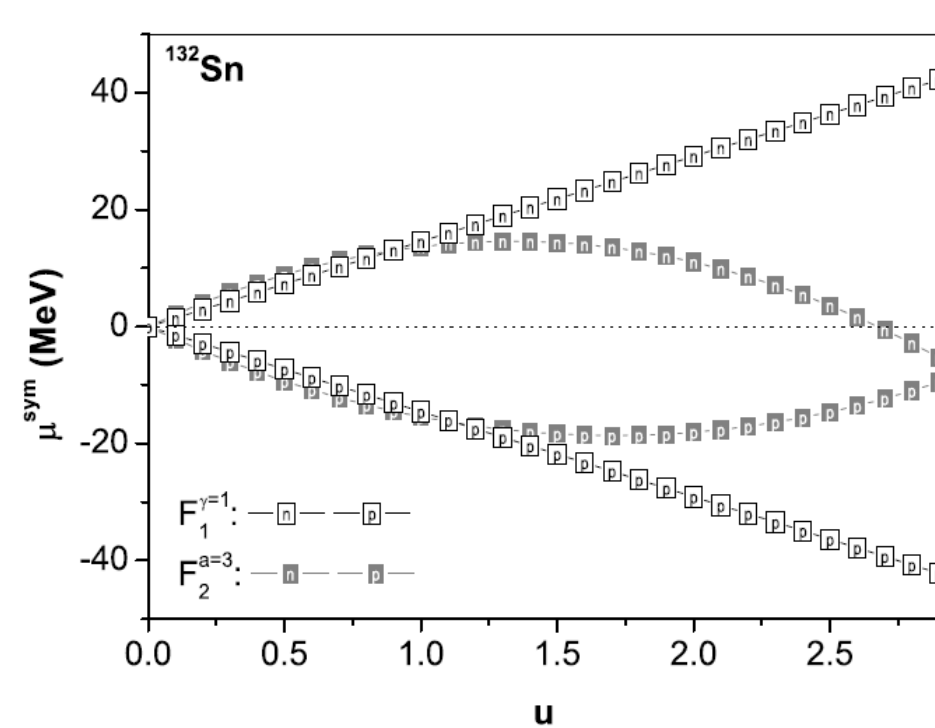


K^0/K^+ yield is not so sensitive to the symmetry energy! Lower energy and more neutron-rich system???



对称能高密探针： Σ 比率

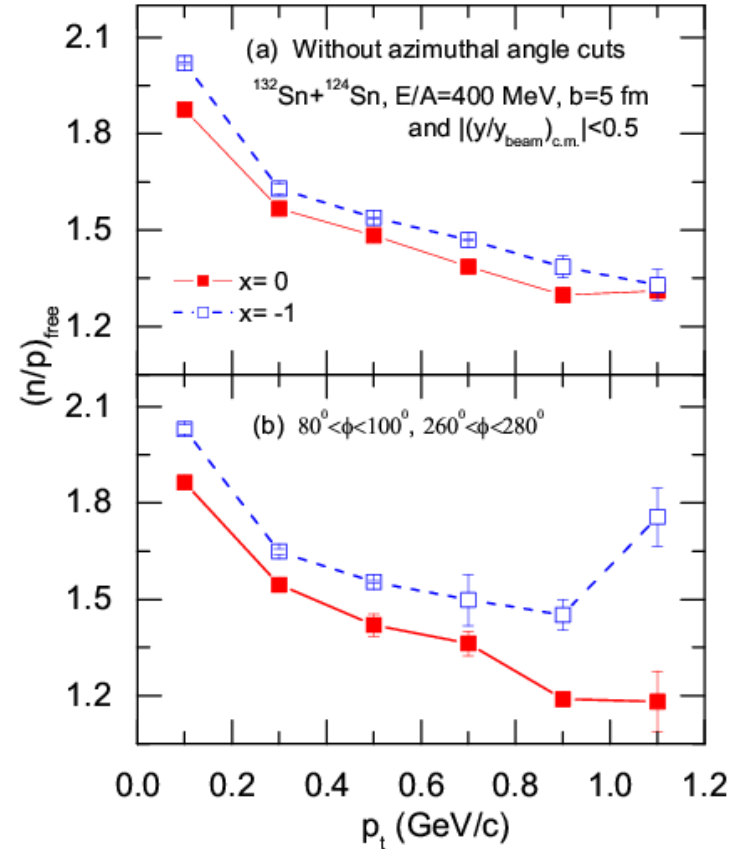
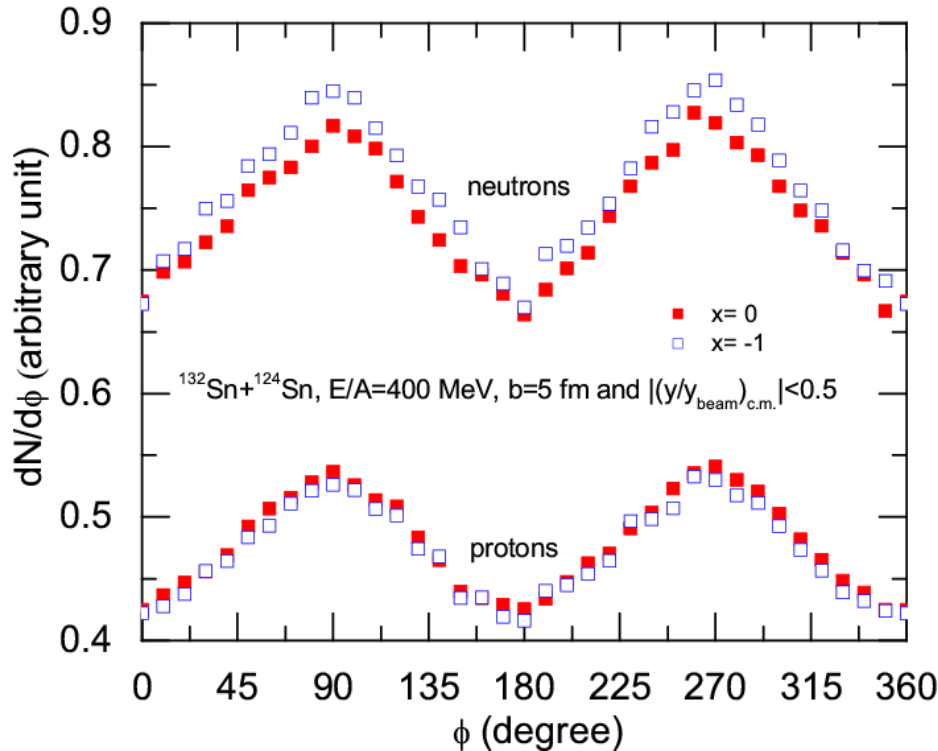
Q.F. Li, Z.X. Li, E.G. Zhao, and R.K. Gupta, PRC71, 054907 (2005)





对称能高密探针：挤出n/p比率

In the **squeeze-out** direction: nucleons emitted from the high density participant region have a better chance to escape without being hindered by the spectators. These nucleons thus carry more direct information about the high density phase of the reaction.

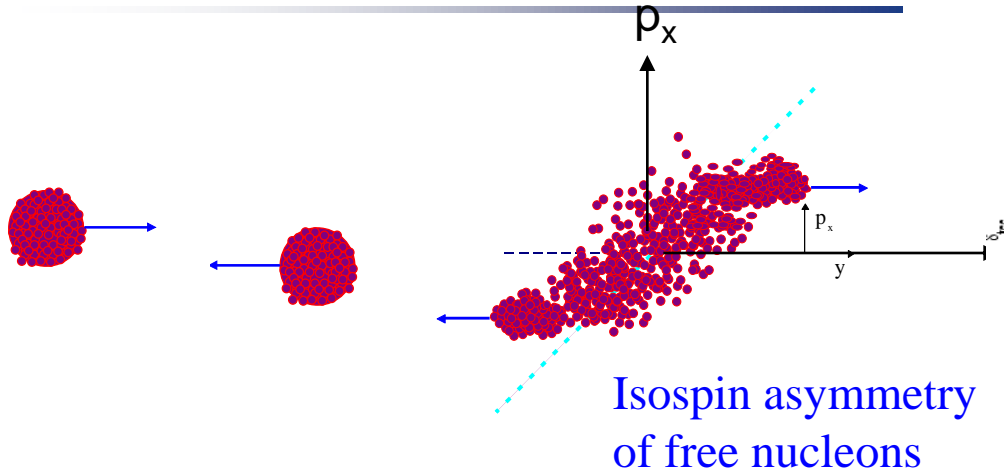


Yong/Li/Chen, nucl-th/0703042
PLB650, 344 (2007)

The effect can be 40% at higher p_T !



对称能高密探针: n-p差分流



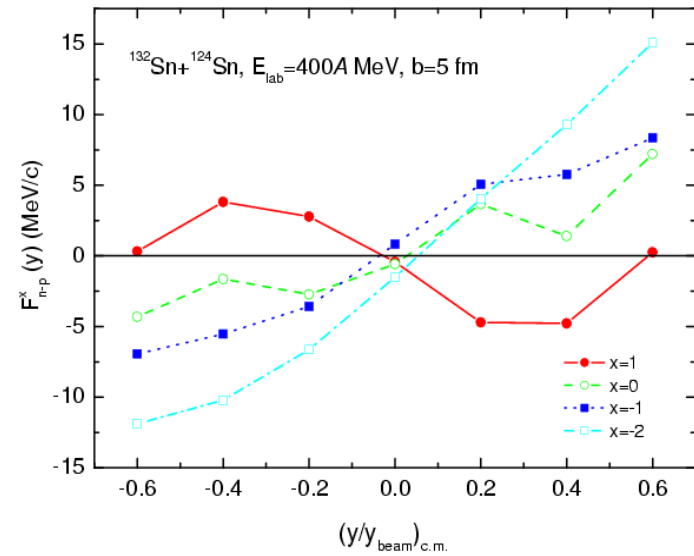
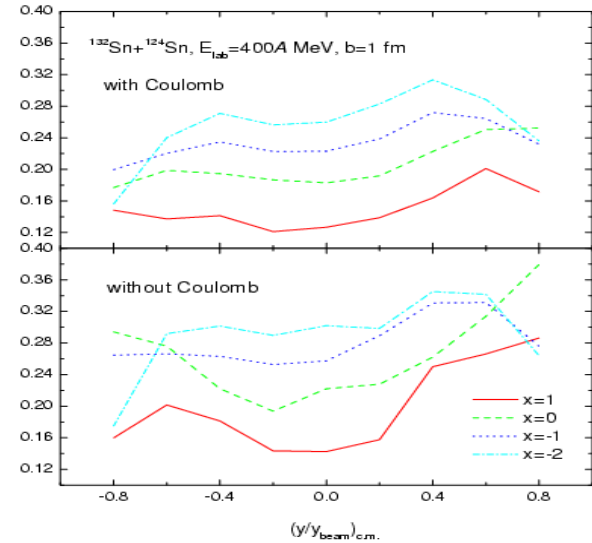
Neutron-proton differential flow

$$F_{n-p}^x(y) \equiv \frac{1}{N(y)} \sum_{i=1}^{i=N(y)} p_i^x \cdot \tau_i$$

$$\tau_i = \pm 1 \text{ for n and p}$$

symmetry potential is generally repulsive for neutrons and attractive for protons

Bao-An Li, PRL 85, 4221 (2000).



Yong/Li/Zuo, High energy physics and nuclear physics (2005).



International Journal of Modern Physics E, Vol. 7, No. 2 (April 1998) 147–229
© World Scientific Publishing Company

ISOSPIN PHYSICS IN HEAVY-ION COLLISIONS AT INTERMEDIATE ENERGIES

BAO-AN LI and CHE MING KO

Department of Physics and Cyclotron Institute
Texas A&M University, College Station, TX 77843-3366, USA

WOLFGANG BAUER

National Superconducting Cyclotron Laboratory
and Department of Physics and Astronomy,
Michigan State University, East Lansing, MI 48824-1321, USA



ELSEVIER

Available online at www.sciencedirect.com



Physics Reports 410 (2005) 335–466

PHYSICS REPORTS

www.elsevier.com/locate/physrep

Reaction dynamics with exotic nuclei

V. Baran^{a,b,1}, M. Colonna^{a,b}, V. Greco^c, M. Di Toro^{a,b,*}

Front. Phys. China, 2007, 2(3): 327–357

DOI 10.1007/s11467-007-0037-0

REVIEW ARTICLE

CHEN Lie-wen, KO Che Ming, LI Bao-an, YONG Gao-chan

Probing the nuclear symmetry energy with heavy-ion reactions induced by neutron-rich nuclei

Physics Reports 464 (2008) 113–281



ELSEVIER

Contents lists available at ScienceDirect

Physics Reports

journal homepage: www.elsevier.com/locate/physrep



Recent progress and new challenges in isospin physics with heavy-ion reactions

Bao-An Li^{a,*}, Lie-Wen Chen^b, Che Ming Ko^c

Eur. Phys. J. A (2014) 50: 29
DOI 10.1140/epja/i2014-14029-6

THE EUROPEAN
PHYSICAL JOURNAL A

Review

Probing isospin- and momentum-dependent nuclear effective interactions in neutron-rich matter*

Lie-Wen Chen^{1,2,a}, Che Ming Ko³, Bao-An Li^{4,5}, Chang Xu⁶, and Jun Xu⁷



Frontiers of Physics

<https://doi.org/10.1007/s11467-020-0961-9>

Front. Phys.
15(5), 54301 (2020)

REVIEW ARTICLE

Progress of quantum molecular dynamics model and its applications in heavy ion collisions

Ying-Xun Zhang^{1,2,*}, Ning Wang^{3,2,†}, Qing-Feng Li^{4,5,‡}, Li Ou^{3,2,§}, Jun-Long Tian^{6,2,¶},
Min Liu^{3,2,***}, Kai Zhao^{1,††}, Xi-Zhen Wu^{1,2,‡‡}, Zhu-Xia Li^{1,2,§§}



四、对称能研究进展

- 引力波时代的对称能
 - PREX-II 铅核中子皮实验的挑战
 - 现状总结
-



核物质状态方程的特征参数

PHYSICAL REVIEW C 80, 014322 (2009)

Higher-order effects on the incompressibility of isospin asymmetric nuclear matter

Lie-Wen Chen,^{1,2} Bao-Jun Cai,¹ Che Ming Ko,³ Bao-An Li,⁴ Chun Shen,¹ and Jun Xu³

¹Department of Physics, Shanghai Jiao Tong University, Shanghai 200240, People's Republic of China

²Center of Theoretical Nuclear Physics, National Laboratory of Heavy Ion Accelerator, Lanzhou 730000, People's Republic of China

³Cyclotron Institute and Physics Department, Texas A&M University, College Station, Texas 77843-3366, USA

⁴Department of Physics, Texas A&M University-Commerce, Commerce, Texas 75429-3011, USA

(Received 27 May 2009; published 30 July 2009)

$$E(\rho, \delta) = E_0(\rho) + E_{\text{sym}}(\rho)\delta^2 + E_{\text{sym},4}(\rho)\delta^4 + O(\delta^6)$$

$$E_0(\rho) = E_0(\rho_0) + \frac{K_0}{2!}\chi^2 + \frac{J_0}{3!}\chi^3 + \frac{I_0}{4!}\chi^4 + O(\chi^5)$$

$$\delta = (\rho_n - \rho_p)/\rho$$

$$E_{\text{sym}}(\rho) = E_{\text{sym}}(\rho_0) + L\chi + \frac{K_{\text{sym}}}{2!}\chi^2 + \frac{J_{\text{sym}}}{3!}\chi^3 + \frac{I_{\text{sym}}}{4!}\chi^4 + O(\chi^5)$$

$$\chi = \frac{\rho - \rho_0}{3\rho_0}$$

$$E_{\text{sym},4}(\rho) = E_{\text{sym},4}(\rho_0) + L_{\text{sym},4}\chi + \frac{K_{\text{sym},4}}{2}\chi^2 + \frac{J_{\text{sym},4}}{3!}\chi^3 + \frac{I_{\text{sym},4}}{4!}\chi^4 + O(\chi^5)$$

Order of the characteristic parameters according to the expansion with χ and δ :

Order-0: $E_0(\rho_0)$; **Order-2:** $K_0, E_{\text{sym}}(\rho_0)$;

Order-3: J_0, L ; **Order-4:** $I_0, K_{\text{sym}}(\rho_0), E_{\text{sym},4}(\rho_0)$



核物质状态方程的特征参数

Order of the characteristic parameters according to the expansion with χ and δ :

Order-0: $E_0(\rho_0)$; Order-2: $K_0, E_{\text{sym}}(\rho_0)$;

Order-3: J_0, L ; Order-4: $I_0, K_{\text{sym}}(\rho_0), E_{\text{sym},4}(\rho_0)$

Order-0  $E_0(\rho_0) = -16 \pm 1 \text{ MeV}$

Order-2  $K_0 = 240 \pm 20 \text{ MeV}, E_{\text{sym}}(\rho_0) = 32.5 \pm 2.5 \text{ MeV}???$

Order-3  $L = 55 \pm 25 \text{ MeV}???, J_0 = ???$

Order-4  $I_0 = ???, K_{\text{sym}}(\rho_0) = ???, E_{\text{sym},4}(\rho_0) = ???$

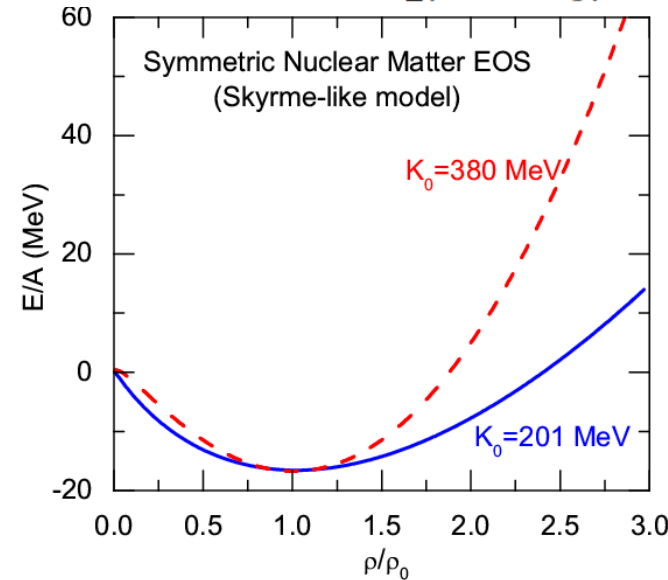


对称核物质的状态方程

(1) EOS of symmetric matter around the saturation density ρ_0

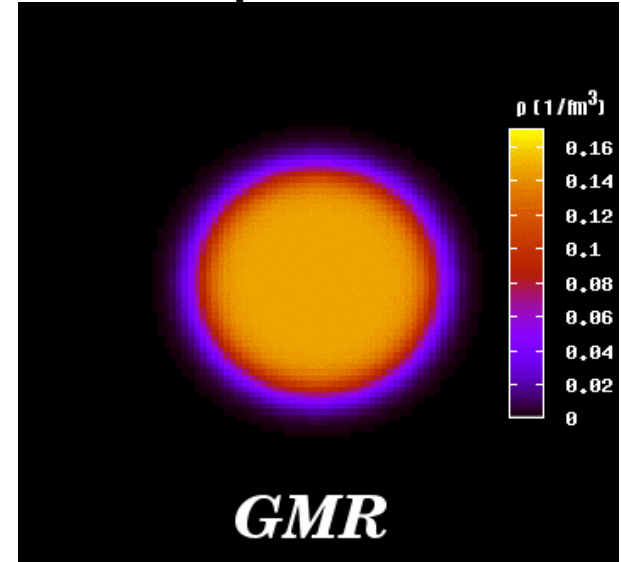
$$E_0(\rho) = E_0(\rho_0) + \frac{K_0}{2!} \chi^2 + \frac{J_0}{3!} \chi^3 + \mathcal{O}(\chi^4) \quad \chi = \frac{\rho - \rho_0}{3\rho_0}$$

Giant Monopole Resonance



Incompressibility:

$$K_0 = 9\rho_0^2 \left(\frac{d^2 E}{d\rho^2} \right)_{\rho_0}$$



$$\text{Frequency } f_{\text{GMR}} \propto \sqrt{K_0}$$

$$K_0 = 231 \pm 5 \text{ MeV}$$

Youngblood/Clark/Lui, PRL82, 691 (1999)

Recent results:

$$K_0 = 240 \pm 20 \text{ MeV}$$

U. Garg et al.

S. Shlomo et al.

G. Colo et al.

J. Piekarewicz et al.

Uncertainty of the extracted K_0 is mainly due to the uncertainty of L (slope parameter of the symmetry energy) and

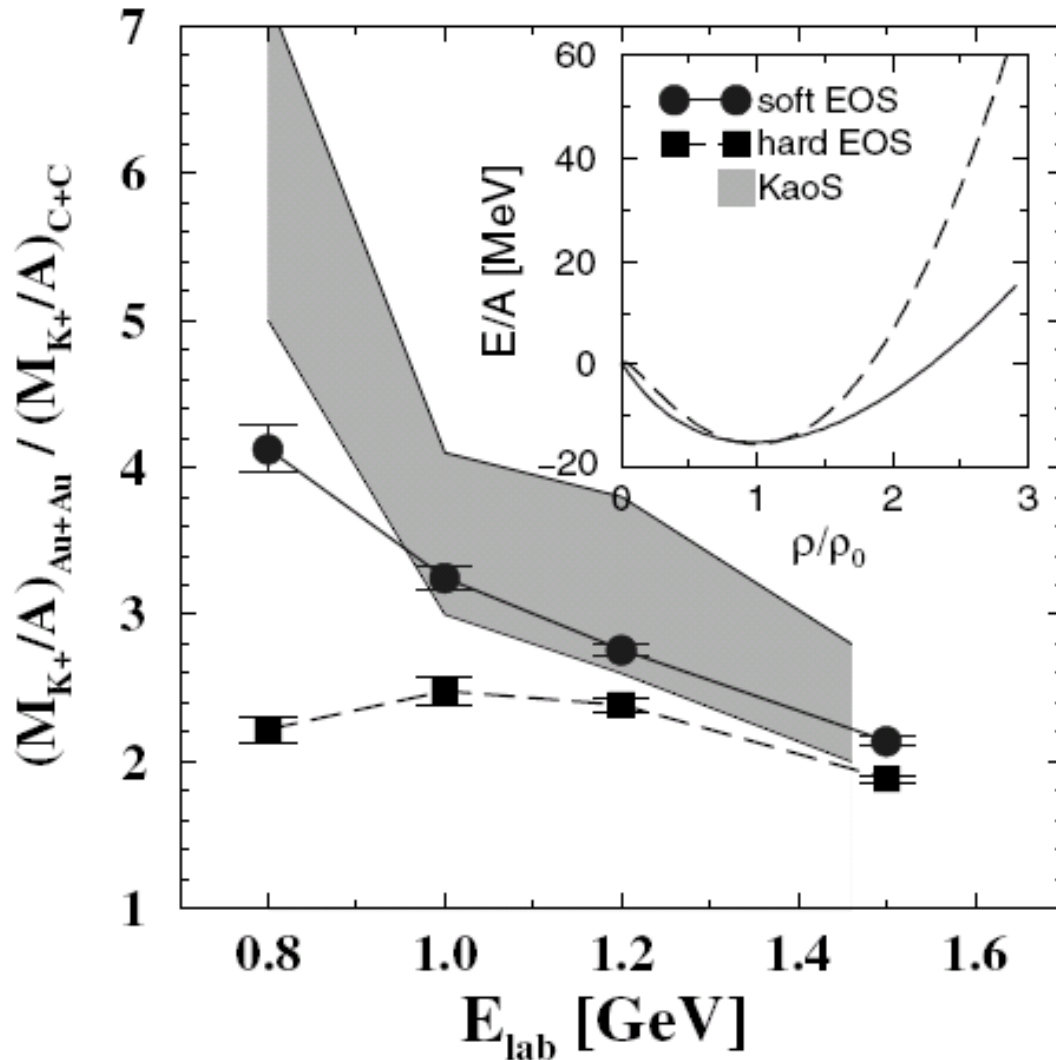
m^*_0 (isoscalar nucleon effective mass)

(See, e.g., LWC/J.Z. Gu, JPG39, 035104(2012))



对称核物质的状态方程

(2) EOS of symmetric matter for $1\rho_0 < \rho < 3\rho_0$ from K^+ production in HIC's



J. Aichelin and C.M. Ko,
PRL55, (1985) 2661

C. Fuchs,
Prog. Part. Nucl. Phys. 56, (2006) 1

C. Fuchs et al,
PRL86, (2001) 1974

Transport calculations indicate that “results for the K^+ excitation function in Au + Au over C + C reactions as measured by the KaoS Collaboration strongly support the scenario with a **soft EOS.**”

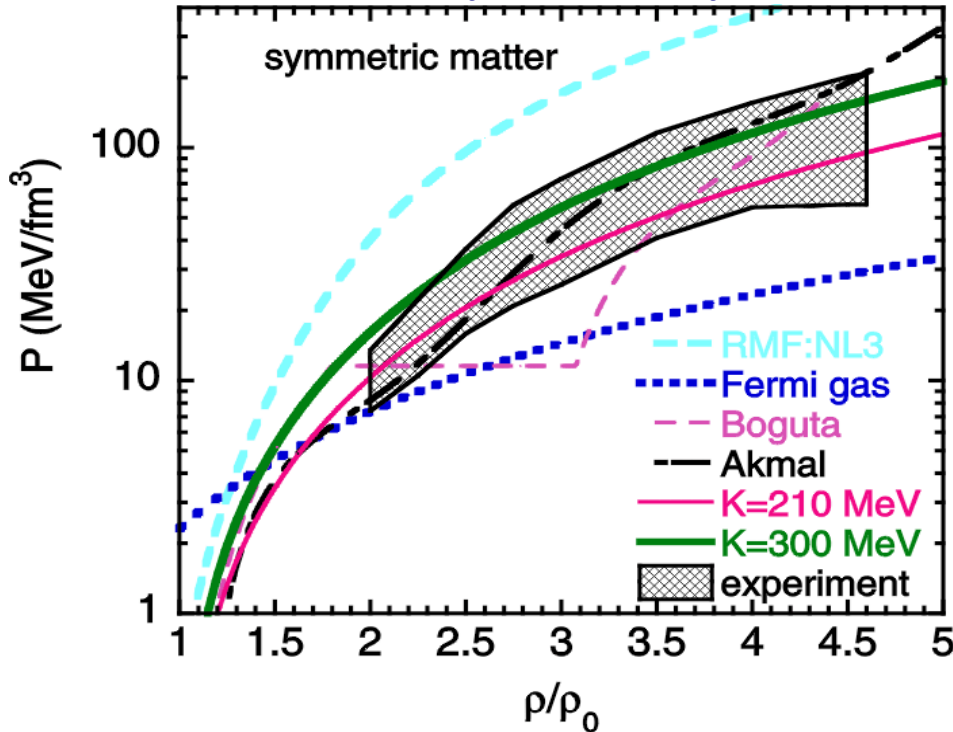
See also: C. Hartnack, H. Oeschler,
and J. Aichelin,
PRL96, 012302 (2006)



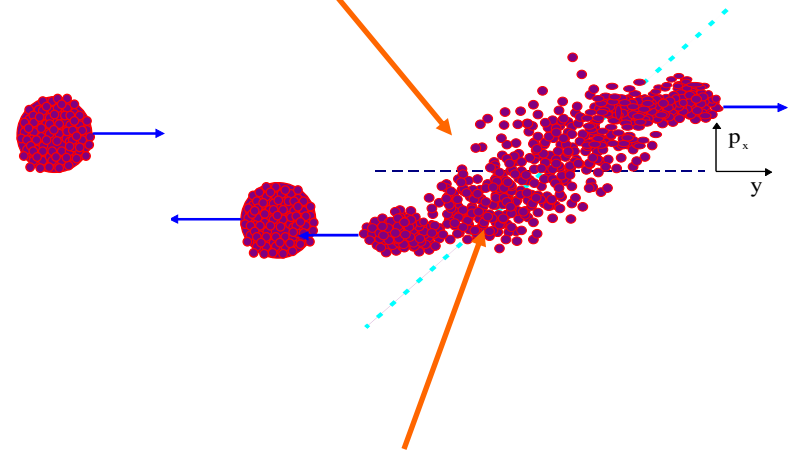
对称核物质的状态方程

(3) Present constraints on the EOS of symmetric nuclear matter for $2\rho_0 < \rho < 5\rho_0$ using flow data from BEVALAC, SIS/GSI and AGS

P. Danielewicz, R. Lacey and W.G. Lynch, *Science* 298, 1592 (2002)



The highest pressure recorded under laboratory controlled conditions in nucleus-nucleus collisions



High density nuclear matter
2 to $5\rho_0$

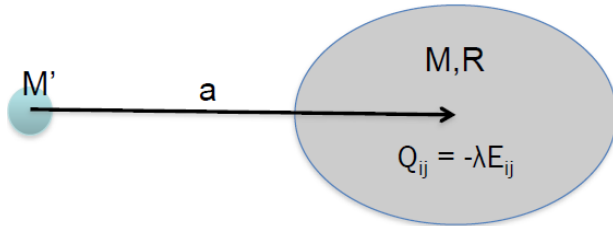
$$\text{Pressure } P(\rho) = \rho^2 \left(\frac{\partial E}{\partial \rho} \right)_s$$

- Use constrained mean fields to predict the EOS for symmetric matter
 - Width of pressure domain reflects uncertainties in comparison and of assumed momentum dependence.



引力波时代的对称能

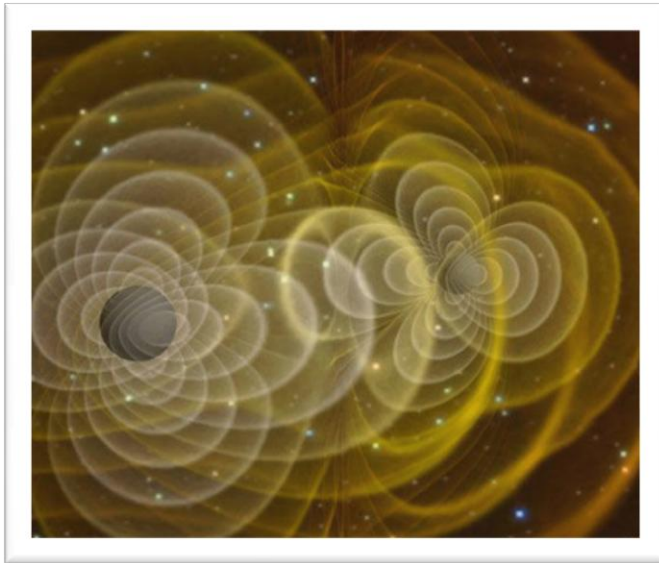
中子星的潮汐极化率 Λ (oscillation response coefficient λ)



$$Q_{ij} = \lambda \varepsilon_{ij}$$

Q_{ij} : Quadrupole moment

ε_{ij} : Tidal field of companion



$$\lambda = \frac{2}{3} k_2 R^5$$

k_2 : Love number

R : Radius

M : Mass

Dimensionless Tidal Deformability

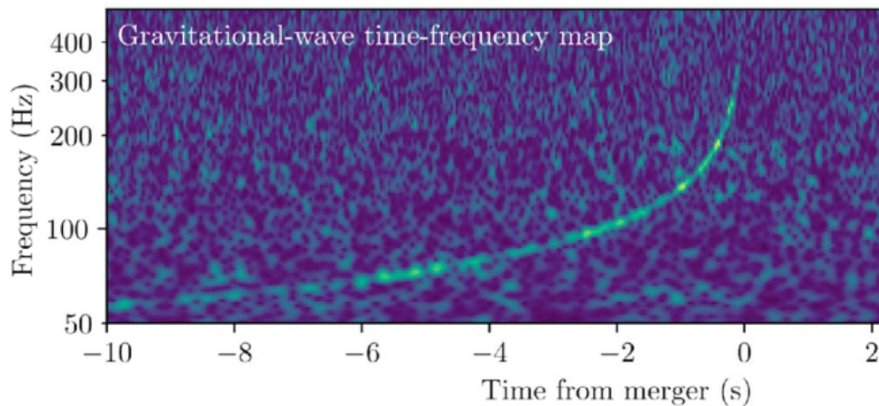
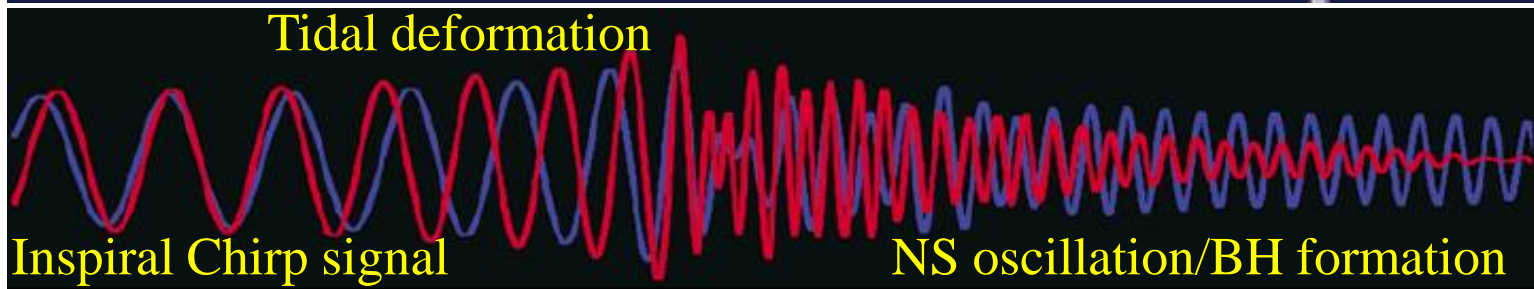
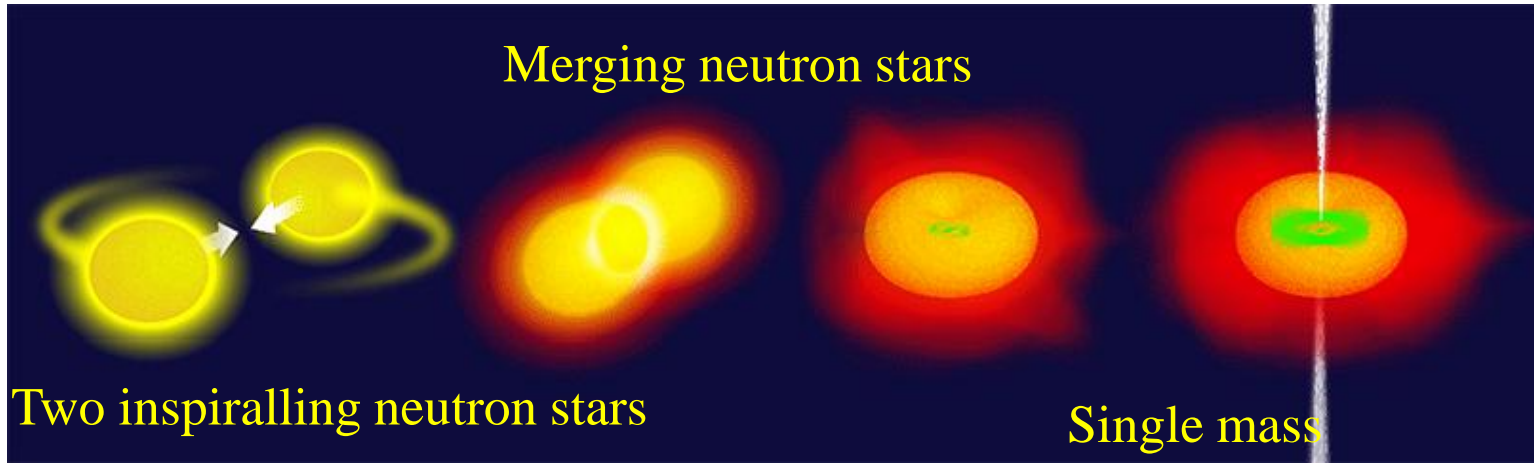
$$\Lambda = \frac{2}{3} k_2 (R / M)^5$$

Éanna É. Flanagan and Tanja Hinderer, Phys.Rev.D 77, 021502(R) (2008)

F.J. Fattoyev, J. Carvajal, W.G. Newton, and Bao-An Li, Phys. Rev. C 87, 015806 (2013)



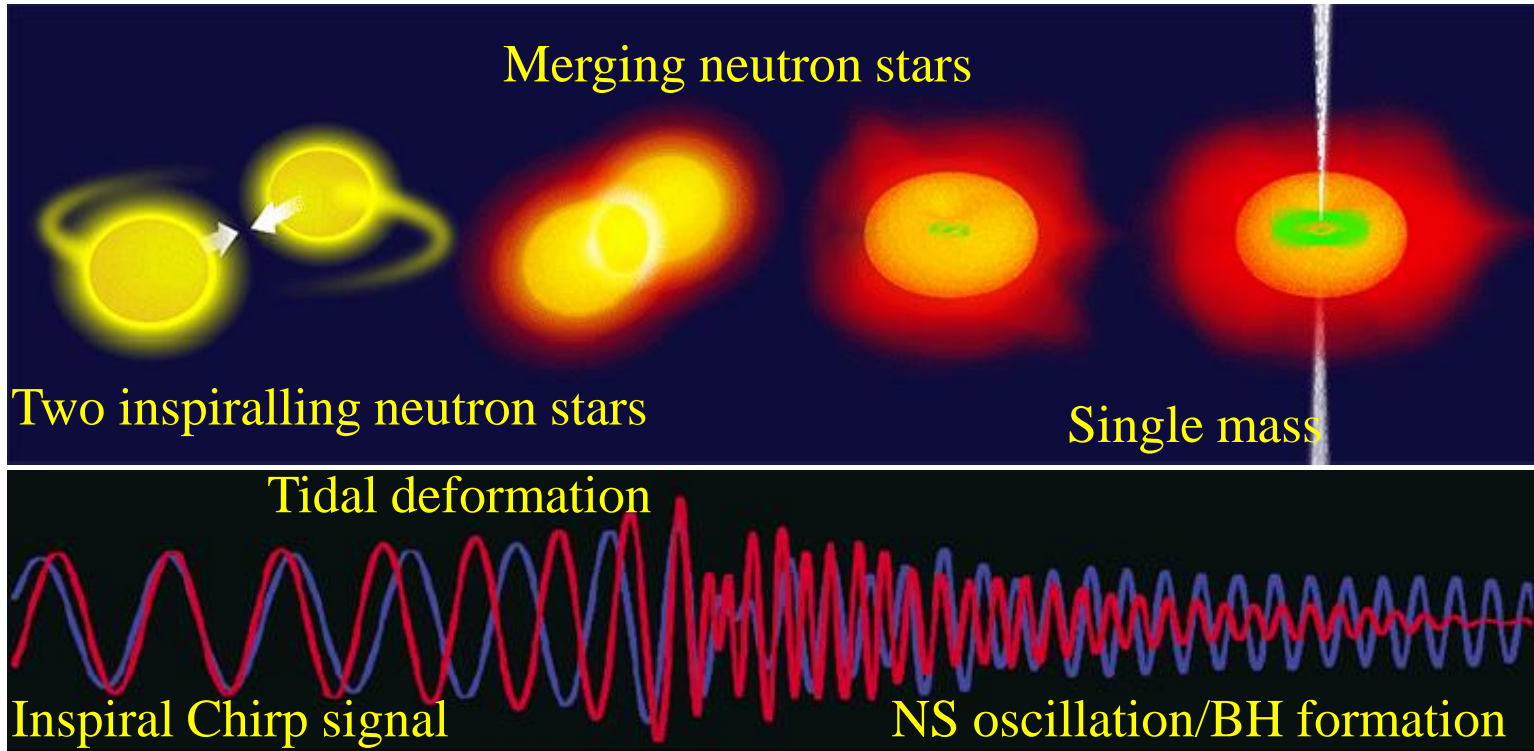
双中子星并合与 Λ



LIGO is sensitive to increase in orbital frequency as system loses energy to both gravitational waves and internal excitation of neutron stars. GW170817 data place limits on polarizability (deformability) Λ of NS and hence limits on NS radius.



双中子星并合与 Λ



中子星并合过程中重子数密度能达到 $\sim 10\rho_0$ 而温度能达到 ~ 50 MeV，但具有非常高的同位旋！

Refs: Elias R. Most et al., PRL122, 061101 (2019), Andreas Bauswein et al., PRL122, 061102 (2019)

对称能的高密行为在中子星并合过程中扮演了非常重要的角色！



引力波事件GW170817

PRL 119, 161101 (2017)

Selected for a Viewpoint in *Physics*
PHYSICAL REVIEW LETTERS

week ending
20 OCTOBER 2017



GW170817: Observation of Gravitational Waves from a Binary Neutron Star Inspiral

B. P. Abbott *et al.**

Citations > 3384

(LIGO Scientific Collaboration and Virgo Collaboration)



- On August 17, 2017, the merger of two neutron stars was observed with gravitational waves (GW) by the LIGO and Virgo detectors.
- The Fermi and Integral spacecrafts independently detected a short gamma ray burst.
- Extensive follow up observations detected this event at X-ray, ultra-violet, visible, infrared, and radio wavelengths.
- No ultra-high-energy gamma-rays and no neutrino candidates consistent with the source were found in follow-up searches. **These observations support the hypothesis that GW170817 was produced by the merger of two neutron stars in NGC 4993 followed by a short gamma-ray burst (GRB 170817A) and a kilonova/macronova powered by the radioactive decay of *r*-process nuclei synthesized in the ejecta**



中子星的潮汐极化率 λ

核物质状态方程EOS +

$$\frac{dy}{dr} = -\frac{1}{r} [y^2 + yF(p, \varepsilon) + r^2 Q(p, \varepsilon)]$$

$$\frac{dp}{dr} = -\frac{(\varepsilon + p)(m + 4\pi r^3 p)}{r(r - 2m)}$$

$$\frac{dm}{dr} = 4\pi r^2 \varepsilon$$



$$\begin{matrix} M \\ R \\ y_R \equiv y(R) \end{matrix}$$



$$k_2 = \frac{1}{20} \left(\frac{R_s}{R} \right)^5 \left(1 - \frac{R_s}{R} \right)^2 \left[2 - y_R + (y_R - 1) \frac{R_s}{R} \right] \left\{ \frac{R_s}{R} \left(6 - 3y_R + \frac{3R_s}{2R} (5y_R - 8) \right) \right.$$

$$+ \frac{1}{4} \left(\frac{R_s}{R} \right)^3 \left[26 - 22y_R + \frac{R_s}{R} (3y_R - 2) + \left(\frac{R_s}{R} \right)^2 (y_R + 1) \right]$$

$$\left. + 3 \left(1 - \frac{R_s}{R} \right)^2 \left[2 - y_R + (y_R - 1) \frac{R_s}{R} \right] \ln \left(1 - \frac{R_s}{R} \right) \right\}^{-1}$$



$$\lambda = \frac{2}{3} k_2 R^5$$

$$F(r) = \frac{r - 4\pi r^3 [\varepsilon(r) - P(r)]}{r - 2M(r)},$$

$$Q(r) = \frac{4\pi r \left[5\varepsilon(r) + 9P(r) + \frac{\varepsilon(r) + P(r)}{c_s^2} - \frac{6}{4\pi r^2} \right]}{r - 2M(r)} - 4 \left\{ \frac{M(r) + 4\pi r^3 P(r)}{r[r - 2M(r)]} \right\}^2.$$



EOS of Neutron Star Matter

□ Core of the neutron stars consist of **infinite β -equilibrium npe μ matter with charge neutrality**. Its EoS is determined by the extended Skyrme-Hartree-Fock(eSHF)

□ The inner crust $2.46 \times 10^{-4} \text{ fm}^{-3} = n_{\text{out}} < n < n_t$

n_t is determined self-consistently
by using dynamical method
(Xu/LWC/Li/Ma, ApJ697,1549(2009))

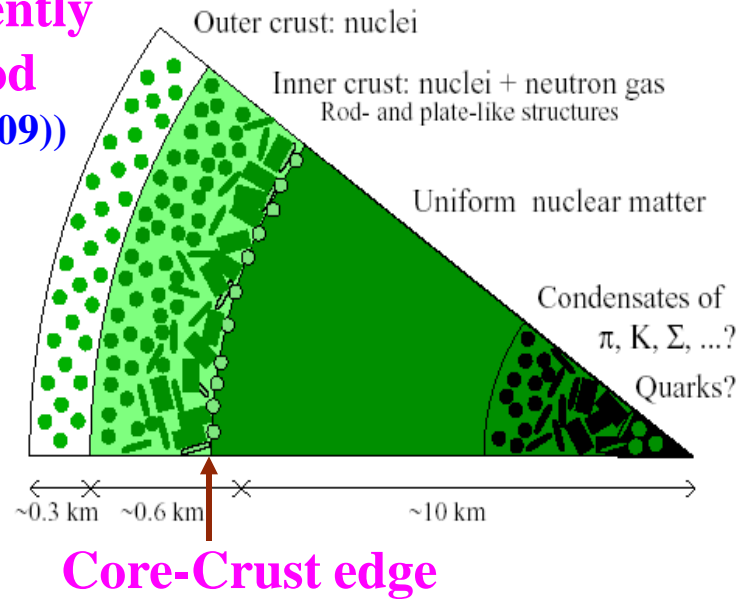
$$P = a + b \rho^{4/3}$$

$$a = \frac{P_{\text{out}} \rho_t^3 - P_t \rho_{\text{out}}^{4/3}}{\rho_t^3 - \rho_{\text{out}}^{4/3}} \quad b = \frac{P_t - P_{\text{out}}}{\rho_t^3 - \rho_{\text{out}}^{4/3}}$$

□ The outer crust

$$6.93 \times 10^{-13} \text{ fm}^{-3} < n < n_{\text{out}} \quad (\text{EOS of BPS})$$

$$4.73 \times 10^{-15} \text{ fm}^{-3} < n < 6.93 \times 10^{-13} \text{ fm}^{-3} \quad (\text{EOS of Feynman-Metropolis-Teller})$$





Extended Skyrme Interaction:

$$\begin{aligned}
 v_{i,j} = & t_0(1 + x_0 P_\sigma) \delta(r) \\
 & + \frac{1}{2} t_1(1 + x_1 P_\sigma) [\mathbf{K}'^2 \delta(r) + \delta(r) \mathbf{K}^2] \\
 & + t_2(1 + x_2 P_\sigma) \mathbf{K}' \cdot \delta(r) \mathbf{K} \\
 & + \frac{1}{6} t_3(1 + x_3 P_\sigma) n(\mathbf{R})^\alpha \delta(r) \\
 & + iW_0(\boldsymbol{\sigma}_i + \boldsymbol{\sigma}_j) \mathbf{K}' \cdot \delta(r) \mathbf{K} \\
 & + \frac{1}{2} t_4(1 + x_4 P_\sigma) [\mathbf{K}'^2 n(\mathbf{R})^\beta \delta(r) + \delta(r) n(\mathbf{R})^\beta \mathbf{K}^2] \\
 & + t_5(1 + x_5 P_\sigma) \mathbf{K}' \cdot n(\mathbf{R})^\gamma \delta(r) \mathbf{K}
 \end{aligned}$$

N. Chamel, S. Goriely, and J.M. Pearson, PRC80, 065804 (2009)

Z. Zhang/LWC, PRC94, 064326 (2016)

LWC/Ko/Li/Xu, PRC82, 024321(2010) Momentum-dependence of many-body forces

13 Skyrme parameters: $\alpha, t_0 \sim t_5, x_0 \sim x_5$ $\mathcal{H} = \mathcal{K} + \mathcal{H}_0 + \mathcal{H}_3 + \mathcal{H}_{\text{eff}} + \frac{G_S}{2}(\nabla\rho)^2 - \frac{G_V}{2}(\nabla\rho_1)^2$

13 macroscopic nuclear properties:

$$-\frac{G_{SV}}{2} \delta\nabla\rho\nabla\rho_1 + \mathcal{H}_{\text{Coul}} + \mathcal{H}_{\text{SO}} + \mathcal{H}_{\text{sg}}, \quad ($$

$$n_0, E_0, K_0, J_0, E_{\text{sym}}, L, K_{\text{sym}}, m_{s,0}^*, m_{v,0}^*, G_S, G_V, G_{SV}, G'_0$$



Why extended SHF EDF?

PHYSICAL REVIEW C 94, 064326 (2016)

Extended Skyrme interactions for nuclear matter, finite nuclei, and neutron stars

Zhen Zhang¹ and Lie-Wen Chen^{1,2,*}

¹*Department of Physics and Astronomy and Shanghai Key Laboratory for Particle Physics and Cosmology, Shanghai Jiao Tong University, Shanghai 200240, China*

²*Center of Theoretical Nuclear Physics, National Laboratory of Heavy Ion Accelerator, Lanzhou 730000, China*

symmetry energy softer at subsaturation densities (favored by experimental constraints and theoretical predictions) but stiffer at higher densities (favored by the observation of $2M_{\odot}$ neutron stars) challenges the SHF model with the conventional Skyrme interactions. For example, the Skyrme interaction TOV-min [28], which is built by fitting properties of both finite nuclei and neutron stars, can successfully support $2M_{\odot}$ neutron stars but predicts a neutron matter EOS significantly deviating from the ChEFT calculations [14] as well as the constraint extracted from analyzing the electric-dipole polarizability in ^{208}Pb [49] at densities below about $0.5\rho_0$.

Furthermore, it is well known that a notorious shortcoming of the conventional standard Skyrme interactions is that they predict various instabilities of nuclear matter around saturation density or at supra-saturation densities, which in principle hinders the application of the Skyrme interactions in the study of dense nuclear matter as well as neutron stars. For instance, most of the conventional standard Skyrme interactions predict spin or spin-isospin polarization in the density region of about $(1 \sim 3.5)\rho_0$ [25,51], including the famous SLy4 interaction [19] which has been widely used in both nuclear physics and neutron star studies and leads to spin-isospin instability of symmetric nuclear matter at densities beyond about $2\rho_0$ [52]. On the other hand, the calculations

- ❑ **The eSHF provides a nice approach that can describe simultaneously nuclear matter, finite nuclei, and neutron stars!**
- ❑ **The eSHF EDF is very flexible to mimic various density behaviors for EOS (13 parameters)**



$$n_0, E_0, K_0, J_0, E_{\text{sym}}, L, K_{\text{sym}}, m_{s,0}^*, m_{v,0}^*, G_S, G_V, G_{SV}, G'_0$$

TABLE I. Experimental data for 12 spherical even-even nuclei binding energies E_B [27], charge r.m.s. radii r_c [28–30], ISGMR energies E_{GMR} and its experimental error [31], and spin-orbit energy level splittings ϵ_{ls}^A [32].

$\frac{A}{2}X$	$E_B(\text{MeV})$	$r_c(\text{fm})$	$E_{\text{GMR}}(\text{MeV})$	$\epsilon_{\text{ls}}^A(\text{MeV})$
^{16}O	-127.619	2.6991	...	6.30(1p ν) 6.10(1p π)
^{40}Ca	-342.052	3.4776
^{48}Ca	-416.001	3.4771
^{56}Ni	-483.995	3.7760
^{68}Ni	-590.408
^{88}Sr	-768.468	4.2240
^{90}Zr	-783.898	4.2694	17.81 \pm 0.35	...
^{100}Sn	-825.300
^{116}Sn	-988.681	4.6250	15.90 \pm 0.07	...
^{132}Sn	-1102.84
^{144}Sm	-1195.73	4.9524	15.25 \pm 0.11	...
^{208}Pb	-1636.43	5.5012	14.18 \pm 0.11	1.32(2d π) 0.89(3p ν) 1.77(2f ν)

Our Strategy:

- Higher-order **J_0** and **K_{sym}** are fixed at various values
- **$E_{\text{sym}}(\rho_c)$** and **$L(\rho_c)$** at $\rho_c = 0.11 \text{ fm}^{-3}$ are fixed at **$E_{\text{sym}}(\rho_c) = 26.65 \text{ MeV}$** and **$L(\rho_c) = 47.3 \pm 7.8 \text{ MeV}$** using heavy isotope binding energy difference and α_D of ^{208}Pb (Z. Zhang/LWC, PLB726, 234(2013); PRC90, 064317(2014))
- Other **9 lower-order parameters** and **W_0** are calibrated to fit data of finite nuclei
- Causality

Minimizing the Chi-square $\chi^2(p)$:

$$\chi^2(P) = \sum_{n=1}^N \left(\frac{O_n^{(\text{th})}(P) - O_n^{(\text{exp})}}{\Delta O_n} \right)^2$$



28 OCTOBER 2010 | VOL 467 | NATURE | 1081

LETTER

doi:10.1038/nature09466

A two-solar-mass neutron star measured using Shapiro delay

P. B. Demorest¹, T. Pennucci², S. M. Ransom¹, M. S. E. Roberts³ & J. W. T. Hessels^{4,5}

Observed heaviest Nstar so far (before 2019):

A Massive Pulsar in a Compact Relativistic Binary

John Antoniadis *et al.*

Science **340**, (2013);

DOI: 10.1126/science.1233232



PSR J0348+0432

2.01 ± 0.04 solar mass (M_{\odot})

Selected for a Viewpoint in *Physics*

PHYSICAL REVIEW LETTERS

week ending
20 OCTOBER 2017

PRL 119, 161101 (2017)



GW170817: Observation of Gravitational Waves from a Binary Neutron Star Inspiral

B. P. Abbott *et al.**

(LIGO Scientific Collaboration and Virgo Collaboration)

PRL121, 161101 (2018)

GW170817: Measurements of neutron star radii and equation of state

The LIGO Scientific Collaboration and The Virgo Collaboration
(compiled 30 May 2018)



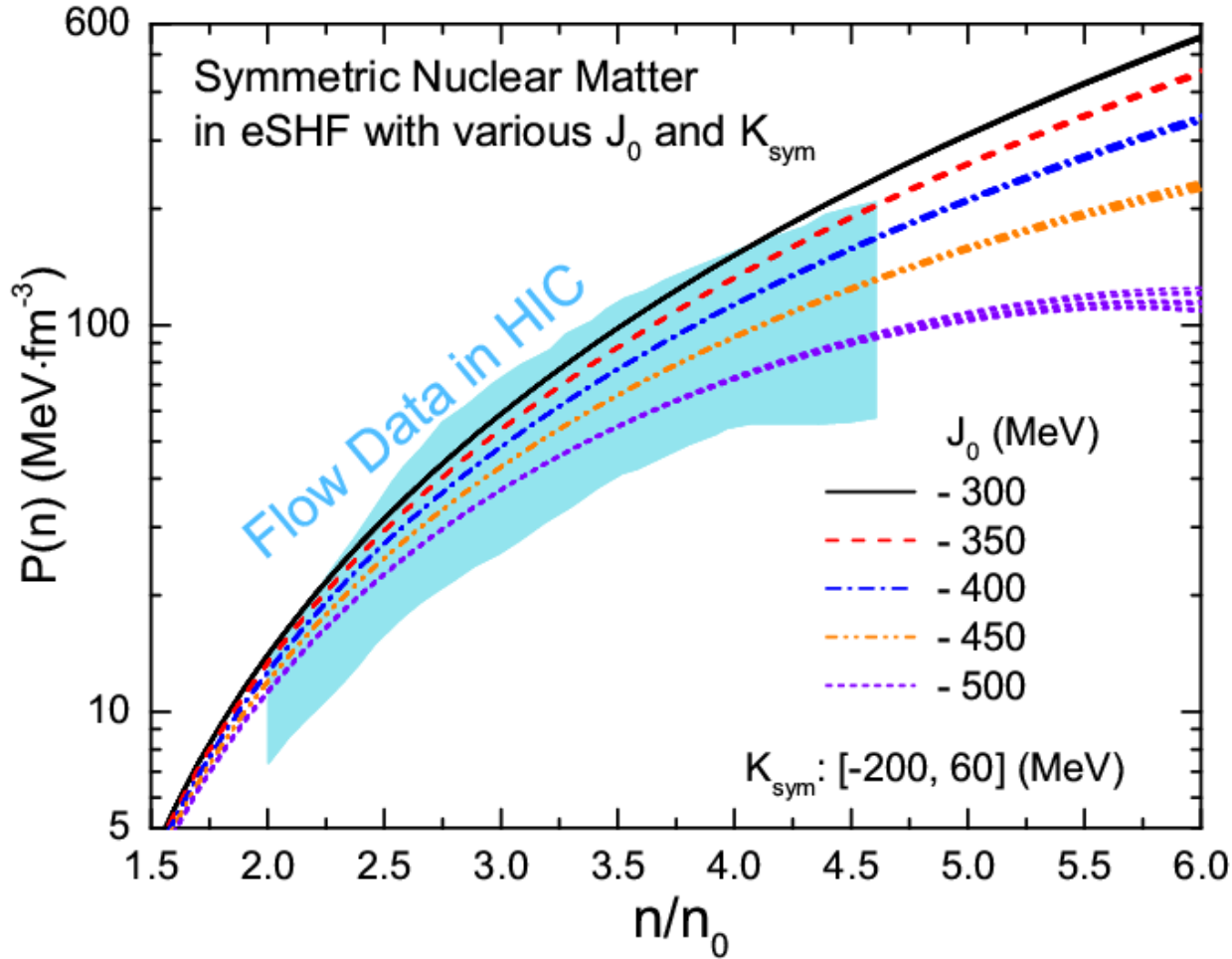
GW170817 (LIGO/Virgo):

$70 < \Lambda_{1.4} < 580$



J₀: Flow data in HIC's

Y. Zhou/LWC/Z. Zhang, PRD99, 121301(R) (2019) [arXiv:1901.11364]



For various J_0 and
 K_{sym} : [-200, 60] MeV

$E_{\text{sym}}(\rho_c) = 26.65$ MeV
 $L(\rho_c) = 47.3$ MeV

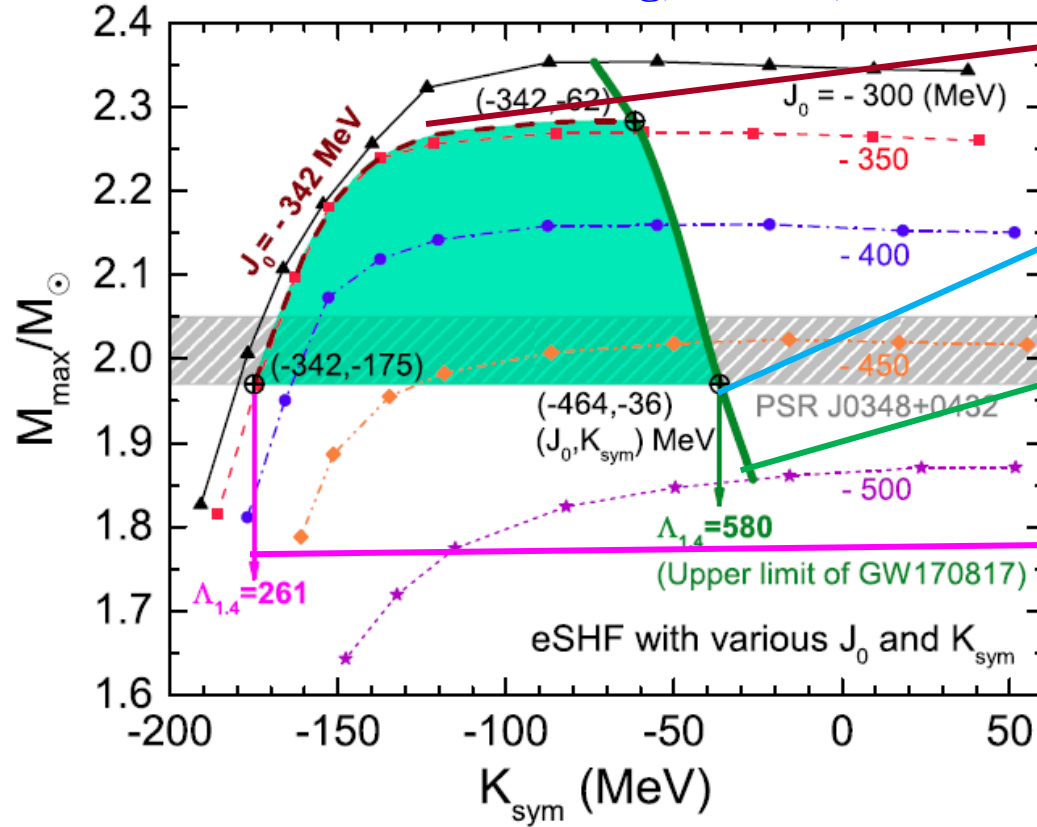
Pressure of SNM is
very sensitive to J_0
but essentially
independent of K_{sym}

-550 MeV $\sim < J_0 < -342$ MeV: Flow Data in HIC's



J0 and Ksym: Flow data, NStar Mass, Λ

Y. Zhou/LWC/Z. Zhang, PRD99, 121301(R) (2019) [arXiv:1901.11364]



$J_0 = -342 \text{ MeV}$

$J_0 = -464 \text{ MeV}$

$K_{\text{sym}} < -36 \text{ MeV}$

$\Lambda_{1.4} < 580$

GW170817 (LIGO/Virgo)

$\Lambda_{1.4} > 261$

Consistent with EM counterpart of GW170817, see, e.g.,
D. Radice et al., ApJL852, L29(2018);
M.W. Coughlin et al., MNRAS 480, 3871(2018)

K_{sym} affects strongly M_{max}
for $K_{\text{sym}} < -100 \text{ MeV}$

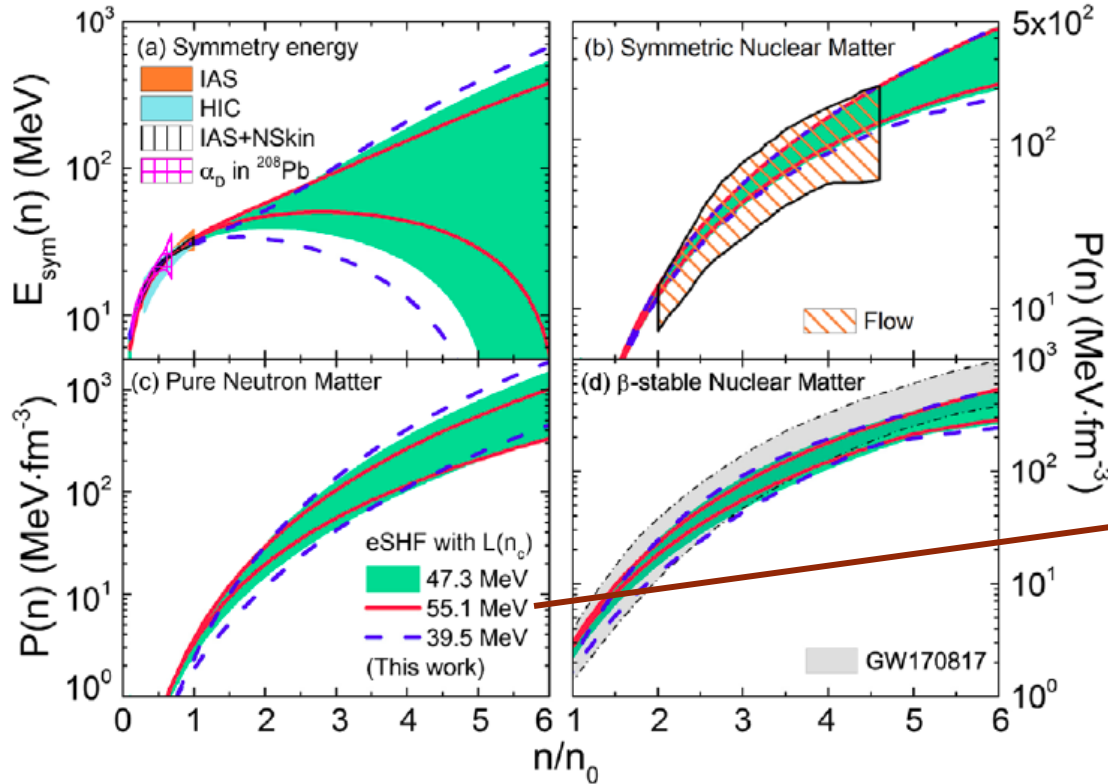
Flow Data in HIC + Mmax:
 $K_{\text{sym}} > -175 \text{ MeV}, \Lambda_{1.4} > 261$

Flow Data in HIC+Mmax+ $\Lambda_{1.4}$:
 $-464 \text{ MeV} < J_0 < -342 \text{ MeV}$:
 $-175 \text{ MeV} < K_{\text{sym}} < -36 \text{ MeV}$:



EOS: Flow data, NStar Mass, Λ

Y. Zhou/LWC/Z. Zhang, PRD99, 121301(R) (2019) [arXiv:1901.11364]



$L(\rho_c)=47.3\pm 7.8$ MeV
using α_D of ^{208}Pb (Z. Zhang, LWC, PRC90, 064317(2014))

$L(\rho_c)$ indeed affects the extraction of E_{sym} at high densities but does not change much the Nstar matter EOS!

$L(\rho_c)=47.3$ MeV:
 J_0 :[-464,-342] MeV,
 K_{sym} :[-175,-36] MeV
 $E_{\text{sym}}(2\rho_0)$:[39.4, 54.5] MeV

$L(\rho_c)=39.5$ MeV:
 J_0 :[-475,-342] MeV,
 K_{sym} :[-203,-34] MeV
 $E_{\text{sym}}(2\rho_0)$:[33.0, 51.3] MeV

$L(\rho_c)=55.1$ MeV:
 J_0 :[-455,-342] MeV,
 K_{sym} :[-138,-38] MeV
 $E_{\text{sym}}(2\rho_0)$:[46.9, 57.6] MeV



E. FONSECA,^{1,2,3,4} H. T. CROMARTIE,^{5,6} T. T. PENNUCCI,^{7,8} P. S. RAY,⁹ A. YU. KIRICHENKO,^{10,11} S. M. RANSOM,⁷ P. B. DEMOREST,¹² I. H. STAIRS,¹³ Z. ARZOUMANIAN,¹⁴ L. GUILLEMOT,^{15,16} A. PARTHASARATHY,¹⁷ M. KERR,⁹ I. COGNARD,^{15,16} P. T. BAKER,¹⁸ H. BLUMER,^{3,4} P. R. BROOK,^{3,4} M. DECESAR,¹⁹ T. DOLCH,^{20,21} F. A. DONG,¹³ E. C. FERRARA,^{22,23,24} W. FIORE,^{3,4} N. GARVER-DANIELS,^{3,4} D. C. GOOD,¹³ R. JENNINGS,²⁵ M. L. JONES,²⁶ V. M. KASPI,^{1,2} M. T. LAM,^{27,28} D. R. LORIMER,^{3,4} J. LUO,²⁹ A. MCEWEN,²⁶ J. W. MCKEE,²⁹ M. A. MCLAUGHLIN,^{3,4} N. MCMANN,³⁰ B. W. MEYERS,¹³ A. NAIDU,³¹ C. NG,³² D. J. NICE,³³ N. POL,³⁰ H. A. RADOVAN,³⁴ B. SHAPIRO-ALBERT,^{3,4} C. M. TAN,^{1,2} S. P. TENDULKAR,^{35,36} J. K. SWIGGUM,³³ H. M. WAHL,^{3,4} AND W. W. ZHU³⁷

¹Department of Physics, McGill University, 3600 rue University, Montréal, QC H3A 2T8, Canada

²McGill Space Institute, McGill University, 3550 rue University, Montréal, QC H3A 2A7, Canada

³Department of Physics and Astronomy, West Virginia University, Morgantown, WV 26506-6315, USA

⁴Center for Gravitational Waves and Cosmology, Chestnut Ridge Research Building, Morgantown, WV 26505, USA

⁵Cornell Center for Astrophysics and Planetary Science and Department of Astronomy, Cornell University, Ithaca, NY 14853, USA
6GNAC U.S. Navy, Ellsworth Air Force Base, Ellsworth, SD 57730, USA

ABSTRACT

We report results from continued timing observations of PSR J0740+6620, a high-mass, 2.8-ms radio pulsar in orbit with a likely ultra-cool white dwarf companion. Our data set consists of combined pulse arrival-time measurements made with the 100-m Green Bank Telescope and the Canadian Hydrogen Intensity Mapping Experiment telescope. We explore the significance of timing-based phenomena arising from general-relativistic dynamics and variations in pulse dispersion. When using various statistical methods, we find that combining ~ 1.5 years of additional, high-cadence timing data with previous measurements confirms and improves upon previous estimates of relativistic effects within the PSR J0740+6620 system, with the pulsar mass $m_p = 2.08^{+0.07}_{-0.07} M_\odot$ (68.3% credibility) determined by the relativistic Shapiro time delay. For the first time, we measure secular variation in the orbital period and argue that this effect arises from apparent acceleration due to significant transverse motion. After incorporating contributions from Galactic differential rotation and off-plane acceleration in the Galactic potential, we obtain a model-dependent distance of $d = 1.14^{+0.17}_{-0.15}$ kpc (68.3% credibility). This improved distance confirms the ultra-cool nature of the white dwarf companion determined from recent optical observations. We discuss the prospects for future observations with next-generation facilities, which will likely improve the precision on m_p for J0740+6620 by an order of magnitude within the next few years.

Relativistic Shapiro delay measurements of an extremely massive millisecond pulsar

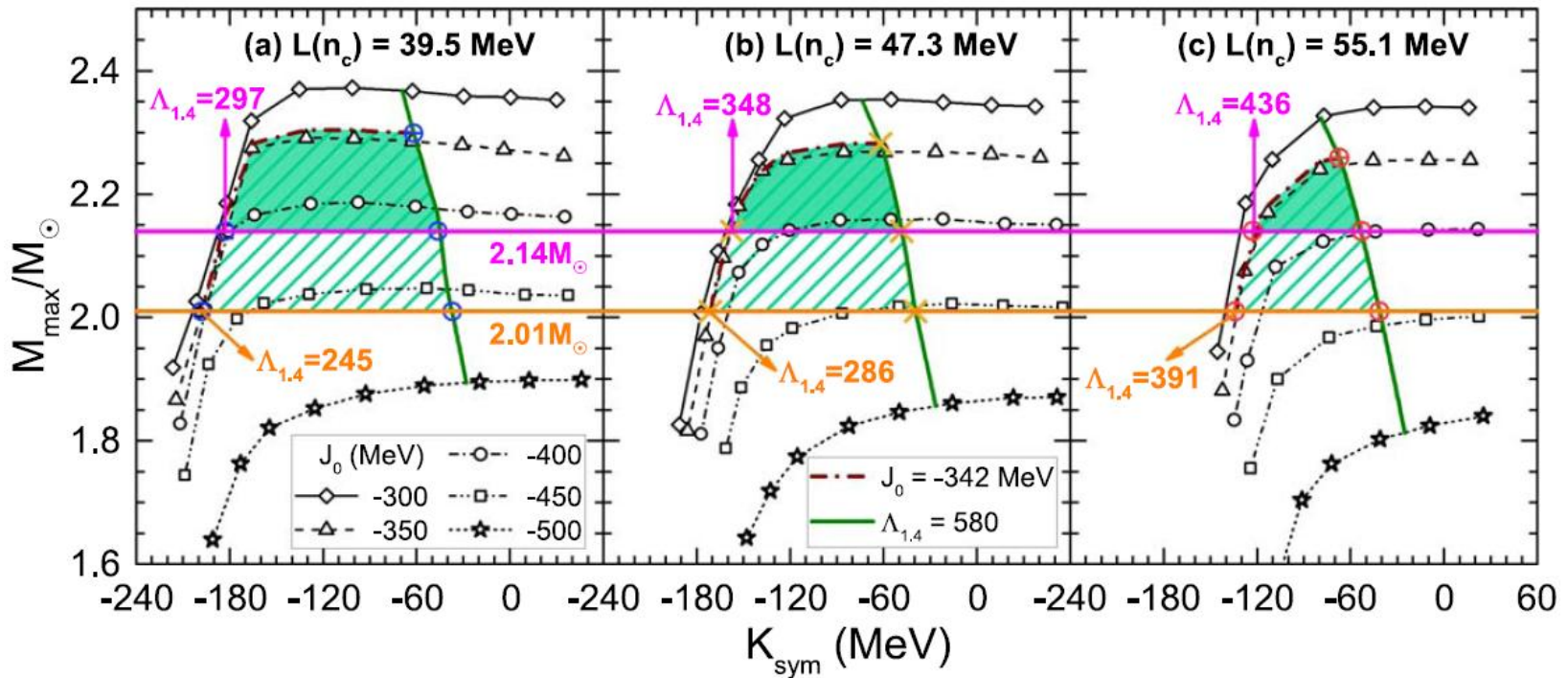
H. T. Cromartie^{1*}, E. Fonseca², S. M. Ransom³, P. B. Demorest⁴, Z. Arzoumanian⁵, H. Blumer^{6,7}, P. R. Brook^{6,7}, M. E. DeCesar⁸, T. Dolch⁹, J. A. Ellis¹⁰, R. D. Ferdman¹¹, E. C. Ferrara^{12,13}, N. Garver-Daniels^{6,7}, P. A. Gentile^{6,7}, M. L. Jones^{6,7}, M. T. Lam^{6,7}, D. R. Lorimer^{6,7}, R. S. Lynch¹⁴, M. A. McLaughlin^{6,7}, C. Ng^{15,16}, D. J. Nice¹⁷, T. T. Pennucci¹⁷, R. Spiewak¹⁸, I. H. Stairs¹⁵, K. Stovall⁴, J. K. Swiggum¹⁹ and W. W. Zhu²⁰

edge-on) binary pulsar systems. By combining data from the North American Nanohertz Observatory for Gravitational Waves (NANOGrav) 12.5-yr data set with recent orbital-phase-specific observations using the Green Bank Telescope, we have measured the mass of the MSP J0740+6620 to be $2.14^{+0.10}_{-0.09} M_\odot$ (68.3% credibility interval; the 95.4% credibility interval is $2.14^{+0.20}_{-0.18} M_\odot$). It is highly likely to be the most massive neutron star yet observed, and serves as a strong constraint on the neutron star interior EoS.



中子星最大质量

Y. Zhou, L.W. Chen*, ApJ886, 52(2019) [arXiv:1907.12284]



$\Lambda_{1.4} > 297$

The maximum mass of static NS is about $2.3M_\odot$!



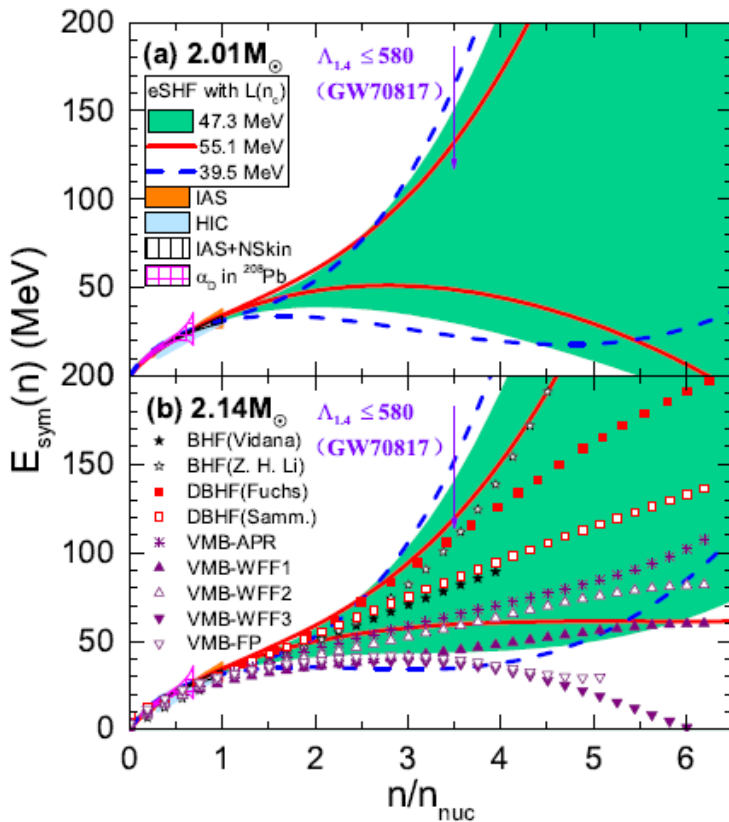
THE ASTROPHYSICAL JOURNAL, 886:52 (6pp), 2019 November 20

Ruling Out the Supersoft High-density Symmetry Energy from the Discovery of PSR J0740+6620 with Mass $2.14_{-0.09}^{+0.10} M_{\odot}$

Ying Zhou and Lie-Wen Chen^{1, @}

School of Physics and Astronomy and Shanghai Key Laboratory for Particle Physics and Cosmology, Shanghai Jiao Tong University, Shanghai 200240, People's Republic of China; lwchen@sjtu.edu.cn

Received 2019 August 1; revised 2019 October 1; accepted 2019 October 1; published 2019 November 19



Y. Zhou, L.W. Chen*, ApJ886, 52(2019) [arXiv:1907.12284]

$$\mu_e = \mu_n - \mu_p = 4\delta E_{\text{sym}}(\rho)$$

“超软”高密对称能的排除意味着中子星内部不存在纯中子物质！



GW190814: 超重中子星???

THE ASTROPHYSICAL JOURNAL LETTERS, 896:L44 (20pp), 2020 June 20

<https://doi.org/10.3847/2041-8213/ab960f>

© 2020. The American Astronomical Society.

OPEN ACCESS



GW190814: Gravitational Waves from the Coalescence of a 23 Solar Mass Black Hole with a 2.6 Solar Mass Compact Object

R. Abbott¹, T. D. Abbott², S. Abraham³, F. Acemese^{4,5}, K. Ackley⁶, C. Adams⁷, R. X. Adhikari¹, V. B. Adya⁸, C. Affeldt^{9,10}, M. Aarthas^{11,12}, K. Arai¹³, N. Arora¹⁴, O. D. Aouar¹⁵, A. Aich¹⁶, I. Aiello^{17,18}, A. Ain³, P. Aith¹⁹, S. Akcay^{11,20}

A. K. Zaitsev⁷⁵, A. Zaitsev⁷⁶, M. Zakharenko⁷⁷, I. Zelenova⁷⁸, J.-F. Zeng⁷⁹, M. Zevin⁸⁰, J. Zhang⁸¹, L. Zhang⁸², T. Zhang⁸³, C. Zhao⁷⁵, G. Zhao¹¹², M. Zhou¹⁴, Z. Zhou¹⁴, X. J. Zhu⁶, A. B. Zimmerman¹⁷⁷, M. E. Zucker^{1,55}, and J. Zweizig¹

LIGO Scientific Collaboration and Virgo Collaboration



2. 6倍太阳质量的致密目标被发现!

夸克星???(The mass of **ud Quark Star** can be $2.77M_{\odot}$,
Z. Cao (曹政), LWC, P.C. Chu (初鹏程), and Y. Zhou (周颖), arXiv:2009.00942.)

中国天眼FAST有望发现更多脉冲星!



四、对称能研究进展

- 引力波时代的对称能
 - PREX-II 铅核中子皮实验的挑战
 - 现状总结
-



中子皮: PREX-II

PHYSICAL REVIEW LETTERS 126, 172502 (2021)

Editors' Suggestion

Featured in Physics

Accurate Determination of the Neutron Skin Thickness of ^{208}Pb through Parity-Violation in Electron Scattering

D. Adhikari,¹ H. Albataineh,² D. Androic,³ K. Aniol,⁴ D. S. Armstrong,⁵ T. Averett,⁵ C. Ayerbe Gayoso,⁵ S. Barcus,⁶

$$R_n - R_p = 0.283 \pm 0.071 \text{ fm}$$

PREX-II: $R_{\text{skin}} = [0.212, 0.354] \text{ fm}$ for Pb208

Huge Nskin!

PREX:

The Lead (Pb) Radius EXperiment

In PREX, the neutron density distribution in ^{208}Pb is determined by measuring the parity-violating electroweak asymmetry in the elastic scattering of polarized electrons off ^{208}Pb and thus is free from the strong interaction uncertainties

PHYSICAL REVIEW LETTERS 126, 172503 (2021)

Editors' Suggestion

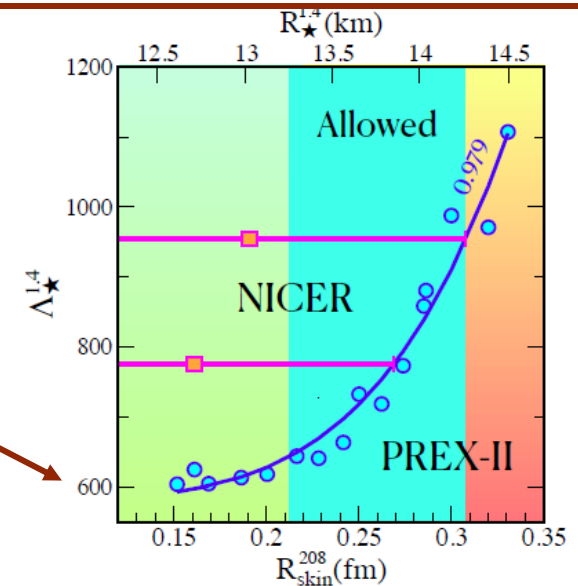
Implications of PREX-2 on the Equation of State of Neutron-Rich Matter

Brendan T. Reed^{1,2,*} F. J. Fattoyev^{3,†} C. J. Horowitz^{2,‡} and J. Piekarewicz^{4,§}

RMF: Inconsistent with GW170817: $\Lambda_{1.4} < 580$!!!

δ meson may be important in the RMF model !!!

F. Li (李帆) et al., in preparation



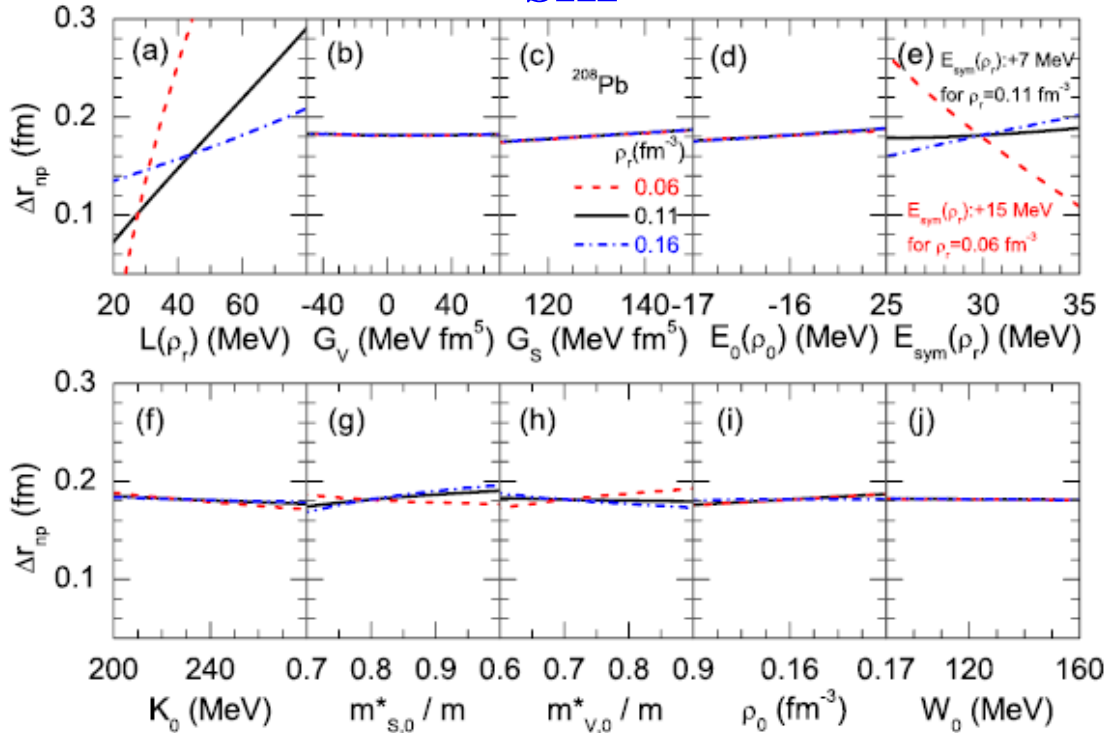
中子皮: PREX-II

What determines the Nskin thickness?

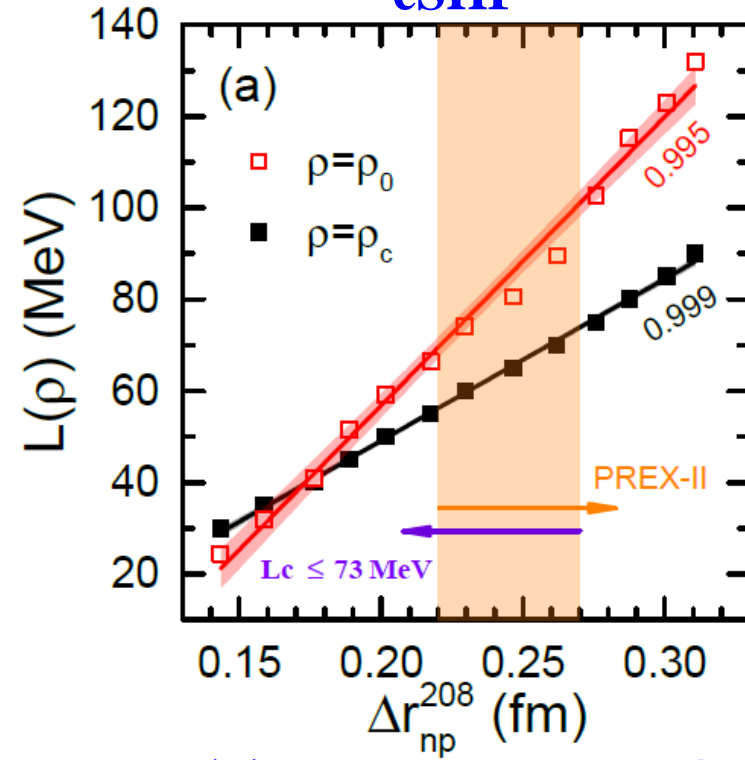
The density slope parameter L , especially L_c at $\rho_c \sim 2\rho_0/3$ (average density of nuclei)!!!

B. A. Brown, PRL85, 5296 (2000); R. J. Furnstahl, NPA706, 85 (2002); L.W. Chen et al., PRC72, 064309 (2005); M. Centelles et al., PRL102, 122502 (2009); L. W. Chen et al., PRC 82, 024321 (2010); X. Roca-Maza et al., PRL106, 252501 (2011),

SHF



eSHF



Z. Zhang (张振) and LWC*, PLB726, 234 (2013)

Citations: 131+ Nskin is determined by L_c !!!

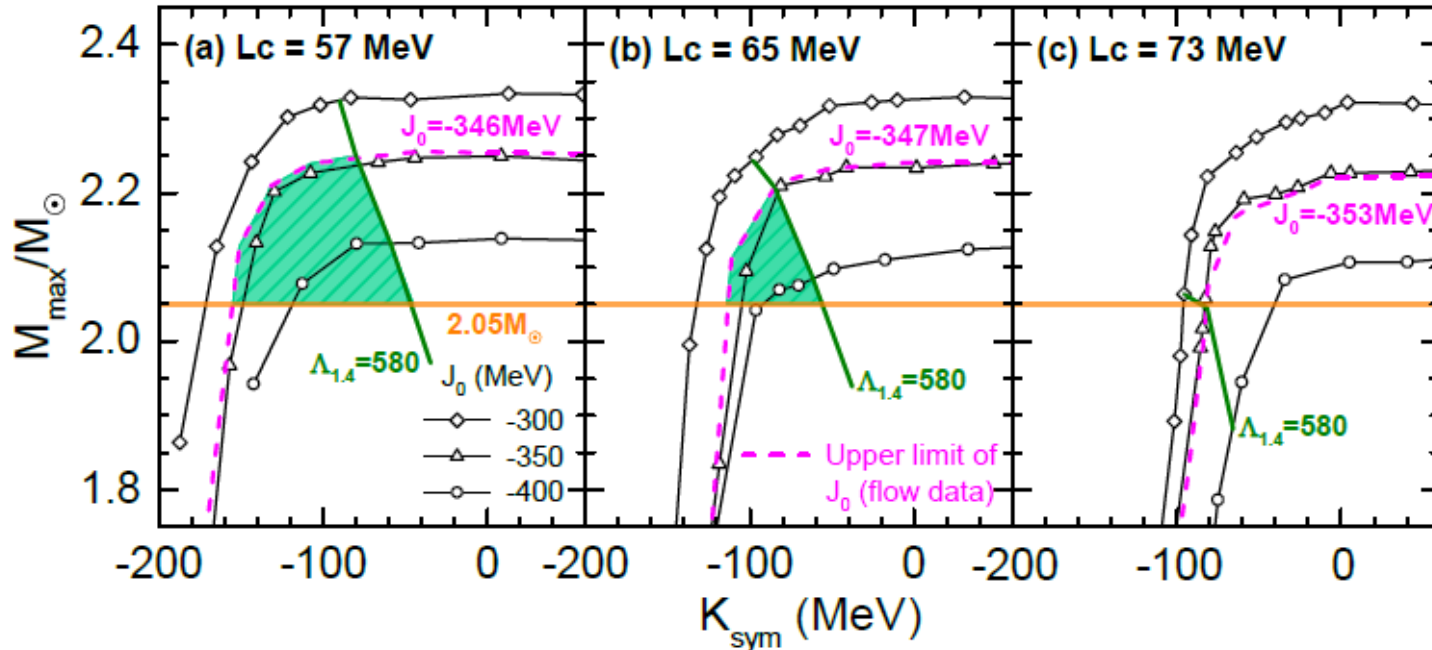
T.G. Yue (岳侗钢), LWC*, Z. Zhang (张振), and Y. Zhou (周颖), arXiv:2102.05267



中子皮: PREX-II

Implications of R_{skin} from PREX-II

T.G. Yue (岳伺钢), LWC*, Z. Zhang (张振), and Y. Zhou (周颖), arXiv:2102.05267



Lc cannot be too big!!! $L_c < 73$ MeV and then set an upper limit on R_{skin}: < 0.27 fm for Pb208

eSHF provides a single unified framework to simultaneously describe the finite nuclei (Eb, Rc, GMR, Nskin-PREX-II) + Flow data in HIC+NStar (e.g., NICER)+GW170817

$$E_{\text{sym}}(\rho_0) = 34.5 \pm 1.5 \text{ MeV and } L = 85.5 \pm 22.2 \text{ MeV}$$



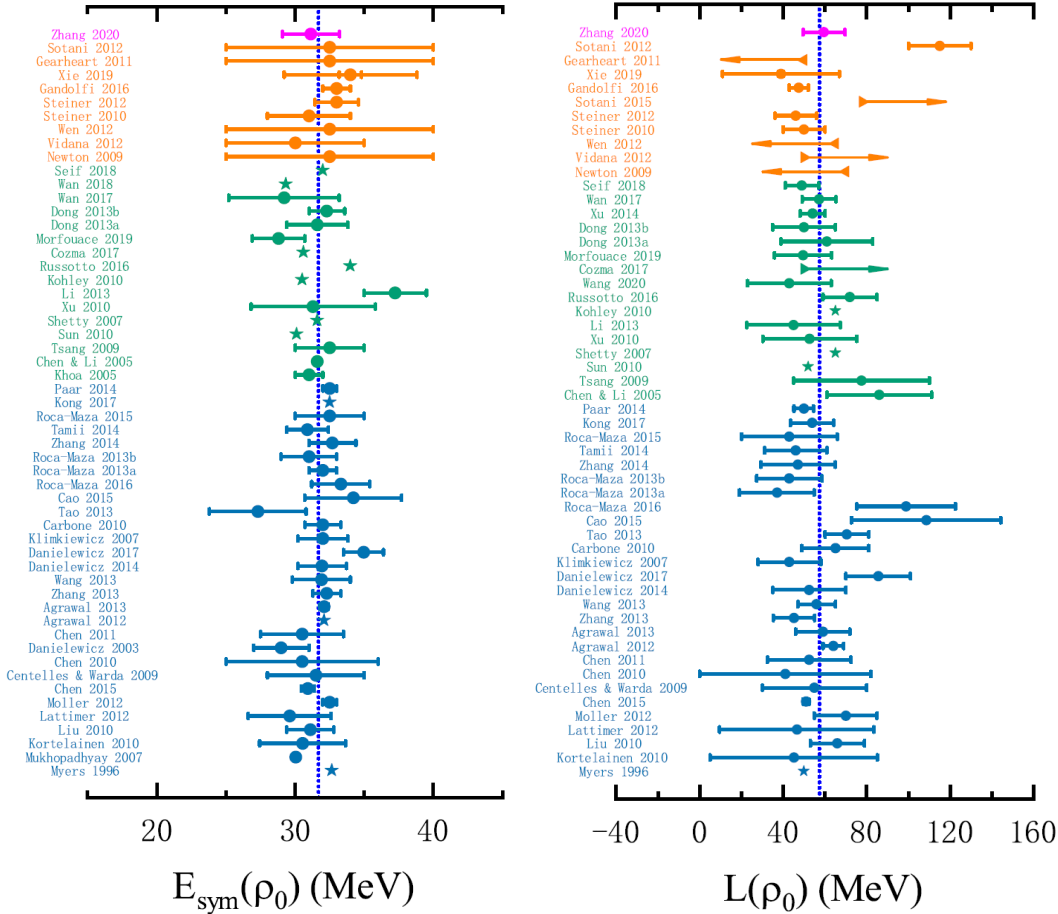
四、对称能研究进展

- 引力波时代的对称能
 - PREX-II 铅核中子皮实验的挑战
 - 现状总结
-



核物质对称能：饱和密度附近

LWC et al., In preparation, Invited Review



58 analyses of terrestrial nuclear experiments and astrophysical observations

$$E_{\text{sym}}(\rho_0) = 31.7 \pm 3.1$$

$$L = 57.5 \pm 24.5 \text{ MeV}$$

Similar conclusion has been obtained in:

B. A. Li and X. Han, Phys. Lett. B727, 276 (2013);
M. Oertel, M. Hempel, T. Klahn, and S. Typel, Rev. Mod. Phys. 89, 015007 (2017).



Assuming all the constraints are equally reliable !!!

Very recent PREX-II+Nuclei+GW et al:

$$E_{\text{sym}}(\rho_0) = 34.5 \pm 1.5 \text{ MeV}$$

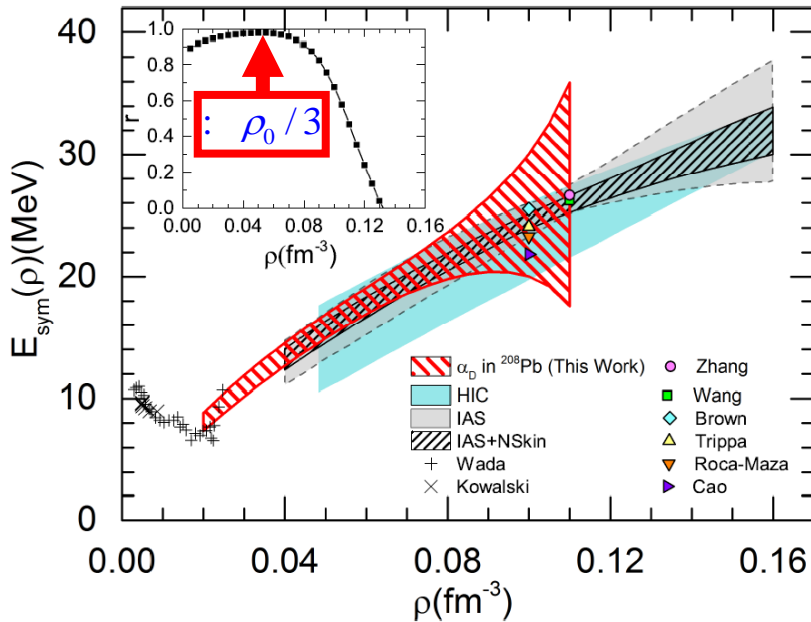
$$L = 85.5 \pm 22.2 \text{ MeV}$$

岳伺钢 et al., arXiv:2102.05267



核物质对称能：亚饱和密度行为

Z. Zhang (张振) and LWC, PRC92, 031301(R) (2015)



$$\bullet \Delta E(A: 208) \propto E_{sym}(\rho_{A=208}), \rho_{A=208} \approx 2/3\rho_0$$

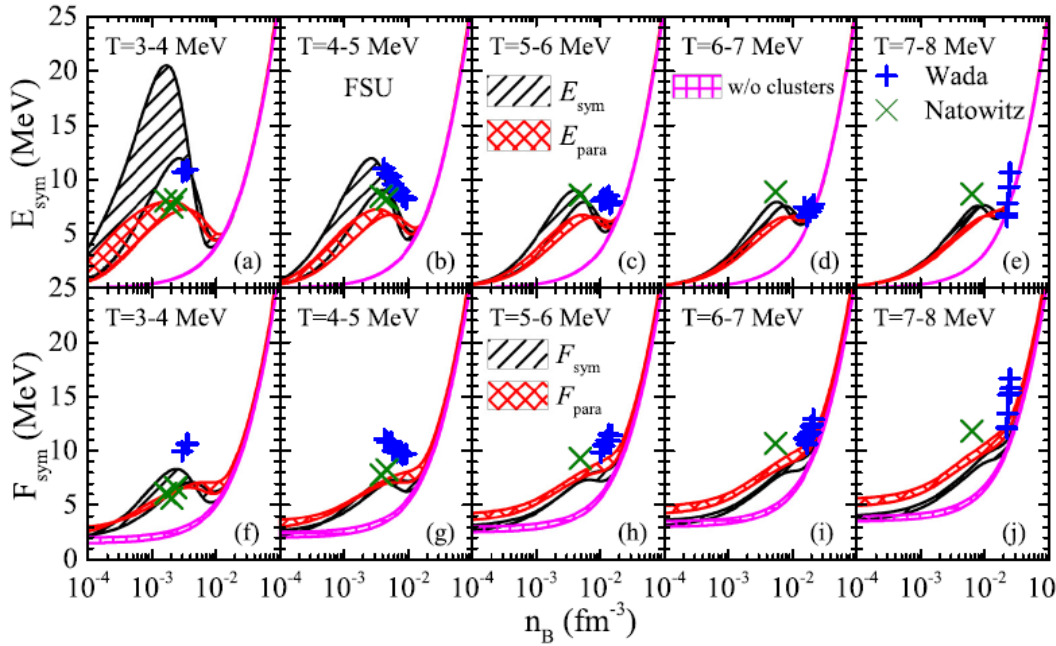
$$\bullet 1/\alpha_D(A=208) \propto E_{sym}(\rho_{A=45}), \rho_{A=45} \approx 1/3\rho_0$$

- **HIC:** Sn+Sn
M.B. Tsang *et al.*, Phys. Rev. Lett. **102**, 122701(2009)
- **IAS and IAS+NSkin**
P. Danielewicz and J. Lee, Nucl. Phys. **A922**, 1 (2014)
- **Zhang:** Isotope binding energy difference
Z. Zhang and L.W. Chen, Phys. Lett. **B726**, 234 (2013)
- **Wang:** Fermi energy difference
N. Wang *et al.*, Phys. Rev. C **87**, 034327 (2013)
- **Brown:** Doubly magic nuclei
B.A. Brown, Phys. Rev. Lett. **11**, 232502 (2013)
- **Trippa:** Giant dipole resonance
L. Trippa *et al.*, Phys. Rev. C **77**
- **Roca-Maza:** Giant quadrupole resonance
X. Roca-Maza *et al.*, Phys. Rev. C **87**, 034301 (2013)
- **Cao:** Pygmy dipole resonance
L.G. Cao and Z.Y. Ma, Chin. Phys. Lett. **25**, 1625 (2008)

Wada and Kowalski: experimental results of the symmetry energies at densities below $0.2\rho_0$ and temperatures in the range 3 ~11 MeV from the analysis of cluster formation in heavy ion collisions.

Wada *et al.*, Phys. Rev. C **85**, (2012) 064618; Kowalski *et al.*, Phys. Rev. C **75**, (2007) 014601. Natowitz *et al.*, Phys. Rev. Lett. **104**, (2010) 202501.

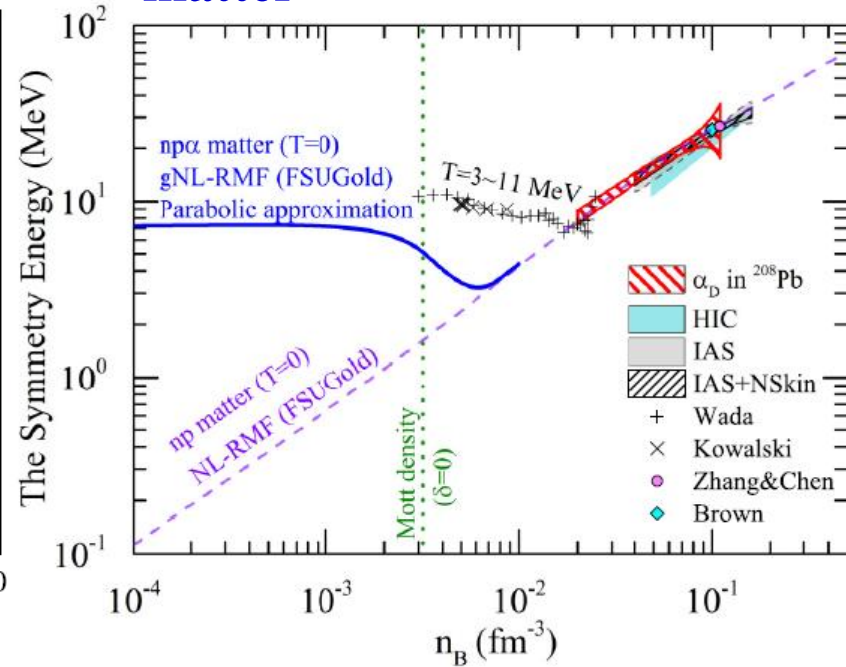
Clustering effects on E_{sym} within NL-RMF for n, p, t, h, α matter



Zhao-Wen Zhang (张肇文) and LWC, PRC95, 064330 (2017)

See also: S. Typel, G. Röpke, T. Klähn, D. Blaschke, and H. H. Wolter, Phys. Rev. C 81, 015803 (2010).

Alpha BEC effects on E_{sym} within NL-RMF for cold $np\alpha$ matter



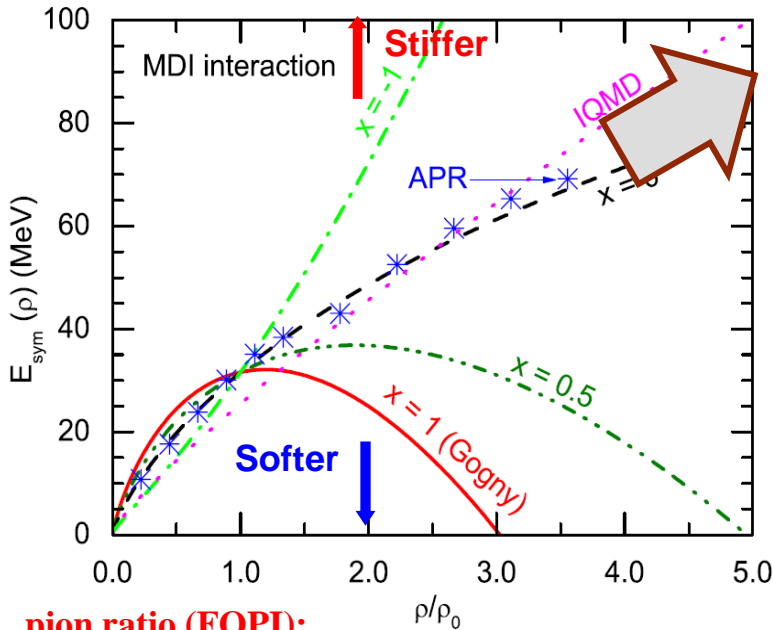
Zhao-Wen Zhang (张肇文) and LWC, PRC100, 054304 (2019)



核物质对称能：超饱和密度行为

A Soft or Stiff E_{sym} at supra-saturation densities ???

pion ratio (FOPI): ImIQMD, Feng/Jin, PLB683, 140(2010)



n/p v2 (FOPI): $(\rho/\rho_0)^\gamma$ with $\gamma = 0.9 \pm 0.4$

Russotto/Trautmann/Li et al.,
PLB697, 471(2011) (UrQMD)

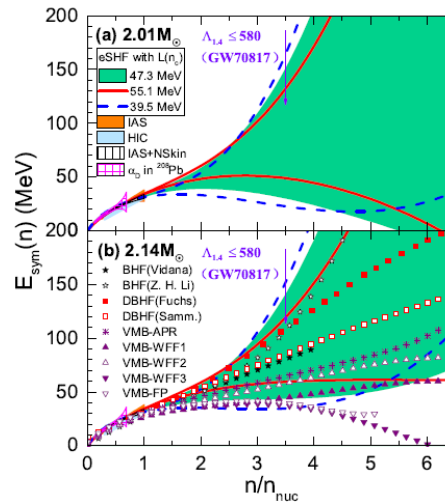
PRC94, 034608 (2016) $\gamma = 0.72 \pm 0.19$

Cozma/Trautmann/Li et al.,
PRC88, 044912 (2013) (Tubingen QMD - MDI)

pion ratio (FOPI):

IBUU04, Xiao/Li/Chen/Yong/Zhang, PRL102,062502(2009)

ImIBL, Xie/Su/Zhu/Zhang, PLB718,1510(2013)



Y. Zhou (周颖), LWC, ApJ886,
52(2019) [arXiv:1907.12284]

- 2.14倍太阳质量中子星的观测排除“超软”对称能
- 中子星并合引力波观测排除“超硬”对称能



核物质对称能：现状

- There are MANY constraints on $E_{\text{sym}}(\rho_0)$ and L , and the world average values are:

$$E_{\text{sym}}(\rho_0) = 31.7 \pm 3.1 \text{ MeV}$$

$$L = 57.5 \pm 24.5 \text{ MeV}$$

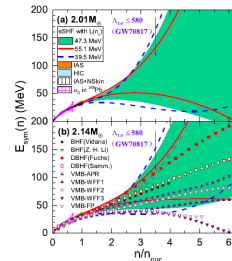
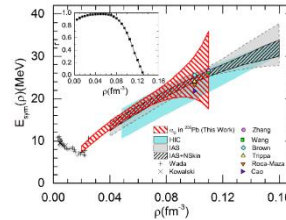
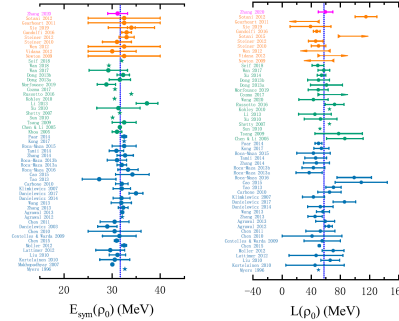
- Very recent PREX-II and GW et al:

$$E_{\text{sym}}(\rho_0) = 34.5 \pm 1.5 \text{ MeV}$$

$$L = 85.5 \pm 22.2 \text{ MeV}$$

- The symmetry energy at subsaturation densities have been relatively well-constrained

- Based on the GW(引力波) multimessenger measurements, the high density E_{sym} cannot be too stiff or too soft but still with large uncertainty!!!



Z. Zhang(张振)/LWC,
PLB726, 234 (2013);
PRC92, 031301(R)(2015)

Y. Zhou (周颖), LWC,
ApJ886, 52(2019)
[arXiv:1907.12284]



NUSYM15

5th INTERNATIONAL SYMPOSIUM ON NUCLEAR SYMMETRY ENERGY

June 29 - July 2, 2015
Kraków, Poland
Auditorium Maximum

Physics topics:

- progress in experimental investigations of the nuclear EoS
- status of theories of the asymmetric nuclear matter
- transport models, their ingredients, reliability and predictive power
- symmetry term in nuclei, heavy ion collisions and in astrophysics
- correlations and clusterization in dense, normal and dilute nuclear matter





上海交通大學
SHANGHAI JIAO TONG UNIVERSITY

NuSYM16 (Tsinghua, Beijing, China)



The 6th International Symposium on Nuclear Symmetry Energy

June 13 - June 17, 2016

Tsinghua University (Beijing, China)





上海交通大學
SHANGHAI JIAO TONG UNIVERSITY

NuSYM17 (GANIL, Caen, France)



NUSYM 2017

7th international symposium on nuclear symmetry energy
SEPTEMBER 4TH - 7TH / GANIL, CAEN, FRANCE





上海交通大学
SHANGHAI JIAO TONG UNIVERSITY

五、展望



- **重离子碰撞**为我们理解非对称核物质的状态方程，尤其是核物质对称能，提供了重要的实验手段
- 决定核物质对称能的**高密行为**依然是一个巨大的挑战 (**Many-body forces, Short range tensor forces, Short range NN correlations, Model cross check, more data,.....**).**丰中子核引起的高能重离子碰撞的实验数据 (HIAF and HIAF-U!!!)**将非常重要!
- **重离子碰撞微观输运理论模型**为理解重离子碰撞动力学提供了重要的理论工具
- 如何改进和发展更为**自洽的同位旋相关的相对论的量子输运模型**仍然是一个巨大的挑战
- **中子星及其并合引发的引力波观测**为约束对称能的高密行为提供了重要途径



上海交通大学
SHANGHAI JIAO TONG UNIVERSITY



谢谢!

